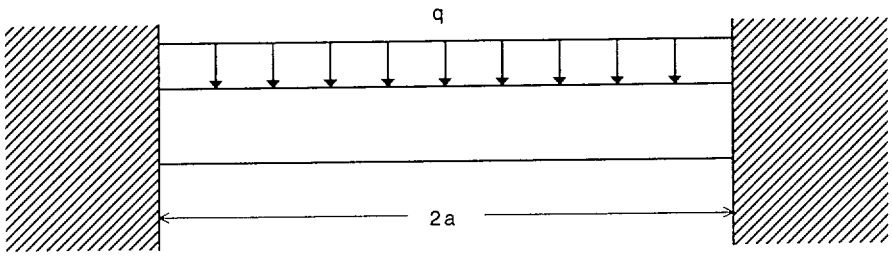

where: $q = 47{,}000$ psi
$a = 1$ in
$t = 1.25$ in
$E = 27 \times 10^6$ psi at 300°F
ν = Poisson's ratio = 0.31.

Because a principal stress is a shear on the edges, a simplified evaluation can be carried out for shear stresses by using the lateral surface of the cover plate:

$$\text{(at edge) } S_{RZ} = \frac{qa}{2t} = 18{,}800 \text{ psi.}$$

Because the maximum port cover temperature is less than 300°F, the ultimate strength of the port cover (conservatively based on 300°F) is 66,000 psi. Therefore, the stress limit is 0.42 S_u = 27,720 psi, the minimum margin of safety is +0.36, and the clearance between the port cover and the valve exceeds 1.5×10^{-4} in.

2.7.2.5 Puncture Accident - Shielding Consequences

The puncture accident causes a localized reduction in the cask shielding. The resulting dose rates are bounded by the loss of neutron shield accident dose rates, which do not exceed the limits of 10 CFR 71.51.

2.7.3 Thermal

In accordance with the requirements of 10 CFR 71.73(c)(4), "Thermal, Hypothetical Accident Conditions," the Universal Transport Cask is analyzed for structural adequacy. The cask is assumed to be subjected to a fire, which produces a surrounding environment of 1,475°F for 30 minutes. The thermal evaluation of the hypothetical fire transient is presented in Section 3.5.

2.7.3.1 Summary of Pressures and Temperatures

The maximum thermal accident condition temperatures are summarized in Tables 3.5-1 and 3.5-2 for the various PWR and BWR cask components. A summary of pressures for the PWR and BWR configurations (both canister and cask pressures) are listed in Tables 2.7.3.1-1 and 2.7.3.1-2. The evaluation for the cask internal pressure of 150 psig is bounded by those pressures presented in Section 2.6 for normal conditions of transport. Stress results for the canister are presented in Tables 2.7.3.1-3 and 2.7.3.1-4 for the PWR canister and in Tables 2.7.3.1-5 and 2.7.3.1-6 for the BWR canister.

Cask closure bolts are qualified for a maximum pressure of 80 psig, which envelopes the maximum pressure developed during the fire.

The Universal Transport Cask inner and outer shells, lid, and lid bolts are demonstrated to be structurally adequate against loss of containment following a Thermal (fire) accident. Therefore, the cask satisfies 10 CFR 71 structural requirements for the fire accident scenario.

2.7.3.2 Differential Thermal Expansion Stress

Differential thermal expansion stresses and through-thickness thermal gradient stresses are induced in the Universal Transport Cask as a result of the Thermal (fire) accident event. All of these thermal stresses are classified as secondary, displacement-limited stresses according to the ASME Boiler and Pressure Vessel Code. Limits on secondary stresses do not apply for accident conditions; the secondary stresses, in themselves, do not compromise the integrity of the cask.

Table 2.7.3.1-1 Summary of Maximum Canister Pressures During Hypothetical Accident Conditions

Pressure Condition	Canister Internal Pressure (PWR)	Canister Internal Pressure (BWR)
Fire Accident and 100% Rod Failure	74.3 psig	43.8 psig
Pressure used for Canister Analysis	80 psig	80 psig

Table 2.7.3.1-2 Summary of Maximum Cask Cavity Pressures During Hypothetical Accident Conditions

Pressure Condition	Cask Cavity Internal Pressure (PWR)	Cask Cavity Internal Pressure (BWR)
Fire Accident and 100% Rod Failure	69.3 psig	42.8 psig
Cask Lid Closure Analysis	80 psig	80 psig
Cask Body Finite Element Analysis	150 psig	150 psig

Table 2.7.3.1-3 PWR Canister P_m Stresses 80 psig Internal Pressure Accident Conditions

Section Location	P_m Stresses (ksi)						Stress Intensity (ksi)	Allowable Stress (ksi)	Margin of Safety
	Sx	Sy	Sz	Sxy	Syz	Sxz			
1	5.7	-4.8	-6.6	-0.9	-0.1	-0.9	12.4	38.4	2.09
2	1.2	0.3	-8.8	1.4	-0.2	-0.8	11.1	38.4	2.46
3	-0.1	2.3	4.2	0	0	0.3	4.3	38.4	7.88
4	-0.1	2.1	4.2	0	0	0.3	4.4	38.4	7.77
5	-0.1	2.1	4.2	0	0	0.3	4.4	38.4	7.74
6	-0.2	2	4.2	0	0	0.3	4.4	38.4	7.69
7	-0.1	2.1	2	0	0.2	0.3	2.4	38.4	14.92
8	-1.1	2.1	0.9	-0.4	0.2	0	3.3	38.4	10.77
9	-3.8	0.6	0	-0.8	0.1	0	4.6	38.4	7.27
10	1.1	-0.2	0.5	0	0.1	-0.1	1.3	38.4	29.15
11	-2.4	-1.5	-0.2	-1.1	0	-0.1	2.9	38.4	12.08
12	-0.9	0.5	0.4	-0.1	0	0	1.4	38.4	26.93
13	1	-1.2	1.1	-0.1	0.1	0	2.2	30.72†	20.94
14	-0.2	0	-0.1	0	0	0	0.1	38.4	304.11
15	0.1	0	0.1	0	0	0	0.1	38.4	266.45

† Allowable Stress includes reduction factor for weld (0.8 x Allowable Stress).

Table 2.7.3.1-4 PWR Canister $P_m + P_b$ Stresses 80 psig Internal Pressure Accident Conditions

Section Location	$P_m + P_b$ Stresses (ksi)						Stress Intensity (ksi)	Allowable Stress (ksi)	Margin of Safety
	Sx	Sy	Sz	Sxy	Syz	Sxz			
1	8.2	20.1	1.4	0.3	0.1	-0.3	18.7	57.5	2.08
2	2.5	-36.8	-16.9	-2.5	-0.2	-1.5	39.7	57.5	0.45
3	1.5	-43.3	-20.4	0.2	-0.4	-3.6	45.4	57.5	0.27
4	-0.1	2.4	4.5	0	0	0.3	4.7	57.5	11.33
5	-0.1	2.1	4.2	0	0	0.3	4.4	57.5	12.09
6	-0.2	2.1	4.4	0	0	0.4	4.6	57.5	11.46
7	-0.2	2.1	4.6	0	0	0.4	4.9	57.5	10.69
8	-0.1	2.4	2.6	-0.1	0.3	0.3	3	57.5	18.39
9	-0.7	4.5	1.6	-0.3	0.2	0.1	5.3	57.5	9.92
10	-3.8	3.1	0.7	-0.3	0.2	0.1	7	57.5	7.26
11	0.6	-2.9	-0.4	0.1	0	-0.2	3.5	57.5	15.34
12	-3.7	-2.4	-0.7	-1.4	0	-0.1	3.9	57.5	13.81
13	-2.4	-0.1	-0.1	-0.2	0	0	2.3	46.0†	19.0
14	24.7	-2	24.7	-0.1	0.3	-0.1	26.7	57.5	1.15
15	-1.8	0	-1.8	0	0	0	1.8	57.5	31.5

†Allowable Stress includes reduction factor for weld (0.8 x Allowable Stress).

Table 2.7.3.1-5 BWR Canister P_m Stresses 80 psig Internal Pressure Accident Conditions

Section Location	P_m Stresses (ksi)						Stress Intensity (ksi)	Allowable Stress (ksi)	Margin of Safety
	Sx	Sy	Sz	Sxy	Syz	Sxz			
1	-1	6.1	2.1	-1.1	0.1	0.1	7.5	38.4	4.15
2	2.6	-4.1	-7.1	-1.3	0	-0.7	10	38.4	2.83
3	1.8	-2.6	-8.2	-0.6	0	-0.7	10.2	38.4	2.76
4	-0.1	2	4.2	0	0	0.3	4.3	38.4	7.91
5	-0.1	2	4.2	0	0	0.3	4.3	38.4	7.95
6	-0.1	2	4.2	0	0	0.3	4.3	38.4	7.95
7	-0.1	2	4.2	0	0	0.3	4.3	38.4	7.94
8	-0.1	2.2	2	-0.1	0.1	0.2	2.4	38.4	14.79
9	-1	2.1	0.9	-0.4	0.1	0	3.3	38.4	10.75
10	-3.8	0.6	0	-0.8	0.1	0	4.7	38.4	7.19
11	1.1	-0.2	0.5	0	0	-0.1	1.3	38.4	28.71
12	-2.4	-1.6	-0.2	-1.1	0	-0.1	2.9	38.4	12.09
13	-0.8	0.5	0.4	-0.1	0	0	1.3	30.72†	22.63
14	1.1	-0.8	1.1	-0.1	-0.1	0	1.9	38.4	18.9
15	-0.2	0	-0.1	0	0	0	0.1	38.4	313.1
16	0.1	0	0.1	0	0	0	0.1	38.4	281.21

†Allowable Stress includes reduction factor for weld (0.8 x Allowable Stress).

Table 2.7.3.1-6 BWR Canister $P_m + P_b$ Stresses 80 psig Internal Pressure Accident Conditions

Section Location	$P_m + P_b$ Stresses (ksi)						Stress Intensity (ksi)	Allowable Stress (ksi)	Margin of Safety
	Sx	Sy	Sz	Sxy	Syz	Sxz			
1	0.6	14.3	0.6	-0.4	0.4	-2.2	15.9	57.5	2.61
2	2.7	-30.1	-14.5	2.2	0.1	1.3	33.1	57.5	0.74
3	2.1	-28.7	-15.6	1.4	0.1	1.3	31	57.5	0.86
4	-0.1	2.1	4.6	0	0	0.4	4.7	57.5	11.18
5	-0.1	2.1	4.7	0	0	0.4	4.8	57.5	10.94
6	-0.1	2.2	4.7	0	0	0.4	4.8	57.5	10.91
7	-0.1	2.2	4.7	0	0	0.4	4.8	57.5	10.93
8	-0.1	2.5	2.5	-0.1	0.3	0.3	2.9	57.5	18.65
9	-0.7	4.6	1.6	-0.3	0.2	0.1	5.3	57.5	9.84
10	-3.9	3.2	0.7	-0.3	0.2	0.1	7.1	57.5	7.13
11	0.6	-3	-0.4	0.1	0	-0.2	3.6	57.5	15.05
12	-3.8	-2.4	-0.8	-1.4	0	-0.1	3.9	57.5	13.78
13	-2.3	-0.1	-0.2	-0.1	0	0	2.3	46.0†	19.00
14	25.4	-1.3	25.4	-0.1	0.1	-0.1	26.8	57.5	1.14
15	-1.8	0	-1.8	0	0	0	1.8	57.5	31.26
16	1	0	1	0	0	0	1	57.5	55.29

†Allowable Stress includes reduction factor for weld (0.8 x Allowable Stress).

2.7.4 Crush

According to the IAEA Safety Series No. 6 Paragraph 627(c), and 10 CFR 71.73(c)(2), this test is not applicable to the Universal Transport Cask because the mass of the cask and contents is greater than 1,100 lb (500 kg) and the cask and contents have an overall density greater than 62.4 lb/ft^3 (1,000 kg/m^3).

2.7.5 Immersion - Fissile Material

According to the requirements of 10 CFR 71.73(c)(5), a package containing fissile material, where water inleakage has not been assumed for criticality analysis, must be subjected to water pressure equivalent to immersion under a head of water of at least 0.9 meters (3 feet) for 8 hours. This immersion is the fourth test in the hypothetical accident sequence of tests for the package. Paragraph No. 633 of IAEA Safety Series No. 6 specifies the same requirements for the international shipment of radioactive materials. A head of water of 0.9 m (3 ft) is equivalent to an external pressure of (3)(0.433) = 1.3 psig.

The analyses presented in Sections 2.7.6 evaluate the Universal Transport Cask for an external pressure of 290 psig. Since the containment boundary is predicted not to be structurally reduced following the hypothetical accident sequence, the external pressure analysis presented in Section 2.7.6 bounds this case.

2.7.6 Immersion - All Packages

According to the requirements of 10 CFR 71.73(c)(6), a package must be subjected to water pressure equivalent to immersion under a head of water of at least 15 meters (50 ft) for 8 hours. Paragraph 630 of IAEA Safety Series No. 6 requires that a package be immersed under a head of water of at least 200 meters (656 ft) for not less than one hour. A head of water of 200 meters (656 ft) is equivalent to an external pressure of (656)(0.433) = 284 psig. In addition, 10 CFR 71.61 requires that a package's undamaged containment system be capable of withstanding an external water pressure of 290 psi for not less than one hour without collapse, buckling, or inleakage of water.

The structural adequacy of the cask body when subjected to an external pressure of 290 psi is demonstrated using classical closed-form solutions of stresses for simplified geometries. Specifically, the formulas for the stresses in these calculations are obtained from Roark [28]. The stresses generated by the 290 psi external pressure are calculated at the following locations:

1) Cask Outer Shell (away from ends)
2) Cask Bottom Forging (at center)
3) Cask Lid (at center)
4) Cask Bottom Plate (at center)
5) Port Cover Plate (at center).

The locations of the stresses evaluated (in the numbered list above) are shown in Figure 2.7.6-1 with the exception of the port cover plate (Item 6).

The bending stresses at the center of the circular plates (Items 3 through 6 in the above list) are evaluated using the formulas in Roark [28], Table 24, Case 10 for simply-supported plates with uniform thickness under a uniformly distributed pressure. The formulas are as follows:

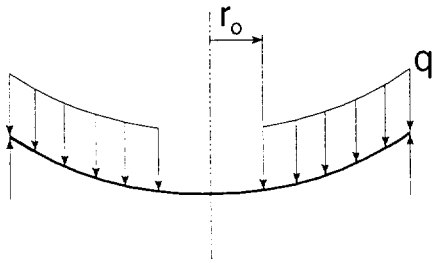

For $r_o = 0$, the bending moment at the center of the plate is

$$M_c = \frac{qa^2(3+\nu)}{16}$$

where M_c = bending moment (in-lb/in)
q = pressure load (lb/in²)
a = outer radius (in.)
ν = Poisson's ratio.

The bending stress at the center of the plate is then calculated as,

$$\sigma_b = \frac{6M_c}{t^2}$$

where σ_b = bending stress at center (lb/in²)
M_c = bending moment (in-lb/in)
t = thickness of the plate (in.).

The primary membrane stresses (Items 1 through 2) in a cylindrical shell with uniform external pressure consist of axial and hoop (circumferential) stresses. Theses stresses are evaluated using formulas in Roark [28], Table 28, Case 1c for cylindrical thin-walled shells with capped ends under external pressure loading. The formulas are as follows:

$$\sigma_1 = \frac{qR}{2t} \quad \text{and} \quad \sigma_2 = \frac{qR}{t}$$

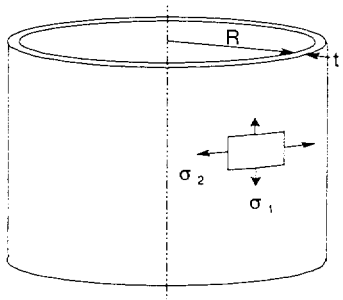

where σ_1 = axial stress (lb/in²)
σ_2 = hoop stress (lb/in²)
q = external pressure (lb/in²)
R = mean radius (in.)
t = thickness of the shell (in.).

From these equations the stresses in the cask body at the locations described above are calculated in the ensuing sections. In addition, a comparison to the allowable stress is made for each stress calculated. Because this is considered to be an accident condition, the calculated stresses are compared to stress allowables as follows (refer to Section 2.1.2):

P_m < the lesser of $2.4S_m$ and $0.7S_u$
$P_m + P_b$ < the lesser of $3.6S_m$ and S_u

The stress allowables for this evaluation are conservatively taken at 400°F since the maximum temperature of the cask is 368°F.

The cask inner shell and port coverplate are constructed of SA240, Type 304 stainless steel. The cask outer shell and bottom are constructed of A240, Type 304 stainless steel. At a temperature

of 400°F, SA240, Type 304 stainless steel has an ultimate strength, S_u, of 64.4 ksi and a design stress intensity, S_m, of 18.7 ksi. Therefore, the stress allowables are:

Primary Membrane:	44.88 ksi ($2.4S_m$)
Primary Membrane + Bending:	64.4 ksi (S_u).

The cask bottom forging, top forging, and lid are constructed of SA336, Type 304 stainless steel. At a temperature of 400°F, SA336, Type 304 stainless steel has an ultimate strength, S_u, of 60.0 ksi and a design stress intensity, S_m, of 18.7 ksi. Therefore, the stress allowables are:

Primary Membrane:	42.0 ksi ($0.7S_u$)
Primary Membrane + Bending:	60.0 ksi (S_u).

2.7.6.1 Membrane Stresses in Cask Outer Shell (away from ends)

The membrane stresses in the cask outer shell are calculated as follows:

$$\sigma_1 = \frac{(-290 \text{ psi})(39.93 \text{ in.})}{2(2.75 \text{ in.})} = -2{,}105 \text{ psi}$$

$$MS = \frac{44{,}880 \text{ psi}}{2{,}105 \text{ psi}} - 1 = +20.32$$

$$\sigma_2 = \frac{(-290 \text{ psi})(34.93 \text{ in.})}{2.75 \text{ in.}} = -4{,}211 \text{ psi}$$

$$MS = \frac{44{,}880 \text{ psi}}{4{,}211 \text{ psi}} - 1 = +9.65$$

2.7.6.2 Bending Stress in the Bottom Forging (at center)

At a temperature of 400°F, SA336, Type 304 stainless steel has a Poison's ratio, ν, = 0.31. The bending stress in the bottom forging at the center is calculated as follows:

$$M_c = \frac{(-290 lb/in^2)(34.805 in.)^2(3+0.31)}{16} = -72{,}676 in-lb/in$$

$$\sigma_b = \frac{6(-72{,}676 in-lb/in)}{(4.25 in.)^2} = -24{,}142 psi$$

$$MS = \frac{60{,}000 psi}{24{,}142 psi} - 1 = +1.48$$

2.7.6.3 Bending Stress in the Cask Lid (at center)

At a temperature of 400°F, SA336, Type 304 stainless steel has a Poisson's ratio, ν, = 0.31. The bending stress in the cask lid at the center is calculated as follows (note the outer radius is taken to be half of the bolt circle):

$$M_c = \frac{(-290 lb/in^2)(36.93 in.)^2(3+0.31)}{16} = -81{,}821 in-lb/in$$

$$\sigma_b = \frac{6(-81{,}821 in-lb/in)}{(6.50 in.)^2} = -11{,}620 psi$$

$$MS = \frac{60{,}000 psi}{11{,}620 psi} - 1 = +4.16$$

2.7.6.4 Bending Stress in the Cask Bottom (at center)

At a temperature of 400°F, A240, Type 304 stainless steel has a Poisson's ratio, ν, = 0.31. The bending stress in the cask lid at the center is calculated as follows:

$$M_c = \frac{(-290 lb/in^2)(41.305 in.)^2(3+0.31)}{16} = -102{,}356 in-lb/in$$

$$\sigma_b = \frac{6(-102{,}356\,\text{in}-\text{lb}/\text{in})}{(5.00\,\text{in.})^2} = -24{,}565\ \text{psi}$$

$$MS = \frac{64{,}400\ \text{psi}}{24{,}565\ \text{psi}} - 1 = +1.62$$

2.7.6.5 Bending Stress in the Port Cover Plate (at center)

At a temperature of 400°F, SA240, Type 304 stainless steel has a Poisson's ratio, $\nu = 0.31$. The bending stress in the cask lid at the center is calculated as follows (note that the outer radius is taken to be half of the bolt circle):

$$M_c = \frac{(-290\,\text{lb}/\text{in}^2)(2.0625\,\text{in.})^2(3+0.31)}{16} = -255\,\text{in}-\text{lb}/\text{in}$$

$$\sigma_b = \frac{6(-255\,\text{in}-\text{lb}/\text{in})}{(1.25\,\text{in.})^2} = -979\ \text{psi}$$

$$MS = \frac{64{,}400\ \text{psi}}{979\ \text{psi}} - 1 = +64.78$$

The minimum margin of safety calculated in this evaluation is +1.48 (for the bottom forging). Because the cask body maintains positive margins of safety when exposed to the 290 psi external pressure, structural adequacy is demonstrated.

Therefore, the Universal Transport Cask satisfies all of the immersion requirements for a package that is used for the domestic and international shipment of radioactive materials.

Figure 2.7.6-1 Cross-Section of Cask Body

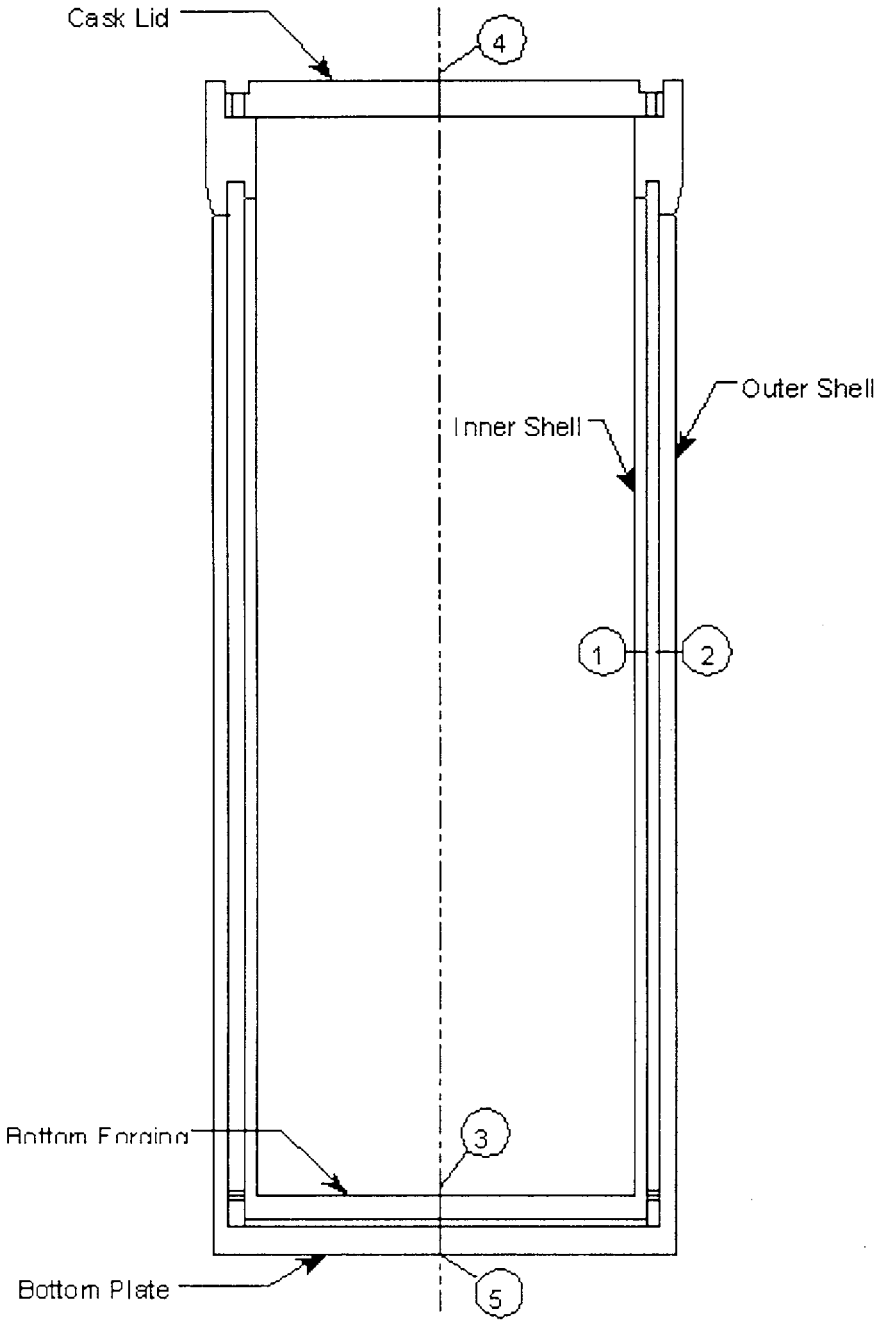

2.7.7 PWR Transportable Storage Canister Analysis – Accident Conditions

This section presents the evaluation of the PWR Transportable Storage Canister for the hypothetical accident conditions. The evaluation of the canister for normal conditions of transport is presented in Section 2.6.12.

The principal components of the canister are the canister shell, including the bottom plate, fuel basket, shield lid, and structural lid. The geometry and materials of construction of the canister, baskets, and spacers are described in Section 1.2.1.2. The general arrangement of the canister, shown with the fuel basket, is shown in Figure 2.6.12-1. The individual components of the canister are shown in Figure 2.6.12-2.

A drop accident stress evaluation is performed for the 30-ft side-drop, top and bottom-end drops, and for the top and bottom-corner drop conditions by applying a 60 g deceleration load. The loads developed in the basket are transferred through the canister wall into the inner shell (for the side-drop and oblique drops), and any axial component is transferred into the ends of the cask cavity. The axial loads are maximized for the end-drops and corner-drop conditions. The lateral loads are maximized in the side-drop since an enveloping acceleration is employed in the analysis. Regardless of the angle of the drop, the canister wall is uniformly supported along its length by the transport cask inner shell, and the load path is not affected by drop orientations close to the side-drop orientation. The oblique orientation will not provide enveloping loading above the side-drop conditions. Therefore, oblique orientations other than the corner drops are not considered.

In addition, the evaluations are performed with and without the 25 psig internal pressure. For the side, top-corner, and bottom-corner drop orientations, basket orientations of 0° and 45° are evaluated. The angles describe the orientation of the basket elements with respect to the symmetry plane of the model. A value of 0° orients the ligaments in the basket elements parallel and perpendicular to the symmetry plane. A value of 45° orients the basket ligaments at +/- 45° from the symmetry plane. In the evaluations, the maximum temperatures present during the normal condition evaluation with 100°F ambient; solar insolation, and maximum decay heat are considered.

2.7.7.1 Analysis Description

The Transportable Storage Canister is a right-circular shell fabricated from rolled 5/8-in. thick, Type 304L stainless steel plate. The canister is closed on its bottom end with a Type 304L stainless steel circular plate that is 1.75-in. thick. The canister is closed at the top end with a 7-in. thick, Type 304 stainless steel shield lid, which is seal welded to the canister shell. The shield lid is covered by a 3-in. thick, Type 304L, stainless steel structural lid welded to the canister shell at its top inside edge. The loaded canister is lifted by using six swivel hoist rings threaded into the top of the structural lid. The canister is the defined confinement boundary for spent fuel contents during long term storage, but no credit is taken for containment in transport. The Universal Transport Cask containment boundary is defined in Section 1.1.

The structural design criteria for the canister are contained in the ASME Code, Section III, Subsection NB, "Class 1 Components." Consistent with this criteria, the structural components of the canister (shell, bottom plate, and structural lid) are shown to satisfy the allowable stress intensity limits presented in Table 2.1.2-3.

For the canister structural lid weld (Section 13, Figure 2.6.12.3-1), base metal properties are used to define the allowable stress limits since the weld filler rod tensile properties are greater than the base metal. Also, the allowable stress is multiplied by a stress reduction factor of 0.8 per ISG-4.

The ANSYS finite element program is used to evaluate the canister for the 30-ft drop conditions in the top and bottom end, top and bottom corner, and side impact orientations. The ANSYS finite element model is the same as that used for the evaluation of the 1-ft drop impacts evaluated for normal conditions of transport. The model is described in Section 2.6.12.2.

2.7.7.2 Analysis Results - PWR Canister

The results of the analysis for the 30-ft side, top and bottom corner, and top and bottom end-drops are presented in Tables 2.7.7.2-1 through 2.7.7.2-10. Only the load cases that result in the worst case margins are presented for each of the drop orientations considered. For the side-drop, the worst configuration is witnout pressure and the basket oriented at 45°. For the bottom drop, the worst case occurs with the canister internal pressure. For the top-end drop, the most severe condition occurs without pressure. For the bottom corner and top-corner drops, the worst case stresses occur without pressure and the basket oriented at 0°.

The section stresses presented in the tables are identified by a section number. The minimum margin at each section is presented by denoting the circumferential angle where the minimum margin of safety occurs. A cross section of the canister showing the section numbers is presented in Figure 2.7.7.2-1. Stresses are evaluated at 9° increments around the circumference for each of the locations shown in Figure 2.7.7.2-1. The minimum margin is denoted by an angular location at each section. The canister minimum margins of safety for the evaluated drop conditions are summarized in Table 2.7.7.2-11.

The methodology used to evaluate the stresses for the side-drop are identical to that used for the normal conditions 1-ft side drop for the PWR canister (Section 2.6.12.6). Sections 9, 10, and 11 at the 0° circumferential position (see Figure 2.6.12.3-1) are not included in the evaluation. These regions are characterized as a bearing stress since they result from the canister shell bearing against cask inner shell. An evaluation of these bearing stresses is not required for accident conditions. Results for Sections 9, 10, and 11 at angular locations other than 0° are included in the evaluation.

The allowable stresses presented in the tables are for Type 304L stainless steel. Because the shield lid is constructed of Type 304 stainless steel, which possesses higher allowable stresses, a conservative evaluation results. These allowables are evaluated at 380°F, unless otherwise indicated. Review of the thermal analyses shows that the maximum temperature of the canister is 399°F (Section 3.4.2), which occurs in the center portion of the canister wall (Sections 5 and 6 described in Figure 2.7.7.2-1). The impact of this temperature increase is addressed by evaluating the margins presented at Sections 5 and 6 where the peak temperature occurs. The minimum margin for all the accident cases considered at Sections 5 or 6 is 4.41, which occurs for the 30-ft bottom-corner drop plus internal pressure. The allowable S_m for Type 304L stainless steel is reduced from 16.0 ksi to 15.8 ksi at 400°F. The margin of safety for this case would be reduced to 4.34. Therefore, the increased peak temperature in the center of the canister will have a negligible impact on the presented minimum margins of safety.

Figure 2.7.7.2-1 Identification of the Sections for Evaluating the Linearized Stresses in the PWR Canister

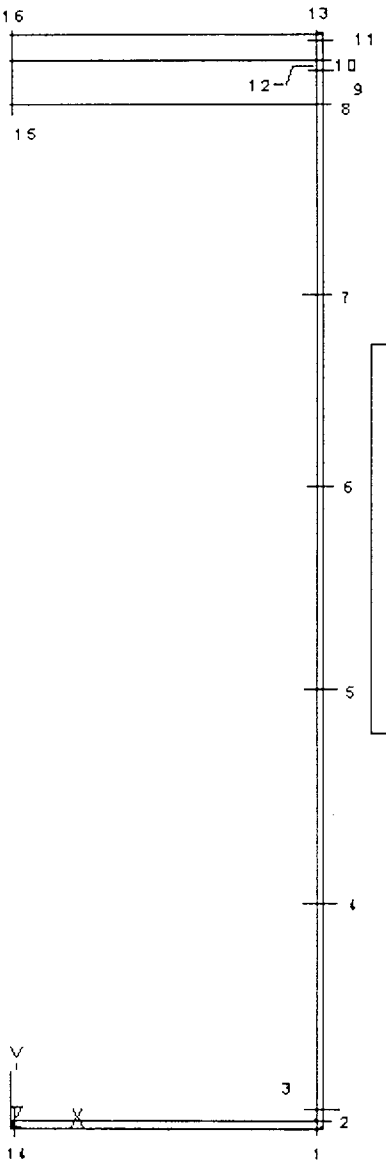

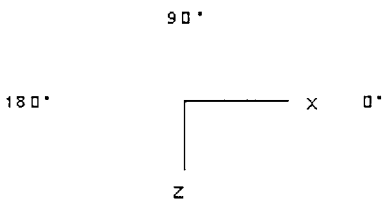

Top View of Axis

Section Coordinates at Z = 0

Axial Section	Node 1		Node 2	
	X	Y	X	Y
1	32.905	0.0	32.905	1.25
2	32.905	1.25	33.53	1.25
3	32.905	2.25	33.53	2.25
4	32.905	34.15	33.53	34.15
5	32.905	66.55	33.53	66.55
6	32.905	98.95	33.53	98.95
7	32.905	131.35	33.53	131.35
8	32.905	163.75	33.53	163.75
9	32.905	170.25	33.53	170.25
10	32.905	170.75	33.53	170.75
11	32.905	172.87	33.53	172.87
12	32.905	170.25	32.905	170.75
13	32.905	172.87	32.905	173.75
14	0.1	0.0	0.1	1.25
15	0.1	163.75	0.1	170.73
16	0.1	170.75	0.1	173.75

Table 2.7.7.2-1 PWR Canister P_m Stresses - 30-Foot Side-Drop - 45° Basket Orientation

Section Location	Angle of peak stress location	P_m Stresses (ksi) Sx	Sy	Sz	Sxy	Syz	Sxz	SI (ksi)	Allow. Stress (ksi)	Margin of Safety
1	0	-20.6	0.4	-12.6	-0.2	-0.3	-1.6	21.3	38.4	0.8
2	0	-15.4	0.4	-12.8	-1.2	-0.9	-0.7	16.3	38.4	1.36
3	0	-4.2	-0.1	-8.9	-0.4	-1.2	-0.9	9.3	38.4	3.11
4	108	-0.2	-2.2	0	2.1	-0.7	0.1	4.8	38.4	7.01
5	9	-2.1	2.1	0.3	0	0	0.4	4.2	38.4	8.03
6	9	-2.1	2.6	0.2	0	-0.1	0.4	4.7	38.4	7.1
7	9	-2.3	2.4	1	0	-0.3	0.5	4.9	38.4	6.9
8	72	0	-0.8	0	-4.5	-1.5	-0.1	9.5	38.4	3.03
9	9	-24.1	6.1	-10.0	-2.9	3.4	1.1	31.5	38.4	0.22
10	9	25	2.7	-13.5	-5.3	2.1	0.8	29.9	38.4	0.28
11	9	-17.7	1.0	-9.5	0.9	2.3	0	19.3	38.4	1.0
12	0	-39.7	-8.1	-17.6	-7.1	1.8	0.8	35	38.4	0.09
13	0	-30.9	-9.5	-12.8	0.2	1.4	-1.5	22	30.72*	0.40
14	0	-2.9	0	1	0	0	-0.1	3.8	38.4	8.98
15	0	-1	0	0.4	-0.1	0	0	1.3	38.4	27.49
16	0	-1.6	0	0.4	0	0	0	2	38.4	18.25

* Allowable stress includes a stress reduction factor for the weld: 0.8 x allowable stress.

Note: All of the allowable stress values presented in this table are based on SA240, Type 304L stainless steel at a temperature of 380°F unless otherwise stated. Localized peak temperatures in the central portion of the canister shell reach 408°F—resulting in slightly lower allowable stress values and subsequently slightly lower margins of safety for sections 5 and 6 than those presented in the table. However, this difference is negligible as discussed in Section 2.7.7.2.

Table 2.7.7.2-2 PWR Canister $P_m + P_b$ Stresses - 30-Foot Side-Drop - 45° Basket Orientation

Section Location	Angle of peak stress location	$P_m + P_b$ Stresses (ksi) Sx	Sy	Sz	Sxy	Syz	Sxz	SI (ksi)	Allow. Stress (ksi)	Margin of Safety
1	0	-23.9	-0.1	-14.1	0.8	0.1	-1.6	24.1	57.5	1.39
2	0	-17.1	1.1	-10.9	-1.7	-0.9	-1.3	18.8	57.5	2.06
3	45	-3.5	-17.8	-3.6	1.6	1.3	-4.2	18.9	57.5	2.05
4	9	-2.3	0.9	3.6	0.1	0.4	0.9	6.3	57.5	8.19
5	9	-2	2.8	2.4	0	0	0.7	4.9	57.5	10.71
6	9	-2	3.3	2.4	0	-0.1	0.7	5.4	57.5	9.62
7	9	-2.3	3	3	0	-0.3	0.8	5.8	57.5	8.88
8	72	0.1	-0.8	0	-5.5	-1.9	-0.1	11.7	57.5	3.91
9	9	-21.8	15.8	-7.9	-2.7	3.9	3.0	39.2	57.5	0.47
10	9	-26.9	0	-11.9	-7.4	1.6	0.5	30.9	57.5	0.86
11	9	-42.1	13	-15.3	0.2	2.4	1.6	55.3	57.5	0.04
12	0	-49	-11.5	-21.2	-7.1	2.5	1.1	40.6	57.5	0.42
13	0	-49.1	-19.1	-21.7	-0.3	2.1	-0.8	31.2	46.0*	0.47
14	0	-2.9	0	1	0	0	-0.1	3.8	57.5	13.95
15	0	-1.9	0	-0.6	-0.1	0	0	1.9	57.5	29.9
16	0	-1.2	0	0.9	0	0	0	2	57.5	27.23

* Allowable stress includes a stress reduction factor for the weld: 0.8 x allowable stress.

Note: All of the allowable stress values presented in this table are based on SA240, Type 304L stainless steel at a temperature of 380°F unless otherwise stated. Localized peak temperatures in the central portion of the canister shell reach 408°F—resulting in slightly lower allowable stress values and subsequently slightly lower margins of safety for sections 5 and 6 than those presented in the table. However, this difference is negligible as discussed in Section 2.7.7.2.

Table 2.7.7.2-3 PWR Canister P_m Stresses - 30-Foot Bottom End-Drop - Internal Pressure

Section Location	Angle of peak stress location	P_m Stresses (ksi) Sx	Sy	Sz	Sxy	Syz	Sxz	SI (ksi)	Allow. Stress (ksi)	Margin of Safety
1	180	0	-2.6	-0.4	0.2	0.1	0	2.6	38.4	13.85
2	180	0.7	-6.3	-1.1	0.3	0.1	0.1	7.1	38.4	4.43
3	180	0.1	-6.9	-1.2	0	0.1	0.1	7	38.4	4.49
4	180	0	-6.3	1.3	0	0	-0.1	7.7	38.4	4.01
5	180	0	-5.8	1.3	0	0	-0.1	7.1	38.4	4.41
6	180	0	-5.2	1.3	0	0	-0.1	6.5	38.4	4.88
7	180	0	-4.6	1.3	0	0	-0.1	6	38.4	5.44
8	81	0.7	-3.1	0.1	0	-0.1	0.1	3.8	38.4	9.03
9	72	-1.7	-1.9	-0.7	-0.1	0.4	-0.4	1.6	38.4	22.94
10	180	1.7	-1.3	-1	-0.3	0	0.2	3.1	38.4	11.5
11	0	-2	0.5	-0.9	0	0	0.1	2.5	38.4	14.17
12	0	0.7	1.8	-0.4	0.2	0.1	-0.1	2.2	38.4	16.18
13	180	0	-2	-1.2	0	0	0.1	2	30.72*	14.36
14	0	0.1	-1.1	0.1	0	0	0	1.2	38.4	30.57
15	171	0.2	-0.1	0.2	0	0	0	0.2	38.4	186.72
16	90	-0.2	0	-0.2	0	0	0	0.2	38.4	223.94

* Allowable stress includes a stress reduction factor for the weld: 0.8 x allowable stress.

Note: All of the allowable stress values presented in this table are based on SA240, Type 304L stainless steel at a temperature of 380°F unless otherwise stated. Localized peak temperatures in the central portion of the canister shell reach 408°F—resulting in slightly lower allowable stress values and subsequently slightly lower margins of safety for sections 5 and 6 than those presented in the table. However, this difference is negligible as discussed in Section 2.7.7.2.

Table 2.7.7.2-4 PWR Canister $P_m + P_b$ Stresses - 30-Foot Bottom End-Drop - Internal Pressure

Section Location	Angle of peak stress location	$P_m + P_b$ Stresses (ksi) Sx	Sy	Sz	Sxy	Syz	Sxz	SI (ksi)	Allow. Stress (ksi)	Margin of Safety
1	180	0.4	-2.9	-0.2	0.3	0.1	0	3.4	57.5	16.11
2	180	0.4	-9.5	-2.1	0.1	0.1	0.2	9.9	57.5	4.84
3	180	0.1	-8.9	-1.8	-0.1	0.1	0.1	9	57.5	5.39
4	180	0	-6.3	1.3	0	0	-0.1	7.7	57.5	6.49
5	0	0	-5.8	1.3	0	0	0.1	7.1	57.5	7.1
6	180	0	-5.2	1.3	0	0	-0.1	6.5	57.5	7.8
7	180	0	-4.6	1.3	0	0	-0.1	6	57.5	8.64
8	90	0.6	-3.4	0.3	0	-0.2	0	4.1	57.5	13.03
9	90	-2.4	-3.9	-0.4	0	0.7	0	3.7	57.5	14.53
10	90	-2.9	-6.6	0.6	0	0.2	0	7.3	57.5	6.91
11	0	-1.1	5.6	0.9	-0.4	0	0.1	6.8	57.5	7.52
12	0	2.6	3.6	0.7	0.7	0	-0.1	3.3	57.5	16.27
13	180	2.3	0.1	0.1	0.4	0.1	0.2	2.4	46.0*	18.17
14	0	0.1	-1.2	0.1	0	0	0	1.3	57.5	43.49
15	81	3.6	0	3.6	0	0	0	3.6	57.5	14.82
16	81	-1.8	0	-1.8	0	0	0	1.8	57.5	31.14

* Allowable stress includes a stress reduction factor for the weld: 0.8 x allowable stress.

Note: All of the allowable stress values presented in this table are based on SA240, Type 304L stainless steel at a temperature of 380°F unless otherwise stated. Localized peak temperatures in the central portion of the canister shell reach 408°F—resulting in slightly lower allowable stress values and subsequently slightly lower margins of safety for sections 5 and 6 than those presented in the table. However, this difference is negligible as discussed in Section 2.7.7.2.

Table 2.7.7.2-5 PWR Canister P_m Stresses - 30-Foot Top End-Drop

Section Location	Angle of peak stress location	P_m Stresses (ksi) Sx	Sy	Sz	Sxy	Syz	Sxz	SI (ksi)	Allow. Stress (ksi)	Margin of Safety
1	0	-0.4	-5.9	-2.2	0.8	0	-0.1	5.8	38.4	5.65
2	0	-3.8	3.7	5.5	0.9	-0.1	0.6	9.5	38.4	3.03
3	0	-0.8	0.1	7.6	-0.7	0.1	0.6	8.9	38.4	3.31
4	135	0	-2.2	0	0	0	0	2.2	38.4	16.27
5	153	0	-2.8	0	0	0	0	2.8	38.4	12.75
6	153	0	-3.4	0	0	0	0	3.4	38.4	10.43
7	180	0	-3.9	0	0	0	0	3.9	38.4	8.77
8	180	0.1	-3.7	0.1	-0.1	0	0	3.8	38.4	9.07
9	180	0.1	-2.8	-0.5	-0.1	0	0	2.8	38.4	12.49
10	144	-0.2	-2.7	-0.3	0	0	0.2	2.6	38.4	13.53
11	135	-0.2	-2.6	-0.2	0	0	0.2	2.6	38.4	13.74
12	36	-0.1	-2.1	-0.2	0.1	-0.1	-0.1	2.1	38.4	17.05
13	180	0	-2.2	-0.3	0	0	0	2.2	30.72*	12.96
14	90	-0.7	0	-0.7	0.2	-0.4	0	1.1	38.4	35.05
15	153	0	-1	0	0	0	0	1.1	38.4	35.42
16	0	0	-1.1	0	0	0	0	1.2	38.4	31.89

* Allowable stress includes a stress reduction factor for the weld: 0.8 x allowable stress.

Note: All of the allowable stress values presented in this table are based on SA240, Type 304L stainless steel at a temperature of 380°F unless otherwise stated. Localized peak temperatures in the central portion of the canister shell reach 408°F—resulting in slightly lower allowable stress values and subsequently slightly lower margins of safety for sections 5 and 6 than those presented in the table. However, this difference is negligible as discussed in Section 2.7.7.2.

Table 2.7.7.2-6 PWR Canister $P_m + P_b$ Stresses - 30-Foot Top End-Drop

Section Location	Angle of peak stress location	$P_m + P_b$ Stresses (ksi) Sx	Sy	Sz	Sxy	Syz	Sxz	SI (ksi)	Allow. Stress (ksi)	Margin of Safety
1	0	-4.3	-14.2	0.2	0.1	-0.1	0.2	14.4	57.5	2.99
2	0	-1.9	27.1	13	2	-0.1	1.1	29.4	57.5	0.96
3	0	-1.6	32.5	16.9	-0.1	0	1.4	34.2	57.5	0.68
4	162	0	-2.3	0	0	0	0	2.3	57.5	24.44
5	153	0	-2.8	0	0	0	0	2.8	57.5	19.63
6	171	0	-3.4	0	0	0	0	3.4	57.5	16.14
7	180	0	-3.9	0	0	0	0	3.9	57.5	13.64
8	180	0.3	-3.6	0.1	-0.2	0	0	3.9	57.5	13.71
9	135	-0.3	-3.2	-0.3	0	0	0.3	3.2	57.5	17.13
10	180	0	-3.1	-0.6	0	0	0	3.1	57.5	17.78
11	135	-0.3	-3	-0.3	0	0	0.2	2.9	57.5	18.74
12	180	0.1	-2	-0.2	-0.2	0	0	2.2	57.5	25.09
13	180	-0.1	-2.3	-0.4	-0.1	0	0	2.2	46.0*	19.91
14	90	-20.4	-0.3	-20.4	0.2	-0.4	0	20.2	57.5	1.85
15	81	0.3	-1	0.3	0	0	0	1.3	57.5	44.4
16	0	0.1	-1.1	0.1	0	0	0	1.2	57.5	47.14

* Allowable stress includes a stress reduction factor for the weld: 0.8 x allowable stress.

Note: All of the allowable stress values presented in this table are based on SA240, Type 304L stainless steel at a temperature of 380°F unless otherwise stated. Localized peak temperatures in the central portion of the canister shell reach 408°F—resulting in slightly lower allowable stress values and subsequently slightly lower margins of safety for sections 5 and 6 than those presented in the table. However, this difference is negligible as discussed in Section 2.7.7.2.

Table 2.7.7.2-7 PWR Canister P_m Stresses - 30-Foot Bottom Corner-Drop

Section Location	Angle of peak stress location	P_m Stresses (ksi) Sx	Sy	Sz	Sxy	Syz	Sxz	SI (ksi)	Allow. Stress (ksi)	Margin of Safety
1	0	-15	-3.3	-6.1	-0.5	-0.1	-1.9	12.1	38.4	2.16
2	18	2.2	-8.7	-1.1	0.3	-0.8	-1.9	11.9	38.4	2.23
3	27	-0.2	-9.3	-2.7	0.6	-0.1	-1.1	9.6	38.4	2.99
4	0	-0.4	-6.9	0.3	0	0.1	0.4	7.4	38.4	4.19
5	180	0	-6.8	-0.2	0	0	0	6.8	38.4	4.68
6	180	0	-6.5	-0.2	0	0	0	6.5	38.4	4.92
7	180	0	-5.8	-0.2	0	0	0	5.8	38.4	5.62
8	54	0.1	-3.5	0.1	-0.8	-0.7	0	4.1	38.4	8.26
9	0	-30.6	1	-10.7	-3	1.9	-0.1	32.5	38.4	0.18
10	0	-14	-0.7	-6.2	-2.7	1.4	-0.9	14.8	38.4	1.59
11	0	-36.8	-1.4	-12.2	-0.4	2	-0.3	35.8	38.4	0.07
12	0	-23.2	-5.3	-7.5	-3.8	1.3	-1.2	20.1	38.4	0.9
13	0	-23.6	-7.4	-7.7	0.3	1.4	-2.1	17.8	30.72*	0.73
14	0	-1.1	-1	0.4	0	0	0	1.5	38.4	24.48
15	0	-0.2	0	0.3	0	0	0	0.5	38.4	81.71
16	0	-0.9	0	0	0	0	0	0.9	38.4	43.06

* Allowable stress includes a stress reduction factor for the weld: 0.8 x allowable stress.

Note: All of the allowable stress values presented in this table are based on SA240, Type 304L stainless steel at a temperature of 380°F unless otherwise stated. Localized peak temperatures in the central portion of the canister shell reach 408°F—resulting in slightly lower allowable stress values and subsequently slightly lower margins of safety for sections 5 and 6 than those presented in the table. However, this difference is negligible as discussed in Section 2.7.7.2.

Table 2.7.7.2-8 PWR Canister $P_m + P_b$ Stresses - 30-Foot Bottom Corner-Drop

Section Location	Angle of peak stress location	$P_m + P_b$ Stresses (ksi) Sx	Sy	Sz	Sxy	Syz	Sxz	SI (ksi)	Allow. Stress (ksi)	Margin of Safety
1	0	-16.3	-2	-6.2	0.8	0.1	-2	14.8	57.5	2.89
2	18	0.4	-18.8	-3.5	-0.1	-0.1	-2	20	57.5	1.87
3	27	-0.8	-18	-4.6	0.1	-1.1	-2.1	18.2	57.5	2.15
4	0	-0.4	-6.1	2.8	0	0.1	0.7	9	57.5	5.37
5	0	-0.4	-4.8	2.6	0	0	0.6	7.5	57.5	6.64
6	0	-0.5	-3.9	2.6	0	0	0.5	6.6	57.5	7.76
7	0	-0.4	-3.2	2.6	0	0	0.6	5.9	57.5	8.81
8	18	0.4	-2.7	-1.3	1	1.8	-0.7	5	57.5	10.54
9	0	-30.5	7.2	-11.3	-2.5	1.8	0.4	38.2	57.5	0.51
10	0	-14.3	-0.9	-4.2	-4.2	1	-1.4	16.3	57.5	2.53
11	0	-32.9	8	-10.2	-0.2	2	0.5	41.2	57.5	0.4
12	0	-30.2	-7.8	-10.2	-3.7	1.7	-0.8	24.5	57.5	1.35
13	0	-38	-15	-14.3	-0.1	1.9	-1.5	25.5	46.0*	0.80
14	0	-1	-1	0.5	0	0	0	1.5	57.5	37.12
15	81	3.9	0	4.3	0	0	0	4.3	57.5	12.39
16	0	-2.7	0	-1.9	0	0	0	2.7	57.5	20.31

* Allowable stress includes a stress reduction factor for the weld: 0.8 x allowable stress.

Note: All of the allowable stress values presented in this table are based on SA240, Type 304L stainless steel at a temperature of 380°F unless otherwise stated. Localized peak temperatures in the central portion of the canister shell reach 408°F—resulting in slightly lower allowable stress values and subsequently slightly lower margins of safety for sections 5 and 6 than those presented in the table. However, this difference is negligible as discussed in Section 2.7.7.2.

Table 2.7.7.2-9 PWR Canister P_m Stresses - 30-Foot Top Corner-Drop

Section Location	Angle of peak stress location	P_m Stresses (ksi) Sx	Sy	Sz	Sxy	Syz	Sxz	SI (ksi)	Allow. Stress (ksi)	Margin of Safety
1	9	-2.1	-7	-4.8	0.7	-1.1	-1	5.9	38.4	5.53
2	0	-38	-1.4	-10.4	-5.2	0.7	-0.2	38.1	38.4	0.01
3	0	-12.1	-2.5	-2.6	-5.3	0.5	-0.3	14.5	38.4	1.65
4	180	0	-2.7	-0.2	0	0	0	2.7	38.4	13.07
5	180	0	-3.5	-0.2	0	0	0	3.5	38.4	9.89
6	180	0	-3.9	-0.2	0	0	0	3.9	38.4	8.82
7	72	0.1	-3.5	0	-0.9	-0.3	0	4.1	38.4	8.39
8	45	0.1	-3.9	0.1	-1.1	-1.2	0.1	5.2	38.4	6.31
9	0	-31.3	-4.8	-10.8	-3.4	0.9	-0.1	27.5	38.4	0.39
10	0	-21.1	-9.8	-8.9	-4	0.2	-0.7	14.2	38.4	1.7
11	0	-30.8	-14.9	-12.3	-1.5	0.7	-0.7	18.9	38.4	1.03
12	0	-27.7	-13.5	-9.2	-5.6	0.4	-1.1	20.7	38.4	0.85
13	0	-26.9	-17.7	-9.7	-1.6	0.4	-1.9	17.9	30.72*	0.72
14	90	-1.4	0	-0.3	0.1	-0.3	0	1.7	38.4	21.81
15	0	-0.4	-1	0.1	0	0	0	1.1	38.4	33.99
16	0	-0.6	-1.1	0.2	0	0	0	1.3	38.4	29.2

* Allowable stress includes a stress reduction factor for the weld: 0.8 x allowable stress.

Note: All of the allowable stress values presented in this table are based on SA240, Type 304L stainless steel at a temperature of 380°F unless otherwise stated. Localized peak temperatures in the central portion of the canister shell reach 408°F—resulting in slightly lower allowable stress values and subsequently slightly lower margins of safety for sections 5 and 6 than those presented in the table. However, this difference is negligible as discussed in Section 2.7.7.2.

Table 2.7.7.2-10 PWR Canister $P_m + P_b$ Stresses - 30-Foot Top Corner-Drop

Section Location	Angle of peak stress location	$P_m + P_b$ Stresses (ksi) Sx	Sy	Sz	Sxy	Syz	Sxz	SI (ksi)	Allow. Stress (ksi)	Margin of Safety
1	0	-28.1	-15.6	-10.7	-7.5	-0.1	-1.1	21.2	57.5	1.71
2	0	-37.9	17.6	-5.7	-2.1	1.6	0.5	55.8	57.5	0.03
3	180	-1.4	29.4	15.6	0.1	0	-1.3	30.9	57.5	0.86
4	27	0.3	-1.7	-2.1	0	-0.1	-1.4	3.7	57.5	14.66
5	0	-0.4	-0.9	2.6	0	0	0.6	3.6	57.5	15.02
6	0	-0.4	-1.6	2.6	0	-0.1	0.6	4.3	57.5	12.39
7	0	-0.4	-2.5	2.8	0	-0.1	0.7	5.4	57.5	9.58
8	45	0.4	-3.8	0.4	-1.3	-1.6	0.2	6	57.5	8.53
9	0	-31.6	0.8	-11.8	-2.4	0.9	0.4	32.8	57.5	0.75
10	0	-23.1	-12.1	-8	-6.7	0	-1.3	18.7	57.5	2.08
11	0	-34	-18.9	-12.5	-2.5	0.9	-1.3	22.1	57.5	1.6
12	0	-30.1	-13	-9.8	-4.6	0.9	-0.8	21.9	57.5	1.63
13	0	-31.3	-21.6	-12.2	-2.7	0.7	-1.8	20.2	46.0*	1.28
14	72	-19.1	-0.3	-17.3	0.1	-0.3	0	18.8	57.5	2.06
15	72	-0.2	-0.9	0.4	0	0	0	1.3	57.5	43.02
16	0	-0.6	-1	0.3	0	0	0	1.3	57.5	43.39

* Allowable stress includes a stress reduction factor for the weld: 0.8 x allowable stress.

Note: All of the allowable stress values presented in this table are based on SA240, Type 304L stainless steel at a temperature of 380°F unless otherwise stated. Localized peak temperatures in the central portion of the canister shell reach 408°F—resulting in slightly lower allowable stress values and subsequently slightly lower margins of safety for sections 5 and 6 than those presented in the table. However, this difference is negligible as discussed in Section 2.7.7.2.

Table 2.7.7.2-11 Summary of Minimum Margins of Safety for PWR Canister - 30-Foot Drops

Drop Orientation	**Loading Condition**	**Stress Evaluated**	**Min. Margin of Safety**	**Section No.***
Side	30-ft impact (45 degree basket)	P_m	0.09	12
Side	30-ft impact (45 degree basket)	$P_m + P_b$	0.04	11
Bottom end	30-ft impact + pressure (25 psi)	P_m	4.01	4
Bottom end	30-ft impact + pressure (25 psi)	$P_m + P_b$	4.84	2
Top end	30-ft impact	P_m	3.03	2
Top end	30-ft impact	$P_m + P_b$	0.68	3
Bottom Corner	30-ft impact	P_m	0.07	11
Bottom Corner	30-ft impact	$P_m + P_b$	0.4	11
Top Corner	30-ft impact	P_m	0.01	2
Top Corner	30-ft impact	$P_m + P_b$	0.03	2

* See Figure 2.7.7.2-1 for section locations.

2.7.7.3 Canister Buckling Evaluation for 30-Foot End Drop

Code Case N-284-1 [12] of the ASME Boiler and Pressure Vessel Code is used to analyze the PWR canister for the accident condition 30-foot end drop (both top and bottom end drops). The evaluation requirements of Regulatory Guide 7.6, Paragraph C.5, are shown to be satisfied by the results of the buckling interaction equation calculations of Code Case N-284-1. The canister buckling design criteria are described Section 2.1.2.5.3.

The PWR canister for the 30-foot end drop is evaluated for buckling in the same manner as the PWR canister for the 1-foot end drop (see Section 2.6.12.12). The analytical process used for the PWR canister is the same as that described in a step-by-step example presented in Section 2.7.12.3 (for the cask inner shell).

A 60 g deceleration load was used for all the 30-ft drop canister analyses that are presented in Sections 2.7.7.2. The 60 g-load bounds all 30-ft deceleration loads for all other drop angles. The top- and bottom-end drops result in the largest potential for canister shell buckling and, therefore, are the two load cases presented here. The side drop load case is not considered a credible buckling mode of the canister shell and is, therefore, not presented here.

The stress results from the dynamic shell analyses (ANSYS) are screened for the maximum values of the longitudinal compression, circumferential compression, or in-plane shear stresses for the 30-ft drop cases (top- and bottom-end drops) with and without pressure. For each loading case, the largest of each of the three stress components anywhere regardless of location within the PWR canister shell are combined. Combining the maximum stress components in this way produces a conservative, bounding-case buckling evaluation of the PWR canister, one which envelopes all 30-ft PWR canister drop cases including those presented in Tables 2.7.7.2-3 and 2.7.7.2-5.

The geometry parameters used in the PWR canister evaluation are the same as those presented in Table 2.6.12.12-1.

The maximum stress components used in the evaluation and the resulting buckling interaction equation ratios are provided in Table 2.7.7.3-1. The results show that all interaction equation ratios are less than 1.0. Therefore, the buckling criteria of Code Case N-284-1 are satisfied, thus demonstrating that buckling of the PWR canister does not occur.

Table 2.7.7.3-1 Buckling Evaluation Results for the PWR Canister for 30-Foot End Drop

Load Condition	Longitudinal (Axial) Stress* S_ϕ (psi)	Circumferential (Hoop) Stress* S_θ (psi)	In-plane Shear Stress $S_{\phi\theta}$ (psi)	Elastic Buckling Interaction Equations				Plastic Buckling Interaction Equations			
				Q1	Q2	Q3	Q4	Q5	Q6	Q7	Q8
1-Ft Top End Drop	3900	100	700	.012	.084	.015	.012	.084	.015	.084	.015
1-Ft Bottom End Drop	7400	1500	100	.142	.159	.219	.142	.159	.219	.159	.219

Component stresses include thermal stresses.

* Compressive stresses.

2.7.8 PWR Basket Analysis - Accident Conditions

The PWR fuel basket in the Transportable Storage Canister is designed to contain up to 24 PWR fuel assemblies. The basket structure has a right-circular cylinder configuration and consists of 24 square tubes supported by circular support disks and a circular top and bottom plate that are retained by eight axial tie rods. The number of support disks provided in the basket varies, depending upon the class (Class 1, 2, or 3) of PWR fuel the basket is designed to contain.

The support disks and top and bottom plates are separated and supported by split spacers at the tie rods. The configuration of the basket is shown in Figure 2.6.13-1. Design of the basket and its components is discussed in detail in Chapter 1.0.

The PWR fuel basket is evaluated for hypothetical accident loads in this section (evaluation of the basket for loads under normal conditions of transport is presented in Section 2.6.13). Both stress analyses and buckling evaluations are performed and documented in the subsequent sections. The structural analysis of the basket components is in accordance with the ASME Code, Section III, Division 1, Subsection NG [15]. In addition, the stainless steel/BORAL composite fuel tube is evaluated for a postulated impact load.

The fuel tubes are not structural components and are not considered in the basket evaluation. The tie rods and spacers locate and structurally assemble the circular support disks, heat transfer disks, and top and bottom plates to form an integral assembly. The spacers carry the weight of the support disks, heat transfer disks, and endplate and their own weight in the 30-ft end-drop accident loading condition. The end-drop loading condition of the spacers is a classical, closed-form analysis, and the spacers are evaluated independently of the finite element basket model. Two finite element models of a single disk are used to perform the support disk structural evaluation. Figure 2.6.13.2-1 shows the PWR support disk model for the side drop evaluation. For further details of the basket, refer to Section 2.6.13.

2.7.8.1 Stress Evaluation of Support Disk

To determine the structural adequacy of the support disks, 30-ft-drop accident impact loads are evaluated for the worst-case radial orientations of the basket (0°, 18.22°, 26.28°, and 45°). The cask orientations considered are side-drop, end-drop, and oblique drops (0°, 10°, 20°, 23°, 30°, 40°, 50°, 60°, 70°, 75°, 80°, and 88°).

A load equal to the weight of the fuel assembly and fuel tubes multiplied by a 60 *g* amplification factor is applied to the support disk structure to simulate the 30-ft side-drop accident condition. The 60 *g* amplification factor is the design value that envelopes the calculated deceleration values in Section 2.6.7.5 for a 30-ft side-drop accident condition. The fuel assembly loads are transmitted in direct compression through the tube wall to the web structure of each support disk. These loads are transmitted to the canister and to the inner shell of the cask by the support disks, top weldment, and bottom weldment. The support disk configuration is analyzed for four worst-case radial orientations—0°, 18.22°, 26.28°, and 45°—to bound the possible maximum stress cases. The 18.22° orientation is located at the thinnest radial section of the disk perimeter.

For the end-drop condition, the support disk is loaded by the inertia of its own weight multiplied by the 60 *g* end-drop amplification factor.

Two limiting boundary conditions (thermal Case A and B) are considered in the evaluation (See Section 2.6.13.3 for case definition). Note that temperatures in the model are used only to determine material allowables for stress evaluation. However, thermal stresses are considered in the buckling evaluation (Section 2.7.8.3).

The stress evaluation for the support disk is performed according to the ASME Code, Section III, Subsection NG. According to this subsection, linearized stresses of cross sections of the structure are to be compared against the allowable stresses. The allowable stresses for Normal and Accident conditions are taken from Subsection NG as shown below.

	Accident (Level D)
P_m	$0.7\ S_u$
P_m+P_b	$1.0\ S_u$

The allowable limit is $0.7\ S_u$ or $2.4\ S_m$, whichever is less. For the support disk, $2.4\ S_m > 0.7\ S_u$, therefore, $0.7\ S_u$ is limiting.

2.7.8.1.1 Finite Element Model Description

Finite element analyses are performed for the basket support disk for hypothetical accident conditions: the 30-ft side-drop impact condition (60 *g*) and 30-ft end-drop impact condition (60 *g*). The 30-ft oblique impact conditions are evaluated based on the stress results from the end impact and side impact analyses. Two finite element models are used for the basket side impact and end impact evaluations, respectively. These models are the same models used in the evaluation for normal transport conditions. The models are described in Section 2.6.13.2.

2.7.8.1.2 PWR Support Disk Impact Loading Conditions

The lateral impact load applied to the support disk for a side-drop accident includes the inertial weights of the canister, fuel assemblies, stainless steel tubes, and weight of the support disk itself. A detailed description of the loadings is provided in Section 2.6.13.2. The heat transfer disks are considered to be self-supporting. A 60 *g* load factor is used to amplify the weight of the basket components for the 30-ft side-drop condition.

2.7.8.1.3 PWR Support Disk Side-Drop Analysis Results

Finite element stress analyses for the 60 *g* side impact load cases are performed for four different radial basket orientations—0°, 18.22°, 26.28°, and 45°. The analyzed section locations are defined in Section 2.6.13.2 and in Figures 2.6.13.2-3 through 2.6.13.2-4.

The calculated stresses for the sections with the 40 lowest margins of safety are presented in Tables 2.7.8.1-2 through 2.7.8.1-17. The minimum margin of safety is +0.28 for primary membrane plus primary bending stress at Section 107 for Thermal Case B side-drop with the basket orientation equal to 18.22° (Table 2.7.8.1-9). The minimum margins of safety for all side-drop analysis results are summarized in Table 2.7.8.1-1.

2.7.8.1.4 PWR Support Disk End-Drop Analysis Results

Finite element stress analyses of the PWR basket support disk are performed for a 60 *g* end impact (30-ft end-drop) for Thermal Case A and B. The primary membrane stresses in the disk for the end drop conditions are essentially zero. The maximum primary membrane plus bending stresses in the support disk for the 30-ft end-drop accident condition are summarized in

Table 2.7.8.1-18. The calculated stresses for the sections with the 40 lowest margins of safety are presented in Tables 2.7.8.1-19 and 2.7.8.1-20.

2.7.8.1.5 PWR Support Disk Oblique Drop Analysis Results

To evaluate oblique impacts, the stress components (i.e., S_x, S_y, S_{xy}) are combined from the side and end drop cases. These stress combinations are accomplished using the same methodology as described in Section 2.6.13.8 for the normal conditions of transport evaluation. The evaluation considers various cask drop angles (φ = 0°, 23°, 30°, 45°, 60°, 70°, 75°, 80°, 85°, and 88°, and 90°), as well as the basket drop orientation (0°, 18.22°, 26.28°, and 45°). The end drop (φ = 0°) and the side drop (φ = 90°) conditions are included in the evaluation so that the results envelope all cask drop angles.

The maximum stresses in the support disk for the 30-ft oblique accident condition are summarized in Table 2.7.8.1-21.

Table 2.7.8.1-1 Summary of Stress Evaluation of Support Disk—30-Foot Side-Drop

Table Number	Basket Orientation (deg)	Thermal Case	Stress Evaluation	Minimum Margin of Safety
2.7.8.1-2	0	A	P_m	+0.86
2.7.8.1-3	0	A	$P_m + P_b$	+0.49
2.7.8.1-4	0	B	P_m	+0.87
2.7.8.1-5	0	B	$P_m + P_b$	+0.47
2.7.8.1-6	18.22	A	P_m	+1.24
2.7.8.1-7	18.22	A	$P_m + P_b$	+0.30
2.7.8.1-8	18.22	B	P_m	+1.27
2.7.8.1-9	18.22	B	$P_m + P_b$	+0.28
2.7.8.1-10	26.28	A	P_m	+1.37
2.7.8.1-11	26.28	A	$P_m + P_b$	+0.31
2.7.8.1-12	26.28	B	P_m	+1.43
2.7.8.1-13	26.28	B	$P_m + P_b$	+0.30
2.7.8.1-14	45	A	P_m	+1.76
2.7.8.1-15	45	A	$P_m + P_b$	+0.43
2.7.8.1-16	45	B	P_m	+1.76
2.7.8.1-17	45	B	$P_m + P_b$	+0.43

Table 2.7.8.1-2 Pm Stresses for Support Disk—30-Foot Side-Drop, 0° Orientation, Thermal Case A

Section	Sx (ksi)	Sy (ksi)	Sxy (ksi)	Stress Intensity (ksi)	Allowable Stress (ksi)	Margin of Safety
107	-35.5	-27.7	18.3	50.3	93.5	0.86
123	-35.5	-27.7	-18.3	50.3	93.5	0.86
25	20.7	-22.2	0.0	42.8	92.2	1.15
20	18.4	-17.4	0.0	35.7	90.4	1.53
29	0.0	-32.4	0.0	32.4	92.8	1.86
112	13.6	-15.7	0.6	29.4	91.7	2.12
96	13.6	-15.7	-0.6	29.4	91.7	2.12
27	-8.5	-29.1	0.0	29.1	92.2	2.17
28	8.9	-16.6	6.3	28.4	92.2	2.24
26	8.9	-16.6	-6.3	28.4	92.2	2.24
114	8.9	-19.4	1.6	28.4	93.0	2.27
98	8.9	-19.4	-1.6	28.4	93.0	2.27
115	8.7	-18.4	-1.5	27.3	93.0	2.41
99	8.7	-18.4	1.5	27.3	93.0	2.41
24	0.0	-26.7	0.0	26.7	91.3	2.41
21	8.1	-13.7	-5.2	24.1	90.4	2.75
23	8.1	-13.7	5.2	24.1	90.4	2.75
30	-21.3	-24.8	0.0	24.8	93.4	2.77
22	-7.2	-23.9	0.0	23.9	90.5	2.79
2	10.4	-12.5	0.0	22.9	88.1	2.84
95	6.8	-16.2	-2.7	23.6	91.7	2.89
111	6.8	-16.2	2.7	23.6	91.7	2.89
116	0.0	-22.6	0.0	22.7	91.1	3.02
100	0.0	-22.6	0.0	22.7	91.1	3.02
19	0.0	-21.1	0.0	21.1	89.1	3.23
121	0.1	-21.5	-0.2	21.5	92.5	3.29
105	0.1	-21.5	0.2	21.5	92.5	3.29
31	-18.1	-14.8	4.4	21.2	93.4	3.40
32	-18.1	-14.8	-4.4	21.2	93.4	3.40
113	-4.9	-19.8	-0.4	19.8	91.9	3.65
97	-4.9	-19.8	0.4	19.8	91.9	3.65
4	-10.9	-18.2	0.0	18.2	88.1	3.86
8	11.1	-7.1	0.0	18.2	90.5	3.96
37	-5.6	-17.6	-1.1	17.7	90.4	4.10
51	-5.6	-17.6	1.1	17.7	90.4	4.10
101	6.9	-9.9	2.0	17.2	91.9	4.33
117	6.9	-9.9	-2.0	17.2	91.9	4.33
49	4.2	-12.4	1.0	16.7	90.4	4.40
35	4.2	-12.4	-1.0	16.7	90.4	4.40
68	0.0	-15.7	0.0	15.7	91.1	4.82

Table 2.7.8.1-3 $P_m + P_b$ Stresses for Support Disk—30-Foot Side-Drop, 0° Orientation, Thermal Case A

Section	Sx (ksi)	Sy (ksi)	Sxy (ksi)	Stress Intensity (ksi)	Allowable Stress (ksi)	Margin of Safety
107	-57.7	-58.0	31.8	89.6	133.5	0.49
123	-57.7	-58.0	-31.8	89.6	133.5	0.49
25	20.7	-22.2	-1.6	43.0	131.6	2.06
26	28.6	-9.7	-4.1	39.2	131.6	2.36
28	28.6	-9.7	4.1	39.2	131.6	2.36
20	18.4	-17.4	-1.4	35.8	129.1	2.60
23	25.1	-7.6	3.3	33.4	129.1	2.87
21	25.1	-7.6	-3.3	33.4	129.1	2.87
30	-21.3	-24.8	10.2	33.4	133.4	3.00
29	0.0	-32.4	0.0	32.4	132.6	3.09
27	-8.5	-29.1	-7.3	31.4	131.8	3.20
112	9.2	-21.7	0.1	30.9	131.0	3.24
96	9.2	-21.7	-0.1	30.9	131.0	3.24
115	10.6	-20.6	-1.3	31.3	132.8	3.25
99	10.6	-20.6	1.3	31.3	132.8	3.25
31	-23.7	-21.7	8.0	30.8	133.4	3.33
32	-23.7	-21.7	-8.0	30.8	133.4	3.33
111	13.4	-16.5	0.8	29.9	131.0	3.38
95	13.4	-16.5	-0.8	29.9	131.0	3.38
98	5.2	-23.1	-3.7	29.2	132.8	3.55
114	5.2	-23.1	3.7	29.2	132.8	3.55
24	0.0	-26.7	0.0	26.7	130.4	3.88
22	-7.2	-23.9	-6.4	26.0	129.3	3.97
37	-9.2	-23.6	-5.2	25.3	129.1	4.10
51	-9.2	-23.6	5.2	25.3	129.1	4.10
110	25.1	1.8	0.1	25.1	132.3	4.28
94	25.1	1.8	-0.1	25.1	132.3	4.28
117	24.4	0.5	1.8	24.5	131.3	4.35
101	24.4	0.5	-1.8	24.5	131.3	4.35
14	-20.9	-10.6	7.1	24.6	131.6	4.36
12	-20.9	-10.6	-7.1	24.6	131.6	4.36
100	-0.2	-24.1	0.0	24.1	130.1	4.41
116	-0.2	-24.1	0.0	24.1	130.1	4.41
2	10.4	-12.5	-0.8	23.0	125.9	4.47
113	-9.9	-22.1	-4.6	23.6	131.3	4.56
97	-9.9	-22.1	4.6	23.6	131.3	4.56
9	-18.3	-13.3	6.9	23.1	129.1	4.59
7	-18.3	-13.3	-6.9	23.1	129.1	4.59
4	-10.9	-18.2	6.7	22.1	125.9	4.69
121	-0.3	-23.2	-0.4	23.2	132.1	4.69

Table 2.7.8.1-4 P_m Stresses for Support Disk—30-Foot Side-Drop, 0° Orientation, Thermal Case B

Section	Sx (ksi)	Sy (ksi)	Sxy (ksi)	Stress Intensity (ksi)	Allowable Stress (ksi)	Margin of Safety
107	-35.2	-28.2	18.6	50.6	94.5	0.87
123	-35.2	-28.2	-18.6	50.6	94.5	0.87
25	21.3	-22.6	0.0	43.9	94.5	1.15
20	18.9	-17.7	0.0	36.6	94.5	1.58
29	0.0	-33.0	0.0	33.0	94.5	1.86
27	-8.7	-29.7	0.0	29.7	94.5	2.19
28	9.2	-16.9	6.4	29.1	94.5	2.25
26	9.2	-16.9	-6.4	29.1	94.5	2.25
112	13.3	-15.6	0.5	28.9	94.5	2.27
96	13.3	-15.6	-0.5	28.9	94.5	2.27
114	9.2	-19.2	1.4	28.5	94.5	2.32
98	9.2	-19.2	-1.4	28.5	94.5	2.32
24	0.0	-27.3	0.0	27.3	94.5	2.46
115	8.7	-18.2	-1.5	27.1	94.5	2.49
99	8.7	-18.2	1.5	27.1	94.5	2.49
30	-21.4	-25.2	0.0	25.2	94.5	2.75
23	8.1	-14.0	5.4	24.5	94.5	2.85
21	8.1	-14.0	-5.4	24.5	94.5	2.85
22	-7.8	-24.4	0.0	24.4	94.5	2.87
2	11.2	-12.7	0.0	23.9	94.5	2.95
95	6.8	-16.0	-2.5	23.4	94.5	3.04
111	6.8	-16.0	2.5	23.4	94.5	3.04
116	0.0	-22.4	0.0	22.4	94.5	3.22
100	0.0	-22.4	0.0	22.4	94.5	3.22
19	0.0	-21.5	0.0	21.5	94.5	3.39
31	-18.2	-15.0	4.5	21.4	94.5	3.42
32	-18.2	-15.0	-4.5	21.4	94.5	3.42
121	0.1	-21.2	-0.2	21.3	94.5	3.43
105	0.1	-21.2	0.2	21.3	94.5	3.43
113	-4.7	-19.5	-0.4	19.6	94.5	3.83
97	-4.7	-19.5	0.4	19.6	94.5	3.83
8	11.6	-7.3	0.0	18.8	94.5	4.02
4	-11.7	-18.6	0.0	18.6	94.5	4.09
37	-5.2	-17.4	-1.1	17.5	94.5	4.40
51	-5.2	-17.4	1.1	17.5	94.5	4.40
101	6.9	-9.8	2.0	17.1	94.5	4.51
117	6.9	-9.8	-2.0	17.1	94.5	4.51
49	3.8	-12.4	1.1	16.3	94.5	4.79
35	3.8	-12.4	-1.1	16.3	94.5	4.79
11	-15.8	-9.1	0.0	15.8	94.5	4.98

Table 2.7.8.1-5 $P_m + P_b$ Stresses for Support Disk—30-Foot Side-Drop, 0° Orientation, Thermal Case B

Section	Sx (ksi)	Sy (ksi)	Sxy (ksi)	Stress Intensity (ksi)	Allowable Stress (ksi)	Margin of Safety
107	-58.4	-59.7	32.7	91.7	135.0	0.47
123	-58.4	-59.7	-32.7	91.7	135.0	0.47
25	21.3	-22.6	-1.7	44.0	135.0	2.07
26	29.5	-9.9	-4.2	40.3	135.0	2.35
28	29.5	-9.9	4.2	40.3	135.0	2.35
20	18.9	-17.7	-1.5	36.7	135.0	2.68
23	25.8	-7.7	3.4	34.2	135.0	2.95
21	25.8	-7.7	-3.4	34.2	135.0	2.95
30	-21.4	-25.2	10.4	33.8	135.0	2.99
29	0.0	-33.0	0.0	33.0	135.0	3.09
27	-8.7	-29.7	-7.4	32.0	135.0	3.22
31	-23.8	-22.1	8.2	31.1	135.0	3.34
32	-23.8	-22.1	-8.2	31.1	135.0	3.34
115	10.4	-20.5	-1.3	31.0	135.0	3.36
99	10.4	-20.5	1.3	31.0	135.0	3.36
96	8.7	-21.8	0.0	30.4	135.0	3.43
112	8.7	-21.8	0.0	30.4	135.0	3.43
98	6.0	-22.7	-3.4	29.5	135.0	3.57
114	6.0	-22.7	3.4	29.5	135.0	3.57
95	12.9	-16.6	-0.7	29.5	135.0	3.58
111	12.9	-16.6	0.7	29.5	135.0	3.58
24	0.0	-27.3	0.0	27.3	135.0	3.95
22	-7.8	-24.4	-6.5	26.7	135.0	4.06
110	25.4	1.8	0.1	25.4	135.0	4.31
94	25.4	1.8	-0.1	25.4	135.0	4.31
37	-9.0	-23.8	-5.2	25.4	135.0	4.31
51	-9.0	-23.8	5.2	25.4	135.0	4.31
14	-21.5	-10.8	7.3	25.2	135.0	4.36
12	-21.5	-10.8	-7.3	25.2	135.0	4.36
117	24.2	0.6	1.8	24.4	135.0	4.54
101	24.2	0.6	-1.8	24.4	135.0	4.54
2	11.2	-12.7	-1.0	24.0	135.0	4.62
100	-0.2	-23.9	0.0	23.9	135.0	4.64
116	-0.2	-23.9	0.0	23.9	135.0	4.64
9	-19.0	-13.7	7.1	23.9	135.0	4.65
7	-19.0	-13.7	-7.1	23.9	135.0	4.65
113	-9.8	-22.1	-4.6	23.6	135.0	4.73
97	-9.8	-22.1	4.6	23.6	135.0	4.73
121	-0.3	-23.0	-0.4	23.1	135.0	4.86
105	-0.3	-23.0	0.4	23.1	135.0	4.86

Table 2.7.8.1-6 P_m Stresses for Support Disk—30-Foot Side-Drop, 18.22° Orientation, Thermal Case A

Section	Sx (ksi)	Sy (ksi)	Sxy (ksi)	Stress Intensity (ksi)	Allowable Stress (ksi)	Margin of Safety
107	-15.5	-30.6	17.0	41.7	93.5	1.24
120	14.8	-19.3	10.4	39.9	93.0	1.33
112	15.1	-15.6	8.0	34.6	91.7	1.65
21	-3.9	-30.9	3.8	31.4	90.4	1.88
123	-27.2	-11.2	-10.4	32.3	93.5	1.89
35	16.2	-8.3	7.7	29.0	90.4	2.12
9	-2.5	-20.1	11.4	28.8	90.4	2.14
98	-5.7	-28.6	4.5	29.4	93.0	2.16
95	0.7	-26.3	4.1	28.2	91.7	2.25
29	-0.1	-28.2	0.5	28.2	92.8	2.29
37	-20.6	-18.3	7.4	26.9	90.4	2.36
25	8.2	-19.0	1.4	27.4	92.2	2.36
20	10.9	-14.6	3.1	26.3	90.4	2.44
27	-17.1	-25.2	-3.6	26.6	92.2	2.47
23	3.9	6.4	12.8	25.8	90.4	2.51
26	-8.4	-26.1	-0.4	26.1	92.2	2.53
51	11.7	-7.9	8.0	25.3	90.4	2.57
119	-0.1	-25.0	-0.6	25.0	92.6	2.70
22	-11.1	-20.4	-6.2	23.5	90.5	2.85
40	8.6	-12.3	5.8	23.9	92.2	2.86
24	-0.1	-23.0	0.8	23.0	91.3	2.97
114	-7.7	5.9	9.4	23.2	93.0	3.02
116	-0.1	-22.6	0.0	22.6	91.1	3.03
42	-14.7	-19.4	5.2	22.8	92.2	3.05
63	0.2	-14.5	8.1	21.8	91.7	3.20
30	-15.0	-21.3	2.1	21.9	93.4	3.26
28	-4.5	-5.0	10.6	21.2	92.2	3.34
64	-19.0	-10.2	4.8	21.1	91.7	3.35
115	3.1	-15.5	5.2	21.3	93.0	3.36
121	-0.7	-20.7	1.4	20.8	92.5	3.45
14	1.5	-2.7	10.1	20.6	92.2	3.47
49	-12.9	-9.2	8.5	19.7	90.4	3.58
72	-16.8	-12.7	5.1	20.2	93.0	3.60
31	-12.6	-18.0	4.2	20.3	93.4	3.60
2	7.6	-10.3	3.0	18.8	88.1	3.68
19	-0.1	-17.7	2.4	18.5	89.1	3.88
113	-9.0	-18.5	1.8	18.8	91.9	3.88
104	-11.3	-3.9	8.6	18.7	93.0	3.96
8	10.0	-5.4	-4.6	17.9	90.5	4.06
66	-2.0	-8.5	8.5	18.3	93.0	4.09

Table 2.7.8.1-7 $P_m + P_b$ Stresses for Support Disk—30-Foot Side-Drop, 18.22° Orientation, Thermal Case A

Section	Sx (ksi)	Sy (ksi)	Sxy (ksi)	Stress Intensity (ksi)	Allowable Stress (ksi)	Margin of Safety
107	-50.3	-76.3	36.9	102.4	133.5	0.30
4	-55.2	-67.0	9.1	71.9	125.9	0.75
23	64.8	40.7	15.9	72.7	129.1	0.78
37	-46.9	-61.0	15.6	71.1	129.1	0.82
3	-61.3	-59.5	8.4	68.8	125.9	0.83
9	-55.9	-50.3	16.8	70.1	129.1	0.84
20	-36.8	-65.4	2.7	65.6	129.1	0.97
49	-42.2	-55.1	12.9	63.1	129.1	1.05
96	-36.4	-56.4	11.4	61.6	131.0	1.13
21	-35.8	-54.6	12.2	60.6	129.1	1.13
2	-37.6	-57.0	2.4	57.3	125.9	1.20
6	-50.4	-53.1	6.5	58.4	129.1	1.21
112	-14.5	-58.6	5.2	59.2	131.0	1.21
95	-33.0	-54.0	10.8	58.5	131.0	1.24
34	-48.9	-54.2	5.3	57.5	129.1	1.25
120	4.5	-51.5	8.6	58.6	132.8	1.27
51	-17.0	-54.4	6.1	55.4	129.1	1.33
64	-42.5	-42.0	11.7	54.0	131.0	1.43
63	-42.2	-41.5	12.0	53.8	131.0	1.44
42	-29.9	-46.1	11.9	52.4	131.6	1.51
48	-43.9	-50.3	2.1	50.9	129.1	1.53
28	-46.5	-25.7	11.7	51.8	131.6	1.54
35	43.1	33.3	11.5	50.7	129.1	1.55
111	44.2	32.7	11.0	50.9	131.0	1.58
1	-38.8	-48.5	1.9	48.8	125.9	1.58
22	26.8	-16.0	-12.6	49.6	129.3	1.60
50	-11.0	-47.0	-3.1	47.3	129.3	1.73
115	-13.1	-46.7	0.1	46.7	132.8	1.84
25	-17.2	-46.1	1.9	46.3	131.6	1.85
104	-26.7	-36.2	13.0	45.3	132.8	1.93
14	41.3	16.9	10.0	44.9	131.6	1.93
8	43.7	0.3	-2.7	43.9	129.3	1.95
98	-25.2	-36.2	12.6	44.4	132.8	1.99
99	-22.2	-38.9	11.1	44.4	132.8	1.99
36	-4.7	-42.4	4.2	42.8	129.3	2.02
80	-17.4	-42.6	3.9	43.2	131.0	2.03
30	-20.7	-38.7	10.7	43.6	133.4	2.06
123	-33.9	-19.8	-14.4	42.9	133.5	2.11
72	-25.6	-33.1	12.3	42.2	132.8	2.15
39	-30.9	-39.1	4.4	41.0	131.6	2.21

Table 2.7.8.1-8 P_m Stresses for Support Disk—30-Foot Side-Drop, 18.22° Orientation, Thermal Case B

Section	Sx (ksi)	Sy (ksi)	Sxy (ksi)	Stress Intensity (ksi)	Allowable Stress (ksi)	Margin of Safety
120	15.5	-20.0	10.9	41.6	94.5	1.27
107	-13.9	-30.6	17.3	41.5	94.5	1.28
112	15.7	-16.1	8.5	36.1	94.5	1.62
21	-4.7	-32.8	4.5	33.5	94.5	1.82
123	-26.7	-10.5	-10.0	31.5	94.5	2.00
35	18.1	-8.4	8.0	31.0	94.5	2.05
9	-2.5	-21.3	12.0	30.5	94.5	2.10
98	-6.3	-28.6	5.0	29.7	94.5	2.19
95	0.6	-26.6	4.8	28.8	94.5	2.28
37	-21.7	-19.0	8.2	28.6	94.5	2.30
29	-0.1	-28.5	0.5	28.5	94.5	2.31
23	3.9	8.0	13.7	27.6	94.5	2.42
25	8.0	-19.3	1.3	27.4	94.5	2.45
51	14.1	-6.7	8.8	27.3	94.5	2.46
27	-17.7	-25.5	-3.8	27.0	94.5	2.50
26	-9.0	-26.6	0.0	26.6	94.5	2.55
20	10.9	-14.8	3.4	26.6	94.5	2.56
119	-0.1	-25.9	-0.6	25.9	94.5	2.64
40	9.1	-13.0	5.8	25.0	94.5	2.78
114	-8.3	6.7	9.9	24.7	94.5	2.82
22	-11.6	-20.7	-6.7	24.3	94.5	2.89
42	-14.5	-20.1	5.7	23.7	94.5	2.99
116	-0.1	-23.4	0.0	23.4	94.5	3.04
24	-0.1	-23.3	0.8	23.3	94.5	3.06
63	0.6	-15.1	8.5	23.1	94.5	3.09
28	-5.1	-5.0	11.1	22.2	94.5	3.26
30	-14.7	-21.5	2.3	22.2	94.5	3.26
115	3.1	-15.9	5.5	22.0	94.5	3.30
64	-19.6	-10.5	5.1	21.9	94.5	3.32
14	1.6	-2.9	10.5	21.4	94.5	3.41
121	-0.7	-21.3	1.5	21.4	94.5	3.42
49	-14.7	-8.9	8.9	21.2	94.5	3.46
72	-17.2	-13.5	5.2	20.8	94.5	3.54
31	-12.3	-18.6	4.3	20.8	94.5	3.55
104	-11.7	-3.6	9.0	19.7	94.5	3.80
2	8.3	-10.4	3.1	19.6	94.5	3.81
113	-9.6	-19.0	2.0	19.4	94.5	3.86
66	-2.0	-9.0	8.9	19.1	94.5	3.94
8	10.4	-5.4	-4.9	18.7	94.5	4.06
19	-0.1	-18.0	2.7	18.7	94.5	4.07

Table 2.7.8.1-9 $P_m + P_b$ Stresses for Support Disk—30-Foot Side-Drop, 18.22° Orientation, Thermal Case B

Section	Sx (ksi)	Sy (ksi)	Sxy (ksi)	Stress Intensity (ksi)	Allowable Stress (ksi)	Margin of Safety
107	-51.1	-78.9	38.2	105.6	135.0	0.28
4	-60.5	-73.7	9.7	78.8	135.0	0.71
23	69.3	45.0	17.2	78.2	135.0	0.73
37	-50.2	-65.8	16.9	76.6	135.0	0.76
3	-66.9	-65.4	9.0	75.1	135.0	0.80
9	-59.2	-53.4	17.7	74.3	135.0	0.82
20	-41.1	-70.2	3.0	70.5	135.0	0.92
49	-45.9	-57.3	13.8	66.6	135.0	1.03
21	-40.4	-59.0	13.5	66.1	135.0	1.04
96	-40.1	-58.5	12.3	64.7	135.0	1.09
112	-16.1	-62.3	5.5	62.9	135.0	1.15
95	-36.9	-56.5	11.7	61.9	135.0	1.18
6	-53.6	-56.4	6.7	61.9	135.0	1.18
34	-52.1	-58.4	5.7	61.8	135.0	1.19
2	-41.4	-61.2	2.3	61.5	135.0	1.20
120	4.4	-54.1	9.0	61.2	135.0	1.21
51	-16.8	-57.3	6.0	58.2	135.0	1.32
64	-44.4	-43.9	12.3	56.4	135.0	1.39
63	-44.0	-43.5	12.5	56.3	135.0	1.40
42	-30.7	-49.1	12.5	55.4	135.0	1.44
28	-49.5	-26.9	12.3	54.9	135.0	1.46
35	46.6	35.4	12.3	54.5	135.0	1.48
111	46.7	35.5	11.8	54.1	135.0	1.50
48	-48.1	-52.9	2.2	53.8	135.0	1.51
22	-52.9	-25.4	-0.1	52.9	135.0	1.55
1	-42.9	-52.4	1.7	52.7	135.0	1.56
50	-10.1	-49.6	-3.8	49.9	135.0	1.70
115	-13.9	-48.8	0.0	48.8	135.0	1.76
25	-19.3	-47.9	1.9	48.0	135.0	1.81
14	43.3	17.8	10.4	47.0	135.0	1.87
8	46.7	0.7	-3.0	46.9	135.0	1.88
98	-28.0	-37.1	13.4	46.7	135.0	1.89
104	-27.5	-37.1	13.4	46.6	135.0	1.90
99	-24.5	-39.5	11.6	45.9	135.0	1.94
30	-21.1	-40.7	11.0	45.6	135.0	1.96
36	-4.1	-44.5	-4.9	45.1	135.0	1.99
80	-17.5	-43.9	3.8	44.4	135.0	2.04
72	-26.3	-34.3	12.7	43.6	135.0	2.10
39	-31.3	-41.5	4.5	43.2	135.0	2.13
27	-40.4	-26.8	4.8	41.9	135.0	2.22

Table 2.7.8.1-10 P_m Stresses for Support Disk—30-Foot Side-Drop, 26.28° Orientation, Thermal Case A

Section	Sx (ksi)	Sy (ksi)	Sxy (ksi)	Stress Intensity (ksi)	Allowable Stress (ksi)	Margin of Safety
107	-12.2	-29.5	16.6	39.5	93.5	1.37
120	13.2	-17.2	10.8	37.3	93.0	1.49
21	-6.9	-31.5	4.1	32.1	90.4	1.81
112	12.3	-14.0	8.4	31.2	91.7	1.94
9	-3.7	-20.9	11.8	29.1	90.4	2.10
123	-25.4	-9.8	-9.5	29.9	93.5	2.13
98	-6.1	-27.3	5.1	28.5	93.0	2.26
35	14.4	-6.4	9.1	27.6	90.4	2.27
37	-23.2	-16.4	6.8	27.4	90.4	2.30
95	-1.4	-26.4	4.6	27.2	91.7	2.37
23	1.8	7.9	12.9	26.4	90.4	2.42
29	-0.2	-26.8	0.5	26.8	92.8	2.46
27	-17.5	-24.0	-3.8	25.8	92.2	2.58
26	-9.6	-25.7	0.0	25.7	92.2	2.59
25	7.4	-18.0	1.5	25.6	92.2	2.60
114	-9.0	7.0	9.5	24.8	93.0	2.75
51	12.1	-6.4	7.5	23.8	90.4	2.79
20	8.8	-13.8	3.4	23.7	90.4	2.82
22	-12.7	-19.4	-6.5	23.4	90.5	2.87
49	-15.5	-8.5	9.7	22.3	90.4	3.05
72	-19.4	-11.9	5.7	22.5	93.0	3.14
119	-0.1	-22.4	-0.6	22.4	92.6	3.14
64	-20.3	-8.4	5.1	22.2	91.7	3.14
24	-0.2	-21.8	0.8	21.8	91.3	3.18
40	4.3	-11.4	7.6	21.8	92.2	3.23
28	-5.1	-4.1	10.7	21.4	92.2	3.30
42	-15.8	-17.3	4.7	21.3	92.2	3.33
63	-1.2	-13.8	8.1	20.6	91.7	3.46
14	1.8	-2.0	10.1	20.6	92.2	3.48
30	-13.0	-20.0	2.5	20.8	93.4	3.50
116	-0.1	-20.2	0.0	20.2	91.1	3.52
31	-11.7	-18.0	4.0	20.0	93.4	3.68
111	-4.9	4.0	8.5	19.1	91.7	3.80
104	-11.2	-4.0	8.9	19.3	93.0	3.82
115	2.3	-13.8	5.3	19.3	93.0	3.83
121	-0.7	-18.6	1.4	18.7	92.5	3.94
66	-2.6	-9.3	8.7	18.6	93.0	4.01
2	5.7	-9.6	3.9	17.2	88.1	4.13
19	-0.2	-16.8	2.5	17.3	89.1	4.14
80	7.3	-6.2	5.6	17.5	91.7	4.25

Table 2.7.8.1-11 $P_m + P_b$ Stresses for Support Disk—30-Foot Side-Drop, 26.28° Orientation, Thermal Case A

Section	Sx (ksi)	Sy (ksi)	Sxy (ksi)	Stress Intensity (ksi)	Allowable Stress (ksi)	Margin of Safety
107	-48.4	-76.3	36.9	101.8	133.5	0.31
9	-59.7	-52.8	17.5	74.1	129.1	0.74
4	-58.1	-65.5	8.6	71.2	125.9	0.77
3	-65.6	-59.0	8.1	71.0	125.9	0.77
23	63.1	42.6	16.1	71.9	129.1	0.80
37	-49.8	-58.0	15.4	69.9	129.1	0.85
49	-47.1	-59.3	14.7	69.1	129.1	0.87
20	-40.0	-66.3	3.3	66.7	129.1	0.94
2	-42.7	-62.1	3.6	62.7	125.9	1.01
21	-39.9	-55.8	13.1	63.2	129.1	1.04
96	-39.7	-56.9	12.2	63.2	131.0	1.07
6	-53.9	-55.7	6.5	61.3	129.1	1.10
95	-37.0	-54.8	11.7	60.6	131.0	1.16
112	-18.3	-59.1	5.7	59.9	131.0	1.19
34	-53.7	-52.5	4.9	58.1	129.1	1.22
63	-45.6	-42.8	12.3	56.6	131.0	1.32
48	-49.1	-54.0	3.2	55.6	129.1	1.32
64	-45.6	-42.7	12.1	56.3	131.0	1.33
1	-44.5	-52.8	3.3	54.0	125.9	1.33
35	43.8	40.8	12.8	55.2	129.1	1.34
120	1.7	-50.9	8.7	55.4	132.8	1.40
51	-16.8	-51.8	5.2	52.6	129.1	1.46
28	-47.9	-25.3	11.6	52.8	131.6	1.49
111	-51.0	-27.8	5.8	52.3	131.0	1.50
22	-50.9	-23.2	0.0	50.9	129.3	1.54
42	-31.2	-43.0	11.1	49.7	131.6	1.65
36	-9.6	-45.6	-3.3	45.9	129.3	1.81
50	-11.5	-45.4	-4.1	45.8	129.3	1.82
40	-14.4	-44.8	7.5	46.6	131.6	1.83
8	45.3	1.2	-3.2	45.5	129.3	1.84
25	-19.3	-45.9	2.0	46.1	131.6	1.86
14	42.3	18.2	10.3	46.1	131.6	1.86
104	-26.9	-37.1	13.2	46.2	132.8	1.87
72	-28.9	-34.9	13.3	45.6	132.8	1.91
98	-27.7	-35.7	13.1	45.4	132.8	1.92
80	-17.8	-43.4	5.6	43.9	131.0	1.98
115	-13.7	-44.4	0.2	44.4	132.8	1.99
99	-24.2	-37.9	11.3	44.3	132.8	2.00
30	-19.7	-39.6	10.5	44.1	133.4	2.02
44	-39.1	-16.8	7.7	41.5	133.4	2.21

Table 2.7.8.1-12 P_m Stresses for Support Disk—30-Foot Side-Drop, 26.28° Orientation, Thermal Case B

Section	Sx (ksi)	Sy (ksi)	Sxy (ksi)	Stress Intensity (ksi)	Allowable Stress (ksi)	Margin of Safety
120	13.8	-17.8	11.4	38.9	94.5	1.43
107	-10.5	-28.7	16.7	38.6	94.5	1.45
21	-7.8	-33.5	4.7	34.3	94.5	1.75
112	12.7	-14.5	9.0	32.6	94.5	1.90
9	-3.5	-22.8	12.5	31.5	94.5	2.00
35	16.0	-6.5	9.7	29.7	94.5	2.18
37	-24.6	-17.1	7.6	29.3	94.5	2.22
123	-24.7	-9.1	-9.0	28.9	94.5	2.27
98	-6.9	-27.3	5.6	28.8	94.5	2.28
23	1.6	9.6	13.7	28.4	94.5	2.32
95	-1.6	-26.8	5.2	27.8	94.5	2.40
29	-0.2	-27.0	0.6	27.1	94.5	2.49
114	-9.6	7.8	9.9	26.4	94.5	2.58
27	-18.1	-24.2	-3.9	26.1	94.5	2.62
26	-10.2	-26.0	0.3	26.1	94.5	2.63
51	14.4	-5.3	8.3	25.7	94.5	2.68
25	7.1	-18.2	1.4	25.4	94.5	2.72
49	-17.6	-8.2	10.4	24.3	94.5	2.89
22	-13.2	-19.6	-7.1	24.2	94.5	2.90
20	8.7	-14.0	3.7	23.8	94.5	2.97
119	-0.1	-23.1	-0.6	23.1	94.5	3.08
72	-19.4	-12.5	6.1	23.0	94.5	3.11
40	4.5	-12.0	7.9	22.9	94.5	3.13
64	-20.6	-8.6	5.6	22.8	94.5	3.14
63	-0.5	-15.2	8.6	22.6	94.5	3.18
28	-5.8	-4.1	11.2	22.4	94.5	3.21
42	-15.9	-17.9	5.1	22.1	94.5	3.27
24	-0.2	-22.0	0.8	22.0	94.5	3.29
14	2.0	-2.1	10.5	21.3	94.5	3.43
116	-0.1	-21.0	0.0	21.0	94.5	3.51
30	-12.6	-20.1	2.7	20.9	94.5	3.51
111	-5.5	4.7	9.0	20.7	94.5	3.57
31	-11.4	-18.6	4.1	20.5	94.5	3.62
104	-11.6	-3.7	9.3	20.3	94.5	3.66
115	2.3	-14.2	5.6	19.9	94.5	3.75
66	-2.5	-9.7	9.0	19.4	94.5	3.88
121	-0.8	-19.2	1.4	19.3	94.5	3.89
80	8.8	-5.7	6.1	18.9	94.5	3.99
8	9.3	-5.0	-5.4	17.9	94.5	4.27
2	6.2	-9.7	4.1	17.9	94.5	4.28

Table 2.7.8.1-13 $P_m + P_b$ Stresses for Support Disk—30-Foot Side-Drop, 26.28° Orientation, Thermal Case B

Section	Sx (ksi)	Sy (ksi)	Sxy (ksi)	Stress Intensity (ksi)	Allowable Stress (ksi)	Margin of Safety
107	-49.0	-77.8	37.9	103.9	135.0	0.30
9	-63.4	-57.0	18.7	79.2	135.0	0.71
4	-63.9	-72.0	9.2	77.9	135.0	0.73
3	-72.0	-64.9	8.6	77.7	135.0	0.74
23	67.5	46.9	17.4	77.4	135.0	0.75
37	-53.8	-62.9	16.7	75.6	135.0	0.79
49	-51.5	-62.7	15.9	74.0	135.0	0.83
20	-44.5	-71.2	3.6	71.7	135.0	0.88
21	-44.6	-60.4	14.4	68.9	135.0	0.96
2	-47.6	-67.7	3.8	68.4	135.0	0.97
96	-43.5	-59.2	13.1	66.6	135.0	1.03
6	-57.4	-60.3	6.8	65.8	135.0	1.05
95	-40.9	-57.5	12.6	64.2	135.0	1.10
112	-20.1	-63.0	6.1	63.8	135.0	1.12
34	-57.8	-56.9	5.3	62.6	135.0	1.16
35	47.8	44.4	13.8	60.0	135.0	1.25
63	-47.5	-45.9	13.0	59.8	135.0	1.26
64	-47.8	-45.9	12.8	59.7	135.0	1.26
48	-54.0	-57.5	3.5	59.7	135.0	1.26
1	-49.7	-57.9	3.4	59.2	135.0	1.28
120	1.5	-53.5	9.1	58.0	135.0	1.33
51	45.7	44.1	11.4	56.3	135.0	1.40
111	-54.7	-29.3	6.1	56.1	135.0	1.41
28	-50.8	-26.5	12.2	55.9	135.0	1.42
22	-54.8	-23.6	-0.5	54.8	135.0	1.46
42	-32.5	-45.9	11.7	52.7	135.0	1.56
36	-9.8	-48.9	-3.9	49.3	135.0	1.74
40	-15.3	-47.3	7.9	49.1	135.0	1.75
8	48.7	1.0	-3.6	49.0	135.0	1.75
50	-11.1	-48.0	-4.8	48.6	135.0	1.77
14	44.2	19.0	10.7	48.1	135.0	1.81
72	-29.8	-37.2	14.0	48.0	135.0	1.82
104	-27.9	-38.3	13.7	47.8	135.0	1.83
98	-30.4	-36.6	13.9	47.7	135.0	1.83
25	-21.5	-47.5	2.0	47.6	135.0	1.83
115	-14.6	-46.5	0.2	46.5	135.0	1.90
80	-18.3	-45.9	3.7	46.3	135.0	1.91
30	-19.9	-41.7	10.8	46.1	135.0	1.93
99	-26.5	-38.5	11.9	45.8	135.0	1.95
79	34.7	36.0	8.4	43.8	135.0	2.08

Table 2.7.8.1-14 P_m Stresses for Support Disk—30-Foot Side-Drop, 45° Orientation, Thermal Case A

Section	Sx (ksi)	Sy (ksi)	Sxy (ksi)	Stress Intensity (ksi)	Allowable Stress (ksi)	Margin of Safety
107	-2.5	-21.4	14.1	33.8	93.5	1.76
37	-29.1	-12.0	4.8	30.3	90.4	1.98
21	-12.0	-29.1	4.8	30.3	90.4	1.98
9	-5.9	-22.3	12.3	29.5	90.4	2.06
49	-22.2	-5.9	12.3	29.5	90.4	2.06
76	-26.6	-10.4	7.2	29.4	93.5	2.18
114	-12.0	9.5	9.9	29.2	93.0	2.18
120	9.4	-12.0	9.9	29.2	93.0	2.19
35	9.3	-2.5	12.3	27.3	90.4	2.31
23	-2.5	9.3	12.3	27.3	90.4	2.31
72	-22.5	-7.6	7.0	25.3	93.0	2.68
98	-7.7	-22.4	6.9	25.2	93.0	2.69
64	-22.8	-5.0	5.8	24.5	91.7	2.75
95	-5.0	-22.8	5.7	24.5	91.7	2.75
111	-9.8	7.8	8.4	24.3	91.7	2.77
112	7.8	-9.7	8.4	24.3	91.7	2.77
42	-22.8	-12.2	1.6	23.0	92.2	3.00
26	-12.3	-22.8	1.6	23.0	92.2	3.01
41	-19.5	-17.5	-4.0	22.6	92.2	3.07
27	-17.5	-19.4	-4.0	22.6	92.2	3.08
40	-1.8	-6.9	10.9	22.4	92.2	3.12
28	-6.9	-1.8	10.9	22.3	92.2	3.13
36	-15.7	-14.6	-6.7	21.8	90.5	3.15
22	-14.5	-15.7	-6.6	21.8	90.5	3.16
123	-19.5	-5.2	-6.3	21.9	93.5	3.27
43	-21.7	-0.3	0.8	21.7	92.8	3.28
124	-5.8	-18.7	-7.1	21.8	93.5	3.29
29	-0.3	-21.6	0.8	21.6	92.8	3.29
54	-0.1	2.5	9.8	19.8	92.2	3.65
14	2.5	0.0	9.8	19.8	92.2	3.66
46	-18.8	-8.9	3.7	20.0	93.4	3.66
63	-3.7	-13.1	8.4	19.2	91.7	3.78
96	-13.1	-3.7	8.3	19.1	91.7	3.80
7	-1.7	13.3	5.6	18.7	90.4	3.83
51	13.2	-1.8	5.5	18.6	90.4	3.85
31	-8.8	-18.1	3.5	19.2	93.4	3.86
39	-14.4	4.3	1.5	18.9	92.2	3.87
25	4.2	-14.4	1.5	18.8	92.2	3.90
66	-4.0	-10.1	8.8	18.6	93.0	3.99
104	-10.1	-3.8	8.7	18.5	93.0	4.03

Table 2.7.8.1-15 $P_m + P_b$ Stresses for Support Disk—30-Foot Side-Drop, 45° Orientation, Thermal Case A

Section	Sx (ksi)	Sy (ksi)	Sxy (ksi)	Stress Intensity (ksi)	Allowable Stress (ksi)	Margin of Safety
107	-42.9	-69.4	34.5	93.1	133.5	0.43
49	-57.5	-66.6	18.7	81.3	129.1	0.59
9	-66.5	-57.5	18.7	81.2	129.1	0.59
2	-54.0	-73.3	6.8	75.4	125.9	0.67
3	-73.2	-53.9	6.7	75.3	125.9	0.67
1	-57.2	-62.3	7.0	67.1	125.9	0.88
4	-62.2	-57.1	6.9	67.0	125.9	0.88
35	43.8	57.6	15.3	67.5	129.1	0.91
23	57.4	43.7	15.3	67.3	129.1	0.92
48	-60.7	-60.2	6.1	66.6	129.1	0.94
6	-60.2	-60.8	6.1	66.6	129.1	0.94
37	-54.7	-47.1	14.0	65.4	129.1	0.97
21	-47.2	-54.7	14.0	65.4	129.1	0.97
34	-63.2	-45.4	3.8	64.0	129.1	1.02
20	-45.4	-63.1	3.8	63.9	129.1	1.02
63	-52.3	-45.9	13.1	62.6	131.0	1.09
96	-45.8	-52.3	13.1	62.5	131.0	1.10
64	-51.9	-44.8	12.8	61.7	131.0	1.13
95	-44.7	-51.8	12.8	61.6	131.0	1.13
76	-59.9	-53.9	4.6	62.4	133.5	1.14
111	-54.8	-22.9	5.9	55.9	131.0	1.35
40	-24.4	-51.9	11.5	56.1	131.6	1.35
112	-22.8	-54.7	5.9	55.8	131.0	1.35
28	-51.8	-24.4	11.5	56.0	131.6	1.35
36	-20.8	-52.9	-0.6	52.9	129.3	1.44
22	-52.9	-20.7	-0.6	52.9	129.3	1.45
50	3.3	48.2	-4.3	48.6	129.3	1.66
8	48.2	3.2	-4.4	48.6	129.3	1.66
7	37.3	40.7	9.1	48.2	129.1	1.68
51	40.5	37.1	9.1	48.1	129.1	1.69
72	-33.1	-35.3	14.4	48.6	132.8	1.73
98	-35.1	-33.1	14.4	48.6	132.8	1.73
14	43.3	21.0	10.7	47.6	131.6	1.76
54	20.9	43.3	10.7	47.6	131.6	1.76
79	37.2	38.6	9.2	47.1	131.0	1.78
80	38.6	37.2	9.2	47.1	131.0	1.78
44	-43.4	-16.5	10.1	46.7	133.4	1.85
30	-16.1	-43.2	10.1	46.6	133.4	1.86
39	-43.8	-26.6	2.2	44.1	131.6	1.99
25	-26.6	-43.8	2.2	44.0	131.6	1.99

Table 2.7.8.1-16 P_m Stresses for Support Disk—30-Foot Side-Drop, 45° Orientation, Thermal Case B

Section	Sx (ksi)	Sy (ksi)	Sxy (ksi)	Stress Intensity (ksi)	Allowable Stress (ksi)	Margin of Safety
107	-0.8	-20.4	14.0	34.2	94.5	1.76
37	-30.9	-12.7	5.4	32.4	94.5	1.91
21	-12.8	-30.9	5.5	32.4	94.5	1.92
9	-5.6	-24.6	13.1	32.3	94.5	1.92
49	-24.6	-5.6	13.1	32.3	94.5	1.93
114	-12.6	10.2	10.5	30.9	94.5	2.06
120	10.1	-12.6	10.4	30.8	94.5	2.07
35	10.8	-2.6	13.1	29.5	94.5	2.20
23	-2.6	10.8	13.1	29.4	94.5	2.21
76	-25.1	-9.3	6.7	27.6	94.5	2.43
111	-10.4	8.3	9.0	25.9	94.5	2.65
112	8.3	-10.3	8.9	25.9	94.5	2.65
72	-22.4	-8.3	7.5	25.7	94.5	2.68
98	-8.4	-22.4	7.5	25.6	94.5	2.69
64	-23.0	-5.2	6.4	25.1	94.5	2.77
95	-5.2	-23.0	6.4	25.1	94.5	2.77
42	-23.1	-12.9	2.0	23.5	94.5	3.03
26	-12.9	-23.1	2.0	23.4	94.5	3.03
40	-1.9	-7.6	11.4	23.4	94.5	3.03
28	-7.6	-1.8	11.4	23.4	94.5	3.03
41	-19.7	-18.1	-4.1	23.1	94.5	3.10
27	-18.1	-19.6	-4.1	23.0	94.5	3.10
36	-15.9	-15.0	-7.2	22.7	94.5	3.17
22	-15.0	-15.9	-7.2	22.6	94.5	3.18
43	-21.9	-0.3	0.9	21.9	94.5	3.31
29	-0.3	-21.8	0.9	21.9	94.5	3.32
63	-2.8	-14.8	8.9	21.5	94.5	3.40
96	-14.8	-2.8	8.9	21.4	94.5	3.41
123	-18.8	-4.5	-5.9	20.9	94.5	3.53
124	-5.0	-17.8	-6.8	20.7	94.5	3.56
46	-19.5	-8.5	3.8	20.7	94.5	3.57
54	-0.1	2.8	10.2	20.5	94.5	3.60
14	2.8	0.0	10.2	20.5	94.5	3.60
7	-0.5	15.7	6.2	20.4	94.5	3.63
51	15.6	-0.6	6.2	20.4	94.5	3.64
31	-8.5	-18.8	3.6	19.9	94.5	3.76
80	12.3	-2.6	6.5	19.7	94.5	3.80
79	-2.6	12.3	6.4	19.7	94.5	3.80
66	-3.9	-10.5	9.1	19.5	94.5	3.86
104	-10.5	-3.7	9.0	19.3	94.5	3.89

Table 2.7.8.1-17 $P_m + P_b$ Stresses for Support Disk—30-Foot Side-Drop, 45° Orientation, Thermal Case B

Section	Sx (ksi)	Sy (ksi)	Sxy (ksi)	Stress Intensity (ksi)	Allowable Stress (ksi)	Margin of Safety
107	-43.5	-70.4	35.1	94.6	135.0	0.43
49	-62.4	-70.6	20.1	87.0	135.0	0.55
9	-70.5	-62.4	20.1	87.0	135.0	0.55
2	-59.6	-80.2	7.1	82.4	135.0	0.64
3	-80.1	-59.5	7.1	82.3	135.0	0.64
1	-63.1	-68.3	7.4	73.5	135.0	0.84
4	-68.3	-63.0	7.3	73.4	135.0	0.84
35	48.0	61.9	16.6	72.9	135.0	0.85
23	61.8	47.9	16.5	72.8	135.0	0.86
6	-64.2	-66.1	6.5	71.8	135.0	0.88
48	-66.1	-64.2	6.5	71.7	135.0	0.88
37	-59.0	-51.8	15.3	71.1	135.0	0.90
21	-51.9	-59.0	15.3	71.1	135.0	0.90
34	-67.8	-49.8	4.1	68.7	135.0	0.96
20	-49.8	-67.7	4.1	68.6	135.0	0.97
63	-54.4	-49.6	14.0	66.2	135.0	1.04
96	-49.6	-54.4	13.9	66.1	135.0	1.04
64	-54.3	-48.7	13.7	65.5	135.0	1.06
95	-48.6	-54.2	13.7	65.4	135.0	1.06
76	-59.6	-55.7	3.6	61.8	135.0	1.18
111	-58.5	-24.5	6.2	59.6	135.0	1.26
112	-24.5	-58.4	6.2	59.5	135.0	1.27
40	-25.8	-54.9	12.1	59.3	135.0	1.28
28	-54.9	-25.7	12.1	59.3	135.0	1.28
36	-21.3	-56.8	-1.0	56.8	135.0	1.38
22	-56.8	-21.3	-1.0	56.8	135.0	1.38
7	42.3	45.4	10.6	54.6	135.0	1.47
51	45.3	42.2	10.6	54.4	135.0	1.48
50	2.7	52.0	-4.9	52.5	135.0	1.57
8	52.0	2.7	-4.9	52.5	135.0	1.57
80	42.4	41.1	10.3	52.1	135.0	1.59
79	41.1	42.4	10.3	52.1	135.0	1.59
72	-34.0	-38.1	15.2	51.3	135.0	1.63
98	-37.9	-34.0	15.2	51.3	135.0	1.63
14	45.3	21.9	11.1	49.8	135.0	1.71
54	21.8	45.3	11.1	49.7	135.0	1.72
44	-45.6	-16.6	10.4	49.0	135.0	1.76
30	-16.2	-45.5	10.4	48.8	135.0	1.76
120	-2.4	-45.3	7.8	46.7	135.0	1.89
114	-45.1	-2.7	7.8	46.5	135.0	1.90

Table 2.7.8.1-18 Summary of Stress Evaluation of Support Disk—30-Ft End-Drop

Table Number	*g*-Load	Thermal Case	Stress Evaluation	Minimum Margin of Safety
2.7.8.1-19	60	A	$P_m + P_b$	+4.63
2.7.8.1-20	60	B	$P_m + P_b$	+4.78

Table 2.7.8.1-19 P_m+P_b Stresses for Support Disk—30-Ft End-Drop, Thermal Case A

Section	Sx (ksi)	Sy (ksi)	Sxy (ksi)	Stress Intensity (ksi)	Allowable Stress (ksi)	Margin of Safety
40	6.1	-17.3	0.7	23.4	131.6	4.63
42	6.1	-17.3	-0.7	23.4	131.6	4.63
54	6.1	-17.3	-0.7	23.4	131.6	4.63
56	6.1	-17.3	0.7	23.4	131.6	4.63
12	-17.2	6.1	0.7	23.4	131.6	4.64
14	-17.2	6.1	-0.7	23.4	131.6	4.64
26	-17.2	6.1	-0.7	23.4	131.6	4.64
28	-17.2	6.1	0.7	23.4	131.6	4.64
39	7.9	-11.2	0.0	19.1	131.6	5.91
53	7.9	-11.2	0.0	19.1	131.6	5.91
11	-11.2	7.9	0.0	19.0	131.6	5.91
25	-11.2	7.9	0.0	19.0	131.6	5.91
67	5.1	15.4	6.8	18.7	132.8	6.09
83	5.1	15.4	-6.8	18.7	132.8	6.09
99	5.1	15.4	6.8	18.7	132.8	6.09
115	5.1	15.4	-6.8	18.7	132.8	6.09
74	15.1	4.7	6.9	18.6	132.8	6.15
106	15.1	4.7	6.9	18.6	132.8	6.15
90	15.1	4.7	-6.9	18.6	132.8	6.15
122	15.1	4.7	-6.9	18.6	132.8	6.15
55	6.7	-10.4	0.0	17.1	131.8	6.70
41	6.7	-10.4	0.0	17.1	131.8	6.70
27	-10.4	6.7	0.0	17.1	131.8	6.71
13	-10.4	6.7	0.0	17.1	131.8	6.71
82	10.2	9.6	-6.1	16.0	132.8	7.31
114	10.2	9.6	-6.1	16.0	132.8	7.31
98	10.2	9.6	6.1	16.0	132.8	7.31
66	10.2	9.6	6.1	16.0	132.8	7.31
72	9.6	10.2	6.0	15.9	132.8	7.34
104	9.6	10.2	6.0	15.9	132.8	7.34
120	9.6	10.2	-6.0	15.9	132.8	7.34
88	9.6	10.2	-6.0	15.9	132.8	7.34
5	0.0	-15.2	0.0	15.2	127.3	7.39
19	0.0	-15.2	0.0	15.2	127.3	7.39
33	-15.2	0.0	0.0	15.2	127.3	7.39
47	-15.2	0.0	0.0	15.2	127.3	7.39
2	-9.1	-14.6	0.0	14.6	125.9	7.61
4	-9.1	-14.6	0.0	14.6	125.9	7.61
3	-14.6	-9.1	0.0	14.6	125.9	7.61
1	-14.6	-9.1	0.0	14.6	125.9	7.61

Table 2.7.8.1-20 P_m+P_b Stresses for Support Disk—30-Foot End-Drop, Thermal Case B

Section	Sx (ksi)	Sy (ksi)	Sxy (ksi)	Stress Intensity (ksi)	Allowable Stress (ksi)	Margin of Safety
40	6.0	-17.3	0.7	23.4	135.0	4.78
42	6.0	-17.3	-0.7	23.4	135.0	4.78
54	6.0	-17.3	-0.7	23.4	135.0	4.78
56	6.0	-17.3	0.7	23.4	135.0	4.78
12	-17.3	6.0	0.7	23.3	135.0	4.79
14	-17.3	6.0	-0.7	23.3	135.0	4.79
26	-17.3	6.0	-0.7	23.3	135.0	4.79
28	-17.3	6.0	0.7	23.3	135.0	4.79
39	7.7	-11.2	0.0	18.9	135.0	6.13
53	7.7	-11.2	0.0	18.9	135.0	6.13
11	-11.2	7.7	0.0	18.9	135.0	6.14
25	-11.2	7.7	0.0	18.9	135.0	6.14
67	5.0	15.3	6.7	18.6	135.0	6.26
83	5.0	15.3	-6.7	18.6	135.0	6.26
99	5.0	15.3	6.7	18.6	135.0	6.26
115	5.0	15.3	-6.7	18.6	135.0	6.26
74	15.0	4.6	6.8	18.4	135.0	6.33
106	15.0	4.6	6.8	18.4	135.0	6.33
90	15.0	4.6	-6.8	18.4	135.0	6.33
122	15.0	4.6	-6.8	18.4	135.0	6.33
55	6.7	-10.4	0.0	17.1	135.0	6.91
41	6.7	-10.4	0.0	17.1	135.0	6.91
27	-10.4	6.6	0.0	17.0	135.0	6.93
13	-10.4	6.6	0.0	17.0	135.0	6.93
82	10.2	9.5	-6.0	15.9	135.0	7.51
114	10.2	9.5	-6.0	15.9	135.0	7.51
98	10.2	9.5	6.0	15.9	135.0	7.51
66	10.2	9.5	6.0	15.9	135.0	7.51
72	9.5	10.2	6.0	15.8	135.0	7.54
104	9.5	10.2	6.0	15.8	135.0	7.54
120	9.5	10.2	-6.0	15.8	135.0	7.54
88	9.5	10.2	-6.0	15.8	135.0	7.54
19	0.0	-15.6	0.0	15.6	135.0	7.64
33	-15.6	0.0	0.0	15.6	135.0	7.64
5	0.0	-15.6	0.0	15.6	135.0	7.64
47	-15.6	0.0	0.0	15.6	135.0	7.64
1	-15.0	-9.4	0.0	15.0	135.0	8.00
2	-9.4	-15.0	0.0	15.0	135.0	8.00
3	-15.0	-9.4	0.0	15.0	135.0	8.00
4	-9.4	-15.0	0.0	15.0	135.0	8.00

Table 2.7.8.1-21 Summary of Stress Evaluation of Support Disk—30-Ft Off-Angle Drop

Thermal Case	Section Number	Drop Angle	Basket Angle	P (kip)	P_{cr} (kip)	M (in-kip)	M_p (in-kip)	M_m (in-kip)	MS1	MS2
A	19	45.0	0.0	11.2	56.5	2.0	8.0	7.1	1.14	1.59
B	29	70.0	0.0	23.3	67.2	0.5	9.8	8.5	1.46	1.97

2.7.8.2 Stress Evaluation of Tie Rods and Spacers

The structural adequacy of the tie rods and spacers in the PWR basket is evaluated following a free drop of the Universal Transport Cask of 30 feet onto a flat, unyielding surface. The design deceleration for the cask for the hypothetical accident 30-ft end-drop is 60 *g*.

The structural capacity of the spacers supporting the basket is evaluated by hand calculations using classical analysis. In accordance with Section III, Subsection NG of the ASME Code [19], accident loading resulting from the 30-ft drop of the fuel basket is compared to the stress limit of 0.7 S_u.

The tie rods serve basket assembly purposes and are not part of the load path for the condition evaluated. The tie rods are loaded during fabrication by a 190 ft-lb preload. Under drop conditions, the preload is reduced. The tie rod design is, therefore, acceptable by inspection, and no detailed evaluation of the rods is required.

During the end drop, the spacers are loaded with the weight of support disks, the aluminum heat transfer disks, one end plate, and their own weight. The load is resisted by the effective area of eight spacers. The compressive stresses are calculated on the effective area of the spacer.

The material allowable stress is conservatively selected at a bounding temperature of 500°F. The temperature near the outer edge of the support disks is below 500°F.

2.7.8.2.1 Design Criteria

Stress limits	=	0.7 S_u (accident condition) (more limiting than 2.4 S_m)
Loading criteria (g)	=	60 *g* (accident condition)
Evaluation temperature	=	500°F

Basket Parameters

Fuel basket weight	=	16,489 lb
Bottom weldment weight	=	527 lb
Fuel tube weight (24 tubes)	=	3,676 lb
Rod diameter	=	1.625 in.
Spacer OD	=	3.0 in.

Materials [21]

Tie rod	=	SA 479 Type 304 Stainless Steel
Spacer	=	SA 479 Type 304 Stainless Steel

Material Allowables

Type 304 stainless steel [21]	=	S_m = 17,500 psi (500°F)
	=	S_u = 63,500 psi (500°F)

2.7.8.2.2 30-Foot End-Drop Condition - Results

The deceleration assumed for the PWR basket in the 30-ft end-drop is 60 *g*. The spacers are loaded with the weight of the support disks, the aluminum heat transfer disks, one end plate and their own weight. These loads are calculated as follows:

Total weight of basket	=	16,489 lb
Less weight of bottom weldment	=	-527 lb
Less weight of fuel tubes	=	-3,676 lb
1 g-load on spacers	=	12,286 lb
Applied g level	=	60 *g*

Therefore,

Accident condition

load on spacers = $12{,}186 \times 60 = 737{,}160$ lb

The effective area of one spacer at each of eight locations supporting the weight of the support disks is equal to the net area of the spacer and is calculated as

$$A = \frac{3.14 \times (3.0^2 - 1.75^2)}{4} = 4.66 \text{ in}^2.$$

The average compressive stress, S_c, in the spacer is

$$S_c = \frac{737{,}160}{8 \times 4.66} = 19{,}774 \text{ psi.}$$

The allowable stress for SA479, Type 304 SS under accident conditions is 0.7 S_u:

S_u = 63,500 psi

0.7 S_u = 0.7 × 63,500 = 44,450 psi.

The margin of safety, which is defined as $\frac{0.7S_u}{S_c} - 1$, is calculated as

$$MS = \frac{44{,}450}{19{,}774} - 1 = +1.24$$

Therefore, the spacers are structurally adequate for a 60 *g* end impact under accident conditions.

2.7.8.3 Buckling Evaluation of Support Disk

During the impact following a 30-ft side drop of the Universal Transport Cask onto an unyielding surface, the support disk is subjected to compressive loading and bending moments in the plane of the disk. For cask impact orientations other than on the side, loads acting perpendicular to the plane of the support disk (out-of-plane) may also be applied. The compressive in-plane loadings in conjunction with the bending moments resulting from in-plane or out-of-plane loadings require that buckling of the support disk be a design consideration.

Buckling of the support disk is evaluated in accordance with the methods and acceptance criteria of NUREG/CR-6322 [16]. The support disk is constructed of SA-693, Type 630, 17-4 PH stainless steel plate. The properties are evaluated at the actual temperature of the linearized cross sections where buckling evaluations are performed.

2.7.8.3.1 Support Disk Buckling Analysis

The buckling evaluation of the support disk web is based on the Interaction Equations 31 and 32 in NUREG/CR-6322. These two equations adopt the "Limit Analysis Design" approach for structural members subjected to stresses beyond the yield limit of the material, i.e., for members deformed elastically as a result of both axial load and bending moment. Other equations applicable to the calculations are listed later in this section.

The maximum forces and moments are determined for the end-drop condition and for four different radial orientations of the support disk for the side-drop condition based on the finite element analysis results. The forces and moments for the cask oblique drop conditions are determined from the end and side drop results based on the drop angle. The buckling evaluations account for both in-plane (about the strong axis of the web) and out-of-plane (about the weak axis of the web) buckling modes. Evaluation for strong axis buckling is performed only for the side drop condition since it is the governing case. Evaluation for weak axis buckling is performed for all end drops and oblique drops (0°, 23°, 30°, 40°, 45°, 50°, 60°, 70°, 75°, 80°, 85°, and 88°).

Detailed buckling calculations are performed using ANSYS macros. The methodology and equations used in the calculations are those from NUREG/CR-6322. The load amplification factors used are 60 *g* for 30-ft end-drop, 30-ft side-drop, and 30-ft oblique drop conditions. The buckling evaluation is performed for each of the sections identified Figures 2.6.13.2-3 and 2.6.13.2-4.

The buckling evaluation methodology/equations are summarized as:

Symbols and Units

P = applied axial compressive load, kips

M = moment, kips-in.

P_a = allowable axial compressive load, kips

P_{cr} = critical axial compression load, kips

P_e = Euler buckling loads, kips

P_y = plastic axial load, equal to profile area times specified minimum yield stress, kips (for normal operating condition)

C_c = column slenderness ratio separating elastic and inelastic buckling

C_m = coefficient applied to bending term in interaction equation

M_m= critical moment that can be resisted by a plastically designed member in the absence of axial load, kip-in.

M_p = plastic moment, kip-in.

F_a = axial compressive stress permitted, ksi

F_e = Euler stress for a prismatic member divided by factor of safety, ksi

k = ratio of effective column length to actual unbraced length

l = unbraced length of member, in.

r = radius of gyration, in.

S_y = yield stress allowable, ksi

A = area of the ligament, in^2

Z_x = plastic section modulus with respect to the major axis, in^3

Σ = allowable reduction factor, dimensionless

From NUREG/CR-6322, the following equations are used to evaluate the support disk:

$$\frac{P}{P_{cr}} + \frac{C_m M}{M_m\left[1 - \frac{P}{P_e}\right]} \leq 1.0$$

$$\frac{P}{P_y} + \frac{M}{1.18\, M_p} \leq 1.0$$

where:

$$P_{cr} = 1.7 \times A \times F_a$$

$$F_a = \frac{P_a}{A} \text{ for} P_a = P_y \left[\frac{1 - \frac{\lambda^2}{4}}{1.11 + 0.5\lambda + 0.17\lambda^2 - 0.28\lambda^3} \right] \text{ and } \lambda = \frac{1}{\pi}\left(\frac{kl}{r}\right)\sqrt{\frac{S_y}{E}}$$

$$P_e = 1.92 \times A \times F_e$$

$$F_e = \frac{\pi^2 \cdot E}{1.92\left(\frac{k \cdot l}{r}\right)^2} \text{ (non-austenitic)}$$

$$F_e = \frac{\pi^2 \cdot E}{1.3\left(\frac{k \cdot l^2}{r}\right)} \text{ (austenitic)}$$

$$P_y = S_y \times A$$

$C_m =$ 0.85 for members with joint translation (sideways).

$$M_p = S_y \times Z_x$$

$$M_m = M_p \cdot \left(1.07 - \frac{\left(\frac{l}{r}\right) \cdot \sqrt{S_y}}{3160} \right) \leq M_p$$

Load Conditions

A buckling evaluation is performed at all sections defined in Figures 2.6.13.2-3 and 2.6.13.2-4. Using the same method described in Section 2.6.13.14, the corresponding force (P) and the bending moment (M) are determined and applied to Equations 31 and 32 of NUREG/CR-6322.

Using the cross-sectional stresses calculated at each of the sections located in the web for each loading condition, the maximum corresponding compressive forces are combined with the maximum out-of-plane moment resulting from the 20 *g* and 60 *g* end-drop conditions to obtain the conservative maximum interaction coefficients. The equations used in the buckling analysis are:

$$P_1 = P/P_{cr} \qquad M_1 = \frac{C_m M}{\left(1 - P/P_e\right) M_m} \quad (P_1 + M_1 \le 1) \quad \text{(Eq. 31, NUREG/CR-6322)}$$

and

$$P_2 = P/P_y \; M_2 = \frac{M}{1.18\, M_p} \quad (P_1 + M_1 \le 1) \quad \text{(Eq. 32, NUREG/CR-6322)}$$

The margins of safety are calculated as:

$$MS1 = \frac{1}{P_1 + M_1} - 1 \qquad \text{(based on Eq. 31, NUREG/CR-6322)}$$

and

$$MS2 = \frac{1}{P_2 + M_2} - 1 \qquad \text{(based on Eq. 32, NUREG/CR-6322)}$$

The following table summarizes the minimum buckling margins of safety for each stress category and thermal case for the accident conditions.

Loading Condition	Stress State*	Thermal Case	Section Number	Drop Angle	Basket Angle	P (kip)	P_{cr} (kip)	M (in-kip)	M_p (in-kip)	M_m (in-kip)	MS1	MS2
Strong Axis Buckling												
Accident	P	A	2	90.00	45.00	5.6	81.8	12.3	23.6	23.6	0.94	0.88
	P+Q	A	2	90.00	45.00	9.2	81.8	11.0	23.6	23.6	0.95	0.85
	P	B	107	90.00	0.00	13.0	40.8	1.1	7.2	6.7	1.13	1.18
	P+Q	B	107	90.00	0.00	13.0	40.8	1.1	7.2	6.7	1.12	1.17
Weak Axis Buckling												
Accident	P	A	107	80.00	0.00	12.9	29.6	0.0	4.2	3.7	1.22	1.56
	P+Q	A	29	85.00	0.00	27.2	59.6	0.0	8.5	7.4	1.17	1.48
	P	B	107	80.00	0.00	12.8	33.2	0.0	4.9	4.2	1.51	1.96
	P+Q	B	107	80.00	0.00	12.8	33.2	0.0	4.9	4.2	1.51	1.96

* P = Primary Stress, P+Q = Primary + Secondary Stresses

As the results demonstrate, the PWR support disks meet the requirements of NUREG/CR-6322.

2.7.8.4 Fuel Tube Analysis

The fuel tube provides a foundation to mount BORAL poison plates within the fuel basket structure. The fuel tube does not serve a structural function relative to the support of the fuel assembly. The fuel tube design is presented in Figure 2.6.13-3. To ensure that the fuel tube remains functional when the cask is subjected to design load conditions, a structural evaluation of the tube is performed for both the end and side-impact load conditions.

2.7.8.4.1 Fuel Tube End Impact Analysis

During the postulated cask end impact, fuel assemblies are supported by the cask bottom for the bottom-end drop and the lid for the top-end drop. The fuel tubes do not carry fuel assembly load. Therefore, evaluation of the fuel tube for the end-impact load is performed by considering the weight of the fuel tube subjected to the cask deceleration carried by the minimum tube cross section. The minimum tube cross section is located at the contact point of the tube with the bottom weldment. From the dimensions of the tube shown in Figure 2.6.13-3, the minimum cross-sectional area is

$$\text{Area} = (\text{thickness})(\text{mean perimeter})\ (0.048)$$
$$= [(8.8+0.048)4] = 1.69\ \text{in}^2.$$

The total bearing load on the tube and BORAL during the cask bottom-end impact is 9,180 lb, (60 g × 153 lb). The maximum compressive and bearing stress in the fuel tube is 5,432 psi (9180/1.69). Limiting the compressive stress level in the tube to the material yield strength ensures that the tube remains in position when the cask is subjected to the postulated end-drop. Type 304 stainless steel yield strength is **19,400** psi at a conservatively high temperature of 500°F for the axial location on the fuel tube that has the minimum cross-section area. Using this criterion to evaluate the tube for the end-drop load, a margin of safety of +2.57 is achieved.

2.7.8.4.2 Fuel Tube Side-Impact Analysis

During the cask side-impact load configuration, the fuel tube is supported by the fuel basket's stainless steel support disks. The fuel basket support disks support the full length of the fuel tube, and are spaced at 4.42 in. apart (which is about one half of the fuel tube width of

8.8 in.). Considering the fuel tube subjected to the 60 *g* [1] side-impact deceleration and the 30 support locations provided by the basket support disks, the fuel tube shear stress is

Impact shear load = (60)(1,602)/30 = 3,204 lb

Shear area of tube = (0.048)(8.8)(2) = 0.845 in^2

Shear stress of tube = 3,204/0.845 = 3,792 psi.

The yield strength of Type 304 stainless steel at 750°F is 17,300 psi. Using an allowable shear stress equivalent to half the yield strength of the tube wall material, 8,650 psi, results in a large positive margin of safety. The conservative evaluation of the tube loading resulting from its own mass during the side-impact configuration indicates that the tube structure will maintain position and will function.

The load transfer of a fuel assembly to the fuel basket support disk when the cask is subjected to a side impact will be through direct bearing and compression of the distributed load of the fuel assembly through the fuel tube to the support disk web. The analysis considers the fuel assembly load as a distributed pressure on the inside tube surface.

The load transfer of the weight of the fuel assembly to the fuel basket support disk in the side impact is through direct bearing and compression of the distributed load of the fuel assembly through the fuel tube to the support disk web. Two load conditions are considered in the fuel tube evaluation. The first considers the fuel assembly load as a distributed pressure on the inside surface of the fuel tube. The second postulates that the fuel assembly grid is located at the center of the span between the support disks and produces a localized distributed load over the effective area of the grid.

Two different ANSYS finite element models of the tube are developed for these two load conditions since the fuel tube structural performance for either load is nonlinear. As shown in the following, the first model represents a fuel tube section with a length of three spans, i.e., the model is supported at four locations by support disks. The model conservatively considers the fuel tube wall thickness of 0.048 inch as the only material subjected to a distributed pressure load representative of the fuel assembly deceleration of 60g. Fuel assembly stiffness is not considered in the development of the imposed pressure load on the fuel tube.

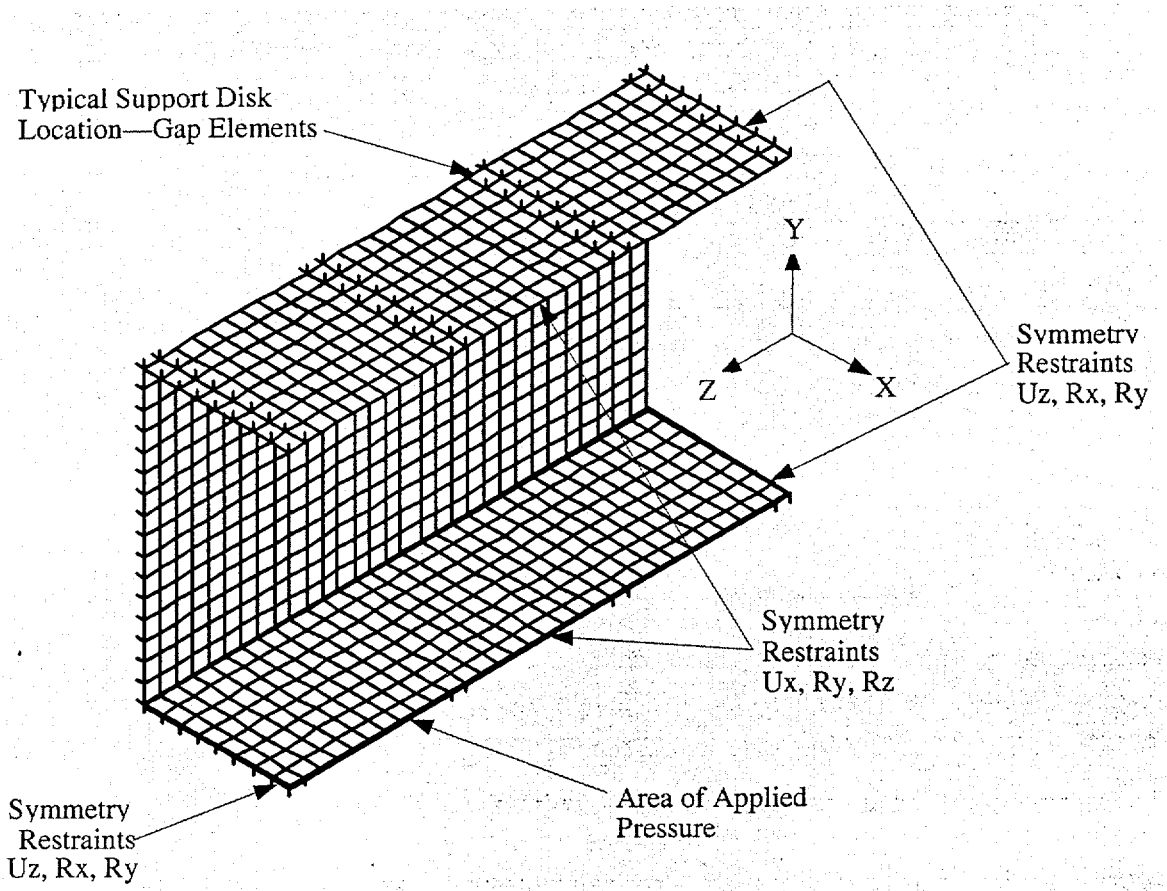

The tube is modeled with the ANSYS plastic, quadrilateral shell element (SHELL43). The support disks are represented by gap elements (CONTAC52). The outer nodes of the gap elements are fully restrained in all three translational directions. Edge restraints were applied to the model to represent symmetry boundary conditions. The effective load on the fuel tube due to the 60g deceleration of the fuel assembly is applied as a pressure to the inside area of the fuel tube.

The finite element analysis results show that the maximum stress in the tube is 23.8 ksi, which is local to the sections of the tube resting on the support disks. At 750°F the ultimate strength for Type 304 stainless steel is 63.1 ksi. The margin of safety is:

$$MS = \frac{63.1}{23.8} - 1 = +1.65$$

The analysis shows that the maximum total strain is 0.026 inch/inch. Defining the acceptable elastic-plastic response of the stainless steel as one half of the material failure strain of 0.40 in./in. at 750°F [24], the resulting margin of safety is:

$$MS = \frac{0.40/2}{0.026} - 1 = +large$$

Similarly, the margin of safety for elastic-plastic stress becomes:

$$MS = \frac{63.1 - 17.3}{23.8 - 17.3} - 1 = 6.05$$

where the yield strength of Type 304 stainless steel is 17.3 ksi at 750°F.

The second finite element model is used to evaluate the load condition with the fuel assembly grid located at the center of the span between two support disks. The fuel tube is subjected to a localized distributed load over the effective area of the grid. As shown in the following, the model is a quarter-symmetry periodic section of the fuel tube. As in the finite element model used for the distributed pressure case, this model conservatively considers a fuel tube wall thickness of 0.048 inch. The BORAL plate (0.075 inch) and stainless steel cover plate (0.018 inch) are conservatively not included in the model. The tube wall is modeled with ANSYS SHELL43 elements. The support disks are modeled with CONTAC52 elements.

Based on the Lawrence Livermore evaluation of the fuel rods for a side impact (UCID-21246) [43], the fuel rods and fuel assemblies maintain their structural integrity during the side impact resulting from a cask tip-over accident and the displacement of the fuel tube is limited. The maximum displacement of the fuel tube section between the support disks will not exceed the "thickness" of the grid spacer, which is the distance between the outer surface of the grid and the outer surface of the fuel rod array. When the displacement of the fuel tube reaches the "thickness" of the grid spacer, the fuel rods will be in contact with the inner surface of the fuel tube and the weight of the fuel rods will be transferred through the tube wall to the support disks. Therefore, a bounding load condition for this model is simulated by applying a constant displacement of 0.08 inch in the negative Y direction to the nodes corresponding to the grid location in the model. Note that 0.08 inch displacement bounds all PWR fuel assemblies. It is assumed that the fuel assembly grid spacer is rigid and therefore a constant displacement is conservatively applied.

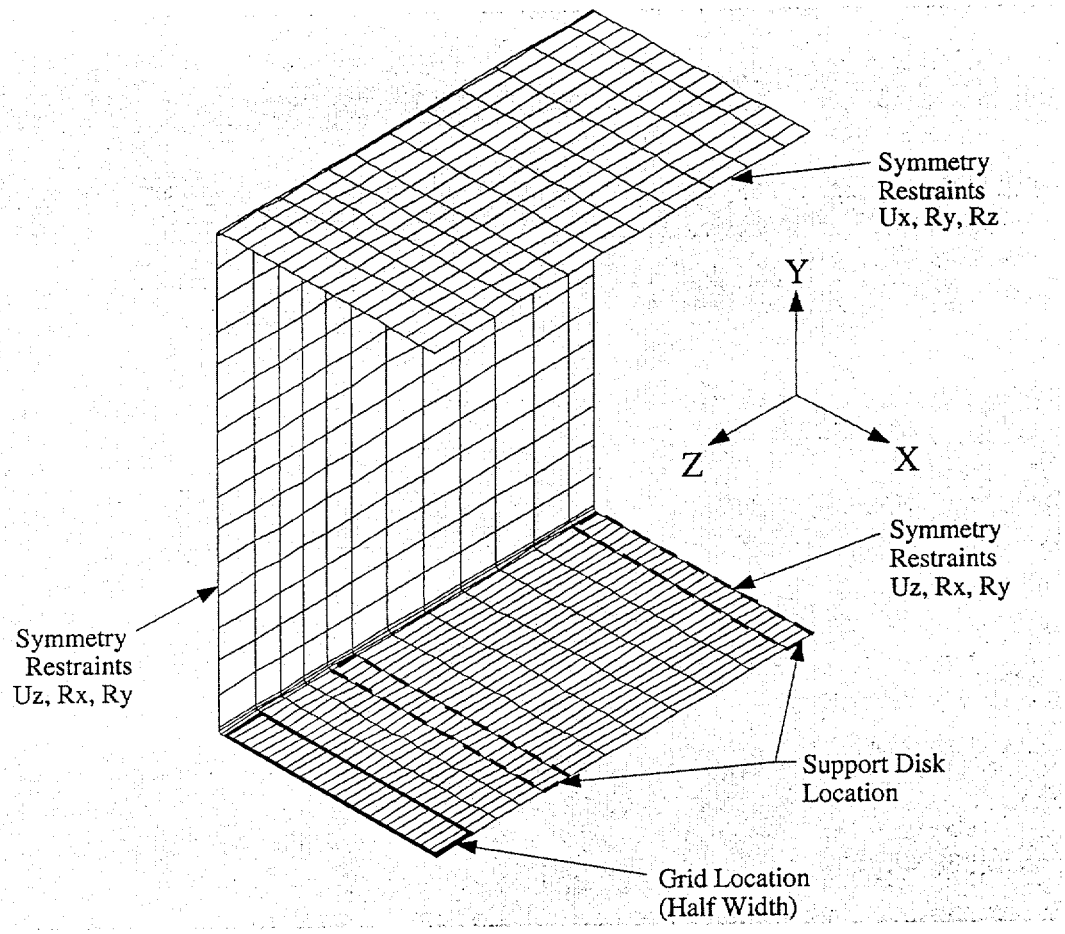

The finite element analysis results show that the maximum stress in the tube is 38.4 ksi, which is local to the corner of the tube at the grid spacer location of the model close to the side wall of the tube. At 750°F the ultimate strength for Type 304 stainless steel is 63.1 ksi. The margin of safety is:

$$MS = \frac{63.1}{38.4} - 1 = +0.64$$

The analysis shows that the maximum total strain is 0.11 inch/inch. Defining the acceptable elastic-plastic response of the stainless steel as one half of the material failure strain of 0.40 in./in. at 750°F [24], the resulting margin of safety is:

$$MS = \frac{0.40/2}{0.11} - 1 = 0.82$$

Similarly, the margin of safety for elastic-plastic stress becomes:

$$MS = \frac{63.1 - 17.3}{38.4 - 17.3} - 1 = 1.17$$

where the yield strength of Type 304 stainless steel is 17.3 ksi at 750°F.

Both the maximum total strain and the elastic-plastic stress analyses indicate that the tube position within the support basket is maintained.

Assurance that the BORAL remains attached to the fuel tube is evaluated by considering that loads produced by the BORAL plate and stainless steel attachment plate, assuming a 60g load, are carried by the attachment plate weld. Total load and resultant stress on the weld are calculated as:

$F_{b/ss} = (g)(\rho)(t)(w)(l)$ Load exerted by BORAL/Stainless Steel Attachment Plate

where:

g = acceleration (g)
ρ = density of material (lb/in^3) (The density of aluminum (0.098 lb/in^3) is conservatively used for the BORAL.
t = thickness of material (in.)
w = width of material (in.)
l = length of material section (in.)

The forces on the weld due to a 12-inch section of BORAL (F_b) and a 12-inch section of stainless steel plate (F_{ss}) are:

F_b = (60g)(0.098 lb/in^3)(0.075 in.)(8.2 in.)(12 in.)
= 43.4 lbs

F_{ss} = (60g)(0.291 lb/in^3)(0.018 in.)(8.7 in.)(12 in.)
= 32.8 lbs

The total load (F_t) on a 1-inch attachment weld for a 12-inch section is:

$F_t = 43.4 \text{ lbs} + 32.8 \text{ lbs} = 76.2 \text{ lbs}$

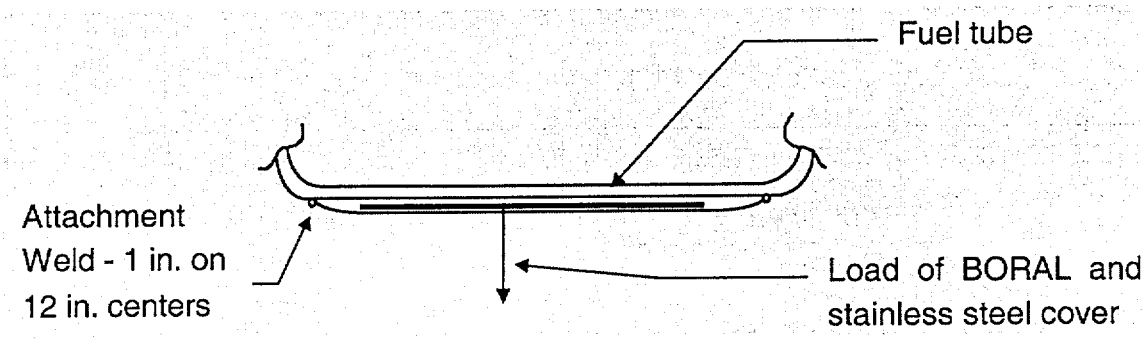

The resulting weld stress is: $\sigma = P/A = (76.2 \text{ lb}/2) / (1 \text{ in.}) (0.018 \text{ in.}) = 2,117 \text{ psi}$

Since the weld material is Type 304 stainless steel, the margin of safety (at 750°F) is:

$$MS = \frac{17,300}{2,117} - 1 = +7.2$$

Therefore, the BORAL remains enclosed on each outer surface of the fuel tube wall.

2.7.8.5 Basket Weldment Analysis for 30-Foot End Drop

The responses of the top and the bottom weldment plates of the fuel basket assembly to a 60 *g* accident condition deceleration load are examined. Two finite element models representing the PWR basket top and bottom weldments are constructed for structural evaluation. The structural evaluations are performed at normal condition temperatures; therefore, prior to the structural evaluation portion of the analyses, the steady-state temperature distribution in the top and bottom weldment models is determined by applying fixed temperatures to the outer circular edge and to the node at the intersection of the symmetry planes and then solving for the intermediate temperatures. These fixed temperatures are obtained from the normal conditions thermal analysis with -40°F ambient temperature and maximum heat generation. The material allowable stresses are based on the maximum temperature of the weldments determined for normal conditions with 100°F ambient temperature and maximum heat generation.

During the temperature solution portion of the analyses, ANSYS three-dimensional thermal shell elements (SHELL57) are used to construct the finite element models. During the structural evaluation portion of the analyses, ANSYS three-dimensional, six-degrees-of-freedom, elastic shell elements (SHELL63) in the weldment plate and structural support plate regions are used to construct the finite element models. BEAM4 elements are used to model the top nut/pads. Contact between the structural support plates and the structural support ring (where applicable) are modeled using CONTACT52 elements. The finite element models represent one-quarter sections of the weldments.

The top and bottom weldments are 1.0-in. and 1.25 in. thick, respectively, and are fabricated from SA-240, Type 304 stainless steel. The top weldment supports its own weight and 24 fuel tubes (without the fuel assemblies) during a top-end drop. Eleven structural support places, eight tie-rod top nuts, and a circumferential ring support the top weldment and its loads during a top-end drop. These structural components are modeled as zero-translation restraints in the direction of the end drop. The finite element models of the top and bottom weldments are presented in Figures 2.6.13.13-1 and 2.6.13.13-2, respectively.

2.7.8.5.1 Results of Basket Weldment Analyses (30-Foot End-Drop)

The maximum stress intensities (SI), for primary membrane plus primary bending ($P_m + P_b$), for the 30-ft end-drop analysis and the corresponding minimum margins of safety are:

Component/Condition	$P_m + P_b$ (ksi)	S_u (ksi)	MS
Top Weldment/30-ft Drop	7.62	62.56	+7.21
Bottom Weldment/30-ft Drop	12.99	63.22	+3.87

Because a large radial temperature gradient occurs through the weldments, the maximum stress intensities presented in the preceding table do not occur at the maximum temperature of the models. Therefore, comparing these stress intensities with stress allowables based upon the maximum temperature is conservative. Therefore, the stress evaluation is performed on a nodal basis. That is, using ANSYS, the maximum stress at each node in each model is compared with the maximum allowable stress at the temperature of the node being evaluated.

For hypothetical accident conditions, the following criteria are used in evaluating the top and bottom weldments nodal stress intensities:

$$P_m + P_b < 3.6S_m \text{ or } S_u, \text{ whichever is less.}$$

(Note: For Type 304 stainless steel in these temperature ranges, S_u is smaller than $3.6S_m$.)

The margin of safety (MS) is calculated as

$$MS = \frac{\text{Allowable Stress}}{\text{Nodal Stress Intensity}} - 1.$$

2.7.8.5.2 Top Weldment Structural Rib Buckling Evaluation

The structural ribs on the top weldment are subjected to axial loads during a top-end drop. End constraints on the ribs during a top-end drop are fixed at the end welded to the top weldment, and free at the other end. Because no closed solutions are readily available for evaluating a plate for buckling loads with end constraints matching those of the top weldment ribs, a closed-form solution for the buckling of a column is used to analyze a 1-in. section of one of the ribs.

For a column under axial loading with one end fixed and the other end free, the critical load (P_{cr}) is determined by

$$P_{cr} = \frac{\pi^2 EI}{(KL)^2}$$

where: I = moment of inertia,
E = modulus of elasticity,
L = length of the column, and
K = effective length factor (K = 2 for a column with one end fixed and the other free).

Evaluating a 1-in. section of one of the ribs at the maximum weldment temperature of 515°F gives

$$P_{cr} = \frac{\pi^2 (25.7\times10^6)\frac{1}{12}(1.0)(1.0)^3}{(2\times8.15)^2} = 8.0 \times 10^4 \text{ lb}$$

For the 30-ft top-end drop, the sum of the forces on the nodes representing the ribs is a maximum of 1,422 lb.

Thus, the margin of safety for buckling of one of the structural ribs of the top weldment during a 30-ft top-end drop is:

$$MS = \frac{8.0 \times 10^4}{1{,}422} - 1 = + \text{Large}$$

2.7.8.5.3 Conclusions

As shown in this section, both the top and bottom weldments maintain positive margins of safety when subjected to the 30-ft end-drop conditions. As shown in the top weldment structural rib buckling calculation, the actual maximum load (P) on one of the structural ribs of the top weldment during a 30-ft drop is much less than the predicted buckling load (P_{cr}). Therefore, the top and bottom weldments are structurally adequate.

2.7.9 BWR Transportable Storage Canister Analysis – Accident Conditions

Evaluation of the BWR Transportable Storage Canister for the hypothetical accident conditions is presented in this section. The evaluation of the canister for normal conditions of transport is presented in Section 2.6.14.

The principal components of the canister assembly are the canister shell, bottom plate, fuel basket, shield lid, and structural lid. The geometry and materials of construction of the canister, baskets, and spacers are described in Section 1.2.1.2. The general arrangement of the canister depicted with the fuel basket is shown in Figure 2.6.14-1. The individual components of the canister are depicted in Figure 2.6.14-2.

A drop accident stress evaluation is performed for the 30-ft side-drop condition, top and bottom end-drops, and for the top and bottom corner-drop conditions by applying a 60 *g* deceleration load. The loads developed in the basket are transferred through the canister wall into the inner shell (for the side drops and oblique drops), and any axial component is transferred into the ends of the cask cavity. The axial loads are maximized for the end-drops and corner-drop conditions. The lateral loads are maximized in the side-drop since an enveloping acceleration is employed in the analysis. Regardless of the angle of the drop, the canister wall is uniformly supported along its length by the transport cask inner shell, and the load path is not affected by drop orientations close to the side-drop orientation. The oblique orientation will not provide enveloping loading above the side-drop conditions. Therefore, oblique orientations other than the corner drops are not considered.

In addition, the evaluations are performed with and without the 25 psig internal pressure. Also, for the side, top corner, and bottom corner-drop orientations, basket orientations of 0° and 45° are evaluated. The angles describe the orientation of the basket elements with respect to the symmetry plane of the model. A value of 0° orients the ligaments in the basket elements parallel and perpendicular to the symmetry plane while a value of 45° orients the basket ligaments at +/-45° from the symmetry plane. The evaluations consider the maximum temperatures present during the normal conditions evaluated with 100°F ambient; solar insolation, and maximum decay heat.

2.7.9.1 Analysis Description

The structural design criteria for the canister are contained the ASME Code, Section III, Subsection NB. Consistent with these criteria, the structural components of the canister (shell, bottom plate, and structural lid) are shown to satisfy the allowable stress intensity limits presented in Table 2.1.2-3. For the canister structural lid weld (Section 13, Figure 2.6.12.3-1), base metal properties are used to define the allowable stress limits since the weld filler rod tensile properties are greater than the base metal. Also, the allowable stress is multiplied by a stress reduction factor of 0.8 per ISG-4.

The ANSYS finite element program is used to evaluate the canister for the 30-ft drop conditions in the top and bottom-end, top and bottom-corner, and side-impact orientations. The ANSYS finite element model is the same as that used for the evaluation of the 1-ft drop impacts evaluated for normal conditions of transport. The model is described in Section 2.6.14.2.

2.7.9.2 Analysis Results - BWR Canister

The detailed results of the analysis for the 30-ft side, top and bottom corner, and top and bottom-end drops are presented in Tables 2.7.9.2-1 through 2.7.9.2-10. Only the load cases that result in the worst case margins are presented for each of the drop orientations considered. For the side drop, the worst case configuration is without pressure and the basket oriented at 0°. For the bottom-drop, the worst case occurs with internal pressure. For the top-end drop, the most severe condition occurs without pressure. For the bottom-corner drops, the worst case stresses occur without pressure and the basket oriented at 0°. For the top-corner drops, the worst case occurs with pressure for primary membrane and without pressure for membrane plus bending.

A drop accident stress evaluation is performed for the 30-ft side-drop, top and bottom-end drops, and for the top and bottom-corner drop conditions by applying a 60 *g* deceleration load. The loads developed in the basket are transferred through the canister wall into the inner shell (for the side-drop and oblique drops), and any axial component is transferred into the ends of the cask cavity. The axial loads are maximized for the end-drops and corner-drop conditions. The lateral loads are maximized in the side-drop since an enveloping acceleration is employed in the analysis. Regardless of the angle of the drop, the canister wall is uniformly supported along its length by the transport cask inner shell, and the load path is not affected by drop orientations close to the side-drop orientation. The oblique orientation will not provide enveloping loading above the side-drop conditions. Therefore, oblique orientations other than the corner drops are not considered.

The section stresses presented in the tables are identified by a section number. The minimum margin of safety at each section is presented by denoting the circumferential angle where the minimum margin of safety occurs. A cross-section of the canister showing the section numbers is presented in Figure 2.7.9.2-1. Stresses are evaluated at 9° increments around the circumference for each of the locations shown in Figure 2.7.9.2-1. The canister minimum margins of safety for the governing drop conditions are summarized in Table 2.7.9.2-11.

The methodology used to evaluate the stresses for the side drop is identical to that used for the normal conditions 1-ft side drop for the BWR canister (Section 2.6.14.6). Sections 9, 10, and 11 at the 0° circumferential position (see Figure 2.6.12.3-1) are not included in the evaluation. These regions are characterized as a bearing stress since they result from the canister shell bearing against cask inner shell. An evaluation of these bearing stresses is not required for accident conditions. Results for Sections 9, 10, and 11 at angular locations other than 0° are included in the evaluation.

Design changes were made to the BWR basket after the initial analyses were performed. The effects of the design changes on the BWR canister are discussed in Section 2.6.14.2. The same procedure used to scale the BWR canister stress intensities in Section 2.6.14.2 is used for the accident conditions in the following evaluation.

The allowable stresses presented in the tables are for Type 304L stainless steel. The shield lid is constructed of Type 304 stainless steel, which possesses higher allowable stresses, resulting in a conservative evaluation. These allowables are evaluated at 380°F, unless otherwise indicated. Review of the thermal analyses shows that the maximum temperature of the canister is 363°F (Section 3.4), so the presented margins of safety are conservative.

Figure 2.7.9.2-1 Identification of Sections for Evaluating Linearized Stresses in BWR Canister

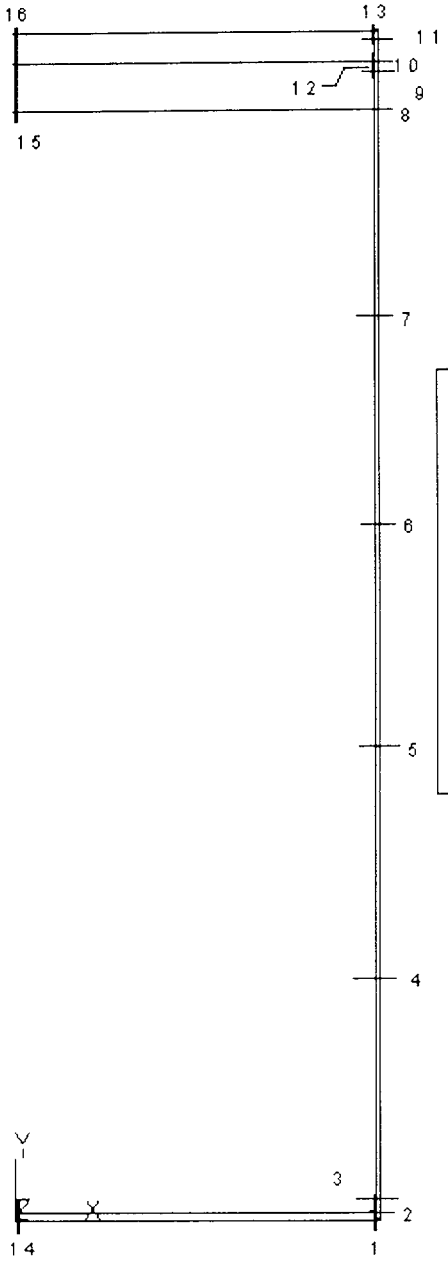

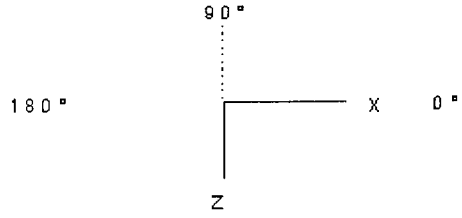

Top View of Axis

BWR Section Coordinates at Z = 0

Axial Section	Nodal		Nodal	
	x	y	x	y
1	32.905	0.0	32.905	1.75
2	32.905	1.75	33.53	1.75
3	32.905	2.25	33.53	2.25
4	32.905	37.79	33.53	37.79
5	32.905	73.83	33.53	73.83
6	32.905	109.87	33.53	109.87
7	32.905	145.91	33.53	145.91
8	32.905	181.95	33.53	181.95
9	32.905	188.45	33.53	188.45
10	32.905	188.95	33.53	188.95
11	32.905	191.07	33.53	191.07
12	32.905	188.45	32.905	188.95
13	32.905	191.07	32.905	191.95
14	0.1	0.0	0.1	1.75
15	0.1	181.95	0.1	188.73
16	0.1	188.97	0.1	191.95

Table 2.7.9.2-1 BWR Canister P_m Stresses - 30-Foot Side Drop

		P_m Stresses (ksi)								
Section Location	Angle of peak stress location	Sx	Sy	Sz	Sxy	Syz	Sxz	SI (ksi)	Allowable Stress (ksi)	Margin of Safety
1	0	-18.3	0.4	-10.7	-0.2	-0.2	-1.7	19.1	38.4	1.01
2	0	-10.4	0.2	-10.2	-0.6	-0.5	-1	11.6	38.4	2.31
3*	0	-7.4	-0.1	-8.7	-0.4	-0.5	-0.9	9.8	38.4	2.92
4*	90	0	0.3	0	2.1	0	0	4.4	38.4	7.73
5*	180	0	-4.5	-0.6	0	-0.1	0	4.7	38.4	7.17
6*	180	0	-4.6	-0.6	0	0	0	4.8	38.4	7.00
7*	0	-1.6	2.4	0.1	0	-0.2	0.2	4.3	38.4	7.93
8*	0	-0.6	6.2	-2.7	-0.1	1	-0.1	9.6	38.4	3.00
9	9	-22.7	5.7	-9.6	-2.7	3.3	1.0	29.7	38.4	0.29
10	0	-24.4	2.5	-13	-5.1	2	0.8	29	38.4	0.32
11	9	-16.3	1.0	-8.9	0.9	2.3	-0.07	18.0	38.4	1.13
12	0	-38.7	-7.9	-16.8	-6.9	1.8	0.7	34.1	38.4	0.13
13	0	-30.2	-9.3	-12.2	0.2	1.4	-1.6	21.6	30.72**	0.42
14	0	-2.4	0	0.8	0	0	-0.1	3.3	38.4	10.66
15	0	-1	0	0.4	-0.1	0	0	1.3	38.4	28.08
16	0	-1.5	0	0.4	0	0	0	1.8	38.4	19.9

* Stresses at these locations are increased by 5% to account for the heavier BWR fuel basket/fuel.

** Allowable stress includes a stress reduction factor for the weld: 0.8 x allowable stress.

Table 2.7.9.2-2 BWR Canister $P_m + P_b$ Stresses - 30-Foot Side Drop

		$P_m + P_b$ Stresses (ksi)								
Section Location	Angle of peak stress location	Sx	Sy	Sz	Sxy	Syz	Sxz	SI (ksi)	Allowable Stress (ksi)	Margin of Safety
1	0	-22.6	-0.1	-12.3	0.6	0	-1.7	22.8	57.5	1.52
2	0	-12.2	0.7	-8.6	-1.1	-0.5	-1.5	13.6	57.5	3.23
3*	0	-8.8	0.6	-6.9	-0.8	-0.5	-1.3	10.8	57.5	4.32
4*	0	-1.6	1	3	0	0.1	0.5	4.9	57.5	10.73
5*	0	-1.7	2.6	2.8	0	0	0.2	4.7	57.5	11.23
6*	0	-1.7	3.1	2.8	0	-0.1	0	5.0	57.5	10.5
7*	0	-1.6	3.1	2.5	0	-0.2	0.3	5.1	57.5	10.27
8*	0	-0.3	6.1	-4.9	-0.1	1	-0.3	11.8	57.5	3.87
9	9	-20.5	14.9	-7.5	-2.5	3.6	2.8	37.0	57.5	0.55
10	0	-26.2	-0.1	-11.4	-7.2	1.5	0.4	30	57.5	0.92
11	0	-41.2	12.5	-14.7	0.1	2.4	1.5	54	57.5	0.06
12	0	-47.8	-11.3	-20.4	-6.8	2.4	1.1	39.5	57.5	0.46
13	0	-48	-18.7	-20.9	-0.3	2.1	-0.8	30.7	46.0	0.50
14	0	-2.5	0	0.8	0	0	-0.1	3.3	57.5	16.41
15	0	-0.3	0	1.5	-0.1	0	0	1.8	57.5	31.74
16	0	-1.2	0	0.9	0	0	0	2	57.5	27.39

* Stresses at these locations are increased by 5% to account for the heavier BWR fuel basket/fuel.

** Allowable stress includes a stress reduction factor for the weld: 0.8 x allowable stress.

Table 2.7.9.2-3 BWR Canister P_m Stresses - 30-Foot Bottom-End Drop, Internal Pressure

		P_m Stresses (ksi)								
Section Location	Angle of peak stress location	Sx	Sy	Sz	Sxy	Syz	Sxz	SI (ksi)	Allowable Stress (ksi)	Margin of Safety
1*	180	-0.1	-2.8	-0.4	0.2	0.1	0	2.8	38.4	12.57
2	180	0.6	-6.5	-1.2	0.3	0.1	0.1	7.1	38.4	4.39
3	180	0.4	-6.7	-1.1	0.2	0.1	0.1	7.1	38.4	4.37
4	180	0	-6.6	1.3	0	0	-0.1	7.9	38.4	3.85
5	180	0	-6	1.3	0	0	-0.1	7.3	38.4	4.27
6	180	0	-5.3	1.3	0	0	-0.1	6.6	38.4	4.77
7	180	0	-4.7	1.3	0	0	-0.1	6	38.4	5.37
8	54	0.5	-3.1	0.3	0	0	0.3	3.8	38.4	9.03
9	72	-1.7	-1.9	-0.7	-0.1	0.4	-0.4	1.6	38.4	22.94
10	180	1.7	-1.3	-1	-0.3	0	0.2	3.1	38.4	11.5
11	0	-2	0.5	-0.9	0	0	0.1	2.5	38.4	14.17
12	0	0.7	1.8	-0.4	0.2	0.1	-0.1	2.2	38.4	16.18
13	180	0	-2	-1.2	0	0	0.1	2	30.72**	14.36
14*	0	0.1	-1.1	0.1	0	0	0	1.3	38.4	29.44
15	180	0.2	-0.1	0.2	0	0	0	0.2	38.4	186.72
16	90	-0.2	0	-0.2	0	0	0	0.2	38.4	223.54

* Stresses at these locations are increased by 5% to account for the heavier BWR fuel basket/fuel.

** Allowable stress includes a stress reduction factor for the weld: 0.8 x allowable stress.

Table 2.7.9.2-4 BWR Canister $P_m + P_b$ Stresses - 30-Foot Bottom-End Drop, Internal Pressure

		$P_m + P_b$ Stresses (ksi)								
Section Location	Angle of peak stress location	Sx	Sy	Sz	Sxy	Syz	Sxz	SI (ksi)	Allowable Stress (ksi)	Margin of Safety
1*	180	0.3	-3.2	-0.3	0.3	0.1	0	3.7	57.5	14.54
2	180	0.3	-9.4	-2.1	0.2	0.1	0.2	9.7	57.5	4.95
3	180	0.2	-9	-1.8	0.1	0.1	0.1	9.2	57.5	5.28
4	180	0	-6.6	1.3	0	0	-0.1	7.9	57.5	6.25
5	0	0	-6	1.3	0	0	0.1	7.3	57.5	6.89
6	180	0	-5.3	1.3	0	0	-0.1	6.7	57.5	7.64
7	180	0	-4.7	1.3	0	0	-0.1	6	57.5	8.54
8	45	0.5	-3.4	0.5	0.1	-0.1	0.2	4.1	57.5	13.03
9	90	-2.4	-3.9	-0.4	0	0.7	0	3.7	57.5	14.53
10	90	-2.9	-6.6	0.6	0	0.2	0	7.3	57.5	6.91
11	0	-1.1	5.6	0.9	-0.4	0	0.1	6.8	57.5	7.52
12	0	2.6	3.6	0.7	0.7	0	-0.1	3.3	57.5	16.27
13	180	2.3	0.1	0.1	0.4	0.1	0.2	2.4	46.0*	18.17
14*	0	0.1	-1.1	0.1	0	0	0	1.4	57.5	37.33
15	90	3.6	0	3.6	0	0	0	3.6	57.5	14.82
16	81	-1.8	0	-1.8	0	0	0	1.8	57.5	31.14

* Stresses at these locations are increased by 5% to account for the heavier BWR fuel basket/fuel.

** Allowable stress includes a stress reduction factor for the weld: 0.8 x allowable stress.

Table 2.7.9.2-5 BWR Canister P_m Stresses - 30-Foot Top-End Drop

Section Location	Angle of peak stress location	P_m Stresses (ksi) Sx	Sy	Sz	Sxy	Syz	Sxz	SI (ksi)	Allowable Stress (ksi)	Margin of Safety
1	0	0.3	-5.2	-1.8	1	-0.1	-0.2	5.8	38.4	5.56
2	0	-2.1	3.5	6.4	1.1	-0.1	0.6	8.8	38.4	3.37
3	0	-1.5	2.3	7.7	0.5	0	0.7	9.3	38.4	3.12
4	135	0	-2.4	0	0	0	0	2.4	38.4	14.87
5	153	0	-3	0	0	0	0	3	38.4	11.62
6	153	0	-3.7	0	0	0	0	3.7	38.4	9.45
7	171	0	-4.3	0	0	0	0	4.3	38.4	7.91
8	180	0.1	-4	0.1	-0.1	0	0	4.2	38.4	8.23
9	180	0.1	-3	-0.5	-0.1	0	0	3	38.4	11.67
10	144	-0.2	-2.9	-0.4	-0.1	0	0.2	2.8	38.4	12.75
11	135	-0.3	-2.8	-0.3	0	0	0.2	2.7	38.4	13.19
12*	36	-0.1	-2.2	-0.2	0.1	-0.1	-0.1	2.3	38.4	15.69
13*	180	0	-2.3	-0.3	0	0	0	2.4	30.72**	11.80
14	90	-0.7	0	-0.7	0.2	-0.4	0	1.1	38.4	32.64
15*	0	0	-1	0	0	0	0	1.1	38.4	33.91
16*	0	0	-1.1	0	0	0	0	1.3	38.4	28.55

* Stresses at these locations are increased by 5% to account for the heavier BWR fuel basket/fuel.

** Allowable stress includes a stress reduction factor for the weld: 0.8 x allowable stress.

Table 2.7.9.2-6 BWR Canister $P_m + P_b$ Stresses - 30-Foot Top-End Drop

Section Location	Angle of peak stress location	$P_m + P_b$ Stresses (ksi) Sx	Sy	Sz	Sxy	Syz	Sxz	SI (ksi)	Allowable Stress (ksi)	Margin of Safety
1	0	-2.1	-11.9	1.9	0.4	-0.1	0.2	13.8	57.5	3.16
2	0	-2.2	24.6	12.6	1.8	-0.1	1.1	27.1	57.5	1.12
3	0	-1.7	23.7	13.8	1.2	-0.1	1.2	25.6	57.5	1.25
4	180	0	-2.4	0	0	0	0	2.4	57.5	22.68
5	153	0	-3	0	0	0	0	3	57.5	17.92
6	162	0	-3.7	0	0	0	0	3.7	57.5	14.68
7	180	0	-4.3	0	0	0	0	4.3	57.5	12.35
8	180	0.3	-4	0.1	-0.2	-0.1	0	4.3	57.5	12.47
9	135	-0.4	-3.5	-0.4	0	0	0.3	3.4	57.5	15.88
10	180	0	-3.3	-0.7	-0.1	0	0.1	3.3	57.5	16.37
11	135	-0.3	-3.1	-0.3	0	0	0.3	3	57.5	18.14
12*	180	0.2	-2.1	-0.3	-0.2	0	0	2.4	57.5	22.81
13*	180	-0.1	-2.5	-0.4	-0.1	0	0	2.4	46.0**	18.17
14	81	-21.9	-0.3	-21.9	0.2	-0.4	0	21.6	57.5	1.66
15*	72	0.3	-1	0.3	0	0	0	1.3	57.5	42.61
16*	0	0.1	-1.1	0.1	0	0	0	1.2	57.5	45.55

* Stresses at these locations are increased by 5% to account for the heavier BWR fuel basket/fuel.

** Allowable stress includes a stress reduction factor for the weld: 0.8 x allowable stress.

Table 2.7.9.2-7 BWR Canister P_m Stresses - 30-Foot Bottom-Corner Drop

Section Location	Angle of peak stress location	P_m Stresses (ksi) Sx	Sy	Sz	Sxy	Syz	Sxz	SI (ksi)	Allowable Stress (ksi)	Margin of Safety
1*	0	-13.6	-3.2	-5	-0.5	0	-2	11.4	38.4	2.37
2	36	-0.2	-8	-1.3	-0.2	0.3	-1.7	9	38.4	3.25
3*	36	-0.3	-8.2	-1.4	-0.1	0.2	-1.5	9.5	38.4	3.04
4*	0	-2.6	-7.9	0.2	0	0	0.1	8.5	38.4	3.52
5*	180	0	-7	-0.2	0	0	0	7.4	38.4	4.19
6*	180	0	-6.7	-0.2	0	0	0	7.0	38.4	4.49
7*	180	0	-6	-0.2	0	0	0	6.3	38.4	5.10
8*	72	0.1	-3.5	0.1	-0.8	-0.4	0	4.2	38.4	8.14
9	0	-29.5	0.8	-10.1	-2.9	1.8	-0.2	31.1	38.4	0.23
10	0	-13.5	-0.8	-5.8	-2.6	1.4	-1	14.2	38.4	1.7
11	0	-35.9	-1.5	-11.6	-0.4	2	-0.3	34.8	38.4	0.1
12	0	-22.4	-5.2	-6.9	-3.7	1.2	-1.3	19.5	38.4	0.97
13	0	-23	-7.2	-7.3	0.3	1.4	-2.2	17.5	30.72**	0.76
14*	0	-0.9	-1	0.4	0	0	0	1.5	38.4	24.60
15	0	-0.1	0	0.3	0	0	0	0.4	38.4	88.61
16	0	-0.8	0	0	0	0	0	0.8	38.4	47.41

* Stresses at these locations are increased by 5% to account for the heavier BWR fuel basket/fuel.

** Allowable stress includes a stress reduction factor for the weld: 0.8 x allowable stress.

Table 2.7.9.2-8 BWR Canister $P_m + P_b$ Stresses - 30-Foot Bottom-Corner Drop

		$P_m + P_b$ Stresses (ksi)								
Section Location	Angle of peak stress location	Sx	Sy	Sz	Sxy	Syz	Sxz	SI (ksi)	Allowable Stress (ksi)	Margin of Safety
1*	0	-16.3	-2.3	-5.5	0.6	0.1	-2	15.1	57.5	2.81
2	27	-0.6	-12.5	-3.5	-0.2	-0.3	-1.8	12.7	57.5	3.53
3*	36	-0.8	-11.6	-2.1	-0.1	0.2	-1.8	12.6	57.5	3.56
4*	0	-2.7	-7.3	2.3	0	0	0.3	10.2	57.5	4.63
5*	0	-2.7	-6	2.3	0	0	0.3	8.7	57.5	5.61
6*	0	-2.6	-5	2.3	0	-0.1	0.3	7.8	57.5	6.37
7*	0	-2.6	-4.3	2.3	0	-0.1	0.3	6.9	57.5	7.33
8*	18	0.5	-3	-1.4	0.9	1.5	-0.6	5.1	57.5	10.27
9	0	-29.4	6.5	-10.8	-2.5	1.8	0.3	36.5	57.5	0.58
10	0	-13.8	-1	-3.8	-4.1	1	-1.4	15.8	57.5	2.65
11	0	-32.1	7.6	-9.8	-0.2	1.9	0.4	39.9	57.5	0.44
12	0	-29.1	-7.5	-9.5	-3.6	1.7	-0.9	23.7	57.5	1.43
13	0	-37	-14.6	-13.7	-0.1	1.9	-1.5	25	46.0**	0.84
14*	0	-0.9	-1	0.4	0	0	0	1.6	57.5	34.94
15	81	3.9	0	4.4	0	0	0	4.4	57.5	12.18
16	18	-2.7	0	-2	0	0	0	2.6	57.5	20.89

* Stresses at these locations are increased by 5% to account for the heavier BWR fuel basket/fuel.

** Allowable stress includes a stress reduction factor for the weld: 0.8 x allowable stress.

Table 2.7.9.2-9 BWR Canister P_m Stresses - 30-Foot Top-Corner Drop, Internal Pressure

Section Location	Angle of peak stress location	P_m Stresses (ksi) Sx	Sy	Sz	Sxy	Syz	Sxz	SI (ksi)	Allowable Stress (ksi)	Margin of Safety
1	9	-0.1	-3.3	-2.8	1.3	-0.9	-1.1	4.9	38.4	6.83
2	0	-20.2	-1.9	-5.8	-1.7	0.4	-1	18.8	38.4	1.04
3*	0	-14.7	-2	-3.8	-1.7	0.4	-1	14.0	38.4	1.74
4*	0	-2.6	-1.8	1.5	0	0	0.3	4.3	38.4	7.93
5*	180	0	-3.2	1.1	0	0	-0.1	4.5	38.4	7.53
6*	180	0	-3.6	1.1	0	0	-0.1	4.9	38.4	6.84
7*	0	-2.5	-3.9	1.3	0	-0.2	0.3	5.6	38.4	5.86
8*	54	0.5	-4	0.3	-1.1	-0.8	0.3	5.8	38.4	5.62
9	0	-30.7	-4.7	-10.3	-3.3	1	-0.2	27	38.4	0.42
10	0	-20.8	-9.6	-8.4	-3.9	0.2	-0.8	14.1	38.4	1.72
11	0	-30.4	-14.7	-11.8	-1.5	0.7	-0.7	19	38.4	1.02
12*	0	-27.1	-13.2	-8.7	-5.5	0.4	-1.2	21.6	38.4	0.78
13*	0	-26.6	-17.3	-9.3	-1.6	0.4	-1.9	18.9	30.72**	0.63
14	90	-1.1	0	-0.1	0.1	-0.2	0	1.3	38.4	28.89
15*	0	-0.4	-1	0.1	0	0	0	1.2	38.4	31.88
16*	0	-0.6	-1.1	0.2	0	0	0	1.3	38.4	27.58

* Stresses at these locations are increased by 5% to account for the heavier BWR fuel basket/fuel.

** Allowable stress includes a stress reduction factor for the weld: 0.8 x allowable stress.

Table 2.7.9.2-10 BWR Canister $P_m + P_b$ Stresses - 30-Foot Top-Corner Drop

Section Location	Angle of peak stress location	$P_m + P_b$ Stresses (ksi) Sx	Sy	Sz	Sxy	Syz	Sxz	SI (ksi)	Allowable Stress (ksi)	Margin of Safety
1	0	-20.3	-11.3	-5.7	-3.8	-0.1	-1.6	16.3	57.5	2.53
2	0	-18	18.3	1.3	1.3	0.9	-0.1	36.4	57.5	0.58
3*	0	-13.4	14.1	1.6	0.4	0.8	-0.3	29.0	57.5	0.98
4*	0	-2.8	-1.8	2.2	0	0	0.3	5.4	57.5	9.65
5*	0	-2.5	-1.8	2.2	0	-0.1	0.4	5.0	57.5	10.50
6*	0	-2.1	-2.3	2.9	0	-0.1	1	5.7	57.5	9.09
7*	0	-2.7	-3.9	2.3	0	-0.2	0.3	6.5	57.5	7.85
8*	54	0.3	-4.2	0.3	-1	-1	0	5.6	57.5	9.27
9	0	-31	0.3	-11.3	-2.3	0.9	0.3	31.7	57.5	0.81
10	0	-22.5	-11.9	-7.5	-6.5	0	-1.3	18.5	57.5	2.11
11	0	-33.4	-18.6	-12	-2.4	0.9	-1.4	22.1	57.5	1.6
12*	0	-29.2	-12.7	-9.2	-4.5	0.8	-0.9	22.7	57.5	1.53
13*	0	-30.9	-21.3	-11.7	-2.7	0.7	-1.8	21.2	46.0**	1.17
14	90	-20.6	-0.3	-19	0.2	-0.3	0	20.3	57.5	1.83
15*	72	-0.2	-0.9	0.4	0	0	0	1.4	57.5	41.24
16*	0	-0.5	-1	0.2	0	0	0	1.3	57.5	41.87

* Stresses at these locations are increased by 5% to account for the heavier BWR fuel basket/fuel.

** Allowable stress includes a stress reduction factor for the weld: 0.8 x allowable stress.

Table 2.7.9.2-11 Summary of Minimum Margins of Safety for BWR Canister - 30-Foot Drops

Drop Orientation	Loading Condition	Stress Evaluated	Minimum Margin of Safety	Section Number*
Side	30-ft impact	P_m	0.13	12
Side	30-ft impact	$P_m + P_b$	0.06	11
Bottom end	30-ft impact + pressure (25 psi)	P_m	3.85	4
Bottom end	30-ft impact + pressure (25 psi)	$P_m + P_b$	4.95	2
Top end	30-ft impact	P_m	3.12	2
Top end	30-ft impact	$P_m + P_b$	1.12	2
Bottom Corner	30-ft impact	P_m	0.10	11
Bottom Corner	30-ft impact	$P_m + P_b$	0.44	11
Top Corner	30-ft impact; internal pressure	P_m	0.42	9
Top Corner	30-ft impact	$P_m + P_b$	0.58	2

* See Figure 2.7.9.2-1 for section locations.

2.7.9.3 Canister Buckling Evaluation for 30-Foot End Drop

Code Case N-284-1 [12] of the ASME Boiler and Pressure Vessel Code is used to analyze the BWR canister for the accident condition 30-foot end-drop (both top- and bottom-end drops). The evaluation requirements of Regulatory Guide 7.6, Paragraph C.5, are shown to be satisfied by the results of the buckling interaction equation calculations of Code Case N-284-1. The canister buckling design criteria are described in Section 2.1.2.5.3.

The BWR canister for the 30-foot end-drop is evaluated for buckling in the same manner as the PWR canister for the 1-foot end-drop (see Section 2.6.12.12). The analytical process used for the BWR canister is the same as that described in a step-by-step example presented in Section 2.7.12.3 (for the cask inner shell).

A 60 g deceleration load was used for all the 30-ft drop canister analyses that are presented in Sections 2.7.9.2. The 60 g-load bounds all 30-ft deceleration loads for all other drop angles. The top- and bottom-end drops result in the largest potential for canister shell buckling and, therefore, are the two load cases presented here. The side drop load case is not considered a credible buckling mode of the canister shell and is, therefore, not presented here.

The stress results from the dynamic shell analyses (ANSYS) are screened for the maximum values of the longitudinal compression, circumferential compression, or in-plane shear stresses for the 30-ft drop cases (top- and bottom-end drops) with and without pressure. For each loading case, the largest of each of the three stress components anywhere regardless of location within the BWR canister shell are combined. Combining the maximum stress components in this way produces a conservative, bounding-case buckling evaluation of the BWR canister, one which envelopes all 30-ft BWR canister drop cases including those presented in Tables 2.7.9.2-3 and 2.7.9.2-5.

The geometry parameters used in the BWR canister evaluation are the same as those presented in Table 2.6.14.12-1.

The maximum stress components used in the evaluation and the resulting buckling interaction equation ratios are provided in Table 2.7.9.3-1. The results show that all interaction equation ratios are less than 1.0. Therefore, the buckling criteria of Code Case N-284-1 are satisfied, thus demonstrating that buckling of the BWR canister does not occur.

Table 2.7.9.3-1 Buckling Evaluation Results for the BWR Canister for 30-Foot End Drop

Load Condition	Longitudinal (Axial) Stress* S_ϕ (psi)	Circumferential (Hoop) Stress* S_θ (psi)	In-plane Shear Stress $S_{\phi\theta}$ (psi)	Elastic Buckling Interaction Equations				Plastic Buckling Interaction Equations			
				Q1	Q2	Q3	Q4	Q5	Q6	Q7	Q8
30-Ft Top End Drop	4300	100	700	.021	.093	.015	.021	.092	.014	.093	.015
30-Ft Bottom End Drop	7100	1300	300	.122	.152	.188	.122	.152	.188	.152	.188

Component stresses include thermal stresses.

* Compressive stresses.

2.7.10 BWR Basket Analysis - Accident Conditions

The BWR fuel basket in the Transportable Storage Canister is designed to contain up to 56 BWR fuel assemblies. The basket structure has a right-circular cylinder configuration and consists of 56 square tubes supported by circular support disks and a circular top and bottom plate that are retained by six axial tie rods. The number of support disks provided in the basket varies, depending upon the class (Class 4 or 5) of BWR fuel the basket is designed to contain. The support disks and top and bottom plates are separated and supported by split spacers at the tie rods. The configuration of the basket is shown in Figure 2.6.15-1. Design of the basket and its components is discussed in detail in Chapter 1.0.

In this section, the BWR fuel basket is evaluated for hypothetical accident loads (evaluation of the basket for normal conditions of transport loads is presented in Section 2.6.15). Both stress analyses and buckling evaluations are performed and documented. The structural analysis of the basket components is in accordance with ASME Code, Section III, Division 1, Subsection NG. In addition, the stainless steel/BORAL composite fuel tube is evaluated for a postulated impact load.

The fuel tubes are not structural components and are not considered in the basket evaluation. The tie rods and spacers locate and structurally assemble the circular support disks, heat transfer disks, and top and bottom plates to form an integral assembly. The spacers carry the weight of the support disks, heat transfer disks, and endplate and their own weight in the 30-ft end-drop accident loading condition. The end-drop loading condition of the spacers is a classical, closed-form analysis and the spacers are evaluated independently of the finite element basket model. A finite element model of a single disk is used to evaluate the support disk structural evaluation. Figure 2.6.15-2 shows the support disk cross-section. For further details of the basket refer to Section 2.6.15.

The basket support disk is designed to restrain 56 fuel assemblies, which would nominally fit into a 6.278-inch square slot. Since a populace of BWR fuel assemblies are not expected to fit into the 6.278-inch square, four oversized fuel assemblies slots are specified as 6.478-inch squares. This will reduce the thickness of the ligament at the outer most corner. However, the size of the web (.65 inch) is not changed. Therefore the oversized slots will not affect the buckling calculations, since they pertain to the in-plane and out of plane buckling of the webs. In an inspection of the maximum stresses of the BWR basket, the ligament, which contains the

reduction due to the oversized slots, does not appear in the maximum stress summaries. The smallest ligament at the corner is still significantly controlled by the .8-inch ligament. Therefore, the use of oversized holes is not considered to alter the model of the BWR basket which employs a slot size of 6.278 inches.

2.7.10.1 Stress Evaluation of Support Disk

To determine the structural adequacy of the support disks, 30-ft-drop accident side impact loads are evaluated for the worst-case radial orientations of the basket. End-drop impact is also considered.

A load equal to the weight of the fuel and tubes multiplied by a 60 *g* amplification factor is applied to the support disk structure to simulate the 30-ft side-drop accident condition. The 60 *g* amplification factor is the design value that envelopes the calculated deceleration values for a 30-ft side-drop accident condition. The fuel assembly loads are transmitted in direct compression through the tube wall to the web structure of each support disk. These loads are transmitted to the canister and to the inner shell by a conservative number of disks, the top weldment, and the bottom weldment. The support disk configuration is analyzed for five worst-case radial orientations (0, 31.82, 49.46, 77.92, and 90°) to bound the possible maximum stress cases. The 31.82, 49.46, and 77.92° orientations are located at the thinnest radial section of the disk perimeter.

For the end-drop condition, the support disk is loaded by the inertia of its own weight multiplied by the 55 *g* end-drop amplification factor. Thermal Case 4 is the limiting boundary condition (See Section 2.6.15.3 for case definition).

To calculate the stresses in a support disk, the ANSYS computer code is used to perform a finite element analysis. In accordance with the ASME Code, Section III, Subsection NG, the maximum primary membrane stress intensity calculated in the support disk is compared with the allowable stress limit, 0.7 S_u or 2.4 S_m, whichever is less. The material strength is taken at the maximum support disk temperature. For the support disk, 2.4 S_m > 0.7 S_u; therefore, 0.7 S_u is limiting.

Temperature boundary conditions are presented in Section 2.6.13.3.

2.7.10.1.1 Finite Element Model Description

Finite element analyses are performed for the basket support disk for two hypothetical accident conditions: the 30-ft side-drop impact condition (60 *g*) and the 30-ft end-drop impact condition (55 *g*). The *g*-loads produced by 30-ft corner-drops and 30-ft oblique drops are bounded by the *g*-loads produced by 30-ft end-drop and side-drop conditions. Therefore, no separate evaluation of 30-ft corner-drop or 30-ft oblique-drop is performed.

The method of analysis of the side-drop impact condition is similar to that used in PWR support disk evaluation (Section 2.7.8.1.1).

An amplification factor of 60 *g* simulates the 30-ft side-drop impact. The thickness option of the planar elements is used to simulate the volume necessary to determine the inertial effects. The fuel weight is simulated as a distributed load over the length of the ligament. The fuel is accelerated by the amplification factor and normalized into horizontal and vertical components on the basis of the orientation angle of the support disk. The amplification factor is oriented in the direction of the drop. A steady-state thermal conduction model is analyzed with temperature boundary conditions from the thermal analyses for the worst thermal case (Thermal Case 2). The resulting nodal temperature distribution is then used as input for the structural model.

The ANSYS finite element model of the support disk for the end-drop impact analysis is generated by changing the PLANE42 elements of the side-drop model to SHELL63 elements. The shell elements are used in the end-drop analyses because they can determine out-of-plane stresses as a result of their extra degrees of freedom. The canister elements and nodes, beam elements, and contact elements in the side-drop model are deleted for the end-drop model.

2.7.10.1.2 Impact Loading Conditions

The lateral impact load applied on the support disk for a side-drop accident, includes the inertial weights of the canister, fuel assemblies, and stainless steel tubes and the weight of the support disk itself. A detailed description of the loadings is provided in Section 2.6.15.2. The heat transfer disks are considered to be self-supporting. A 60 *g*-load factor is used to amplify the weight of the basket components for the 30-ft side-drop condition.

2.7.10.1.3 Side-Drop Analysis Results

Finite element stress analyses are performed for the 60g side impact load cases for five different radial basket orientations—0, 31.82, 49.46, 77.92, and 90°. The analysis section locations are defined in Section 2.6.15.6 and in Figures 2.6.15.6-2 through 2.6.15.6-5. The stress evaluations are performed in accordance with the ASME Code, Section III, Division 1, Subsection NG. The calculated stresses for the sections with the lowest margins of safety are presented in Tables 2.7.10.1-2 through 2.7.10.1-21. The minimum margin of safety is +0.12 for primary membrane stress at Section 27 for the Thermal Case 1 side-drop with the basket orientation equal to 90° (Table 2.7.10.1-18). The minimum margin of safety for all side-drop analysis results are summarized in Table 2.7.10.1-1.

2.7.10.1.4 End-Drop Analysis Results

Finite element stress analyses of the BWR basket support disk are performed for a 55 *g* end impact (30-ft end-drop) on the cask and canister for Thermal Case 1 and for Thermal Case 4. Three layers of stresses are obtained from the shell elements used to model the support disk: primary membrane plus bending stress at the top layer, primary membrane stress at the middle layer, and primary membrane plus bending stress at the bottom layer. The maximum stresses in the support disk for the 30-ft end-drop accident condition are summarized in Table 2.7.10.1-22.

The margin of safety is

$$MS = (Allowable/Stress) - 1.$$

For conservatism, the allowable stresses are interpolated to the maximum disk temperature for the hot thermal condition. From these results, Thermal Case 4 with no thermal stresses has the lowest margin of safety, **+ 0.01**, principally as a result of bending loads, using an allowable stress intensity of 90 ksi.

The allowable stresses are taken at a temperature of 500°F, which is conservative, given the fact that the maximum stresses occur at the outer edges of the disk where the temperatures are lower.

Table 2.7.10.1-1 Summary of Stress Evaluation of Support Disk - 30-Foot Side-Drop

Table Number	Basket Orientation (deg)	Thermal Case	Stress Evaluation	Minimum Margin of Safety
2.7.10.1-2	0	1	P_m	+ 0.49
2.7.10.1-3	0	1	$P_m + P_b$	+ 0.61
2.7.10.1-4	0	2	P_m	+ 0.47
2.7.10.1-5	0	2	$P_m + P_b$	+ 0.60
2.7.10.1-6	31.82	1	P_m	+ 0.75
2.7.10.1-7	31.82	1	$P_m + P_b$	+ 0.16
2.7.10.1-8	31.82	2	P_m	+ 0.72
2.7.10.1-9	31.82	2	$P_m + P_b$	+ 0.15
2.7.10.1-10	49.46	1	P_m	+ 0.82
2.7.10.1-11	49.46	1	$P_m + P_b$	+ 0.36
2.7.10.1-12	49.46	2	P_m	+ 0.60
2.7.10.1-13	49.46	2	$P_m + P_b$	+ 0.32
2.7.10.1-14	77.92	1	P_m	+ 0.46
2.7.10.1-15	77.92	1	$P_m + P_b$	+ 0.35
2.7.10.1-16	77.92	2	P_m	+ 0.46
2.7.10.1-17	77.92	2	$P_m + P_b$	+ 0.35
2.7.10.1-18	90	1	P_m	+ 0.12
2.7.10.1-19	90	1	$P_m + P_b$	+ 0.59
2.7.10.1-20	90	2	P_m	+ 0.13
2.7.10.1-21	90	2	$P_m + P_b$	+ 0.59

Table 2.7.10.1-2 P_m Stresses for Support Disk 30-Foot Side-Drop, 0° Orientation, Thermal Case 1

Section	Stress (ksi)			Stress Intensity (ksi)	Stress Allowable (ksi)	Margin of Safety
	Sx	Sy	Sxy			
293	14.9	-27.4	-0.3	42.4	63.0	0.49
294	17.8	-23.7	-0.8	41.6	63.0	0.52
298	-0.3	-40.3	0.0	40.3	63.0	0.56
227	13.5	-25.7	0.0	39.2	63.0	0.61
232	-0.2	-37.6	-0.5	37.6	63.0	0.68
299	-0.2	-36.7	0.7	36.8	63.0	0.71
290	-0.2	-35.6	0.1	35.6	63.0	0.77
300	10.7	-24.9	0.2	35.6	63.0	0.77
228	14.5	-20.8	0.7	35.3	63.0	0.79
284	10.8	-23.8	-0.1	34.6	63.0	0.82
224	-0.2	-33.2	-0.2	33.2	63.0	0.90
301	9.1	-22.4	-4.0	32.6	63.0	0.93
218	9.8	-22.2	0.4	32.0	63.0	0.97
233	-0.1	-31.9	-0.8	31.9	63.0	0.98
285	12.0	-19.8	-0.6	31.8	63.0	0.98
296	-1.5	-31.6	0.2	31.6	63.0	0.99
259	12.0	-18.6	3.6	31.4	63.0	1.01
291	-0.2	-31.0	0.6	31.0	63.0	1.03
281	-0.2	-31.0	0.1	31.0	63.0	1.03
263	11.7	-16.6	-5.9	30.8	63.0	1.05

Table 2.7.10.1-3 $P_m + P_b$ Stresses for Support Disk 30-Foot Side-Drop, 0° Orientation, Thermal Case 1

Section	Stress (ksi)			Stress Intensity (ksi)	Stress Allowable (ksi)	Margin of Safety
	Sx	Sy	Sxy			
16	-31.2	-35.4	-22.4	55.8	90.0	0.61
15	-29.3	-32.8	19.6	50.7	90.0	0.77
301	7.1	-36.7	-10.8	48.8	90.0	0.84
293	14.0	-29.0	-1.5	43.1	90.0	1.09
297	-14.2	-39.9	-8.5	42.5	90.0	1.12
294	8.5	-33.3	-0.4	41.8	90.0	1.15
298	-0.3	-40.6	0.0	40.6	90.0	1.22
234	3.9	-31.3	9.8	40.3	90.0	1.23
227	18.1	-22.1	-1.2	40.3	90.0	1.24
232	-0.4	-39.7	-0.4	39.7	90.0	1.27
299	-0.5	-39.6	0.7	39.6	90.0	1.28
263	35.0	-3.6	-4.1	39.4	90.0	1.28
235	-2.8	-35.6	10.6	39.2	90.0	1.30
231	-11.8	-36.8	7.1	38.6	90.0	1.33
300	10.8	-24.9	7.3	38.6	90.0	1.33
259	20.7	-16.8	1.3	37.6	90.0	1.39
230	-5.5	-36.0	7.1	37.5	90.0	1.40
262	15.2	-21.9	2.4	37.4	90.0	1.41
260	22.7	-14.1	-1.8	37.0	90.0	1.44
288	-14.2	-33.6	-7.8	36.3	90.0	1.48

Table 2.7.10.1-4 P_m Stresses for Support Disk 30-Foot Side-Drop, 0° Orientation, Thermal Case 2

Section	Stress (ksi)			Stress Intensity (ksi)	Stress Allowable (ksi)	Margin of Safety
	Sx	Sy	Sxy			
293	15.2	-27.6	-0.3	42.8	63.0	0.47
294	18.0	-23.7	-0.8	41.7	63.0	0.51
298	-0.3	-40.6	0.0	40.6	63.0	0.55
227	13.8	-25.9	0.0	39.6	63.0	0.59
232	-0.2	-37.9	-0.5	37.9	63.0	0.66
299	-0.2	-36.8	0.8	36.8	63.0	0.71
300	11.7	-25.0	0.1	36.7	63.0	0.72
290	-0.2	-35.8	0.1	35.8	63.0	0.76
228	14.5	-20.9	0.7	35.7	63.0	0.76
284	10.8	-23.9	-0.1	34.9	63.0	0.81
224	-0.2	-33.5	-0.2	33.5	63.0	0.88
301	9.1	-22.5	-4.4	33.4	63.0	0.88
218	9.8	-22.4	0.4	32.3	63.0	0.95
233	-0.1	-32.1	-0.8	32.2	63.0	0.96
296	12.0	-31.9	0.1	31.9	63.0	0.98
285	-1.5	-19.8	-0.6	31.8	63.0	0.98
259	12.0	-18.7	3.6	31.7	63.0	0.99
281	-0.2	-31.2	0.1	31.2	63.0	1.02
263	-0.2	-16.9	-0.6	31.1	63.0	1.02
291	11.7	-31.0	0.6	31.0	63.0	1.03

Table 2.7.10.1-5 $P_m + P_b$ Stresses for Support Disk 30-Foot Side-Drop, 0° Orientation, Thermal Case 2

Section	Stress (ksi)			Stress Intensity (ksi)	Stress Allowable (ksi)	Margin of Safety
	Sx	Sy	Sxy			
16	-32.0	-35.3	-22.6	56.3	90.0	0.60
15	-30.0	-33.0	19.9	51.5	90.0	0.75
301	7.7	-37.7	-11.1	50.5	90.0	0.78
293	14.1	-29.3	-1.4	43.5	90.0	1.07
297	-14.7	-40.7	-8.7	43.3	90.0	1.08
294	27.8	-13.9	-1.2	41.8	90.0	1.15
234	4.8	-31.6	9.9	41.4	90.0	1.18
298	-0.3	-40.9	0.0	40.9	90.0	1.20
235	-2.0	-36.5	10.9	40.8	90.0	1.21
227	18.4	-22.2	-1.2	40.8	90.0	1.21
232	-0.4	-40.0	-0.4	40.0	90.0	1.25
299	-0.6	-39.9	0.7	39.9	90.0	1.25
263	35.6	-3.4	-4.1	39.8	90.0	1.26
231	-12.4	-37.6	7.3	39.5	90.0	1.28
300	11.5	-25.3	-7.0	39.4	90.0	1.39
259	20.9	-17.0	1.4	38.1	90.0	1.37
230	-5.7	-36.3	7.2	37.9	90.0	1.37
260	23.3	-14.0	-1.9	37.5	90.0	1.40
262	15.0	-22.1	2.5	37.4	90.0	1.41
288	-14.4	-33.8	-7.8	36.6	90.0	1.46

Table 2.7.10.1-6 P_m Stresses for Support Disk 30-Foot Side-Drop, 31.82° Orientation, Thermal Case 1

	Stresses (ksi)			Stress	Stress	Margin of
Section	Sx	Sy	Sxy	Intensity (ksi)	Allow(ksi)	Safety
246	-17.9	10.0	11.3	35.9	63.0	.75
234	6.4	-18.4	12.2	34.9	63.0	.81
300	10.3	-18.8	9.2	34.4	63.0	.83
235	-2.4	-13.7	15.0	32.0	63.0	.97
298	-.3	-31.8	-1.4	31.8	63.0	.98
293	4.7	-21.0	7.0	29.3	63.0	1.15
243	-16.4	9.4	6.3	28.7	63.0	1.20
299	-.2	-28.5	-.8	28.5	63.0	1.21
229	-18.6	3.8	8.8	28.5	63.0	1.21
232	-.2	-27.8	-2.0	28.0	63.0	1.25
290	-.2	-27.6	-2.0	27.8	63.0	1.27
245	-27.3	-.2	-2.1	27.5	63.0	1.29
227	5.0	-18.3	6.8	27.0	63.0	1.33
277	7.8	-10.2	9.6	26.3	63.0	1.39
301	7.3	-16.4	5.7	26.3	63.0	1.40
294	3.6	-18.3	7.2	26.3	63.0	1.40
54	.0	-14.9	10.3	25.4	63.0	1.48
295	2.8	-14.0	9.3	25.0	63.0	1.52
263	-8.3	-24.8	-1.4	24.9	63.0	1.53
257	-6.4	5.5	10.9	24.9	63.0	1.53

Table 2.7.10.1-7 $P_m + P_b$ Stresses for Support Disk 30-Foot Side-Drop, 31.82° Orientation, Thermal Case 1

	Stresses (ksi)			Stress	Stress	Margin of
Section	Sx	Sy	Sxy	Intensity (ksi)	Allow(ksi)	Safety
274	-46.2	-73.0	12.5	77.9	90.0	.16
208	-47.6	-72.5	11.7	77.2	90.0	.17
266	-55.9	-67.6	12.6	75.6	90.0	.19
200	-56.6	-67.2	12.0	75.0	90.0	.20
275	-43.7	-67.2	12.3	72.4	90.0	.24
209	-48.7	-65.5	10.6	70.6	90.0	.27
267	-54.2	-61.6	12.1	70.5	90.0	.28
74	-46.3	-66.0	9.2	69.6	90.0	.29
137	-48.2	-65.8	9.1	69.6	90.0	.29
82	-45.2	-63.6	10.8	68.6	90.0	.31
173	-51.5	-62.3	9.8	68.1	90.0	.32
238	-50.7	-61.8	10.5	68.1	90.0	.32
145	-46.6	-62.8	10.2	67.7	90.0	.33
201	-52.8	-59.9	9.4	66.4	90.0	.36
18	-61.7	-55.1	7.0	66.2	90.0	.36
32	-62.0	-55.6	6.1	65.7	90.0	.37
234	-1.2	-54.9	18.4	65.1	90.0	.38
176	-52.4	-58.3	9.2	65.1	90.0	.38
21	-60.7	-50.8	7.1	64.4	90.0	.40
241	-49.1	-57.0	10.4	64.2	90.0	.40

Table 2.7.10.1-8 P_m Stresses for Support Disk 30-Foot Side-Drop, 31.82° Orientation, Thermal Case 2

	Stresses (ksi)			Stress	Stress	Margin of
Section	Sx	Sy	Sxy	Intensity (ksi)	Allow(ksi)	Safety
246	-17.9	10.2	11.8	36.7	63.0	.72
300	11.4	-18.7	9.7	35.8	63.0	.76
234	6.1	-18.4	12.8	35.5	63.0	.78
235	-3.0	-13.7	15.4	32.6	63.0	.93
298	-.3	-31.9	-1.5	32.0	63.0	.97
229	-19.3	4.0	9.1	29.5	63.0	1.13
293	4.8	-21.1	7.1	29.5	63.0	1.14
243	-16.5	10.0	6.2	29.2	63.0	1.15
299	-.2	-28.9	-.8	28.9	63.0	1.18
277	8.7	-11.3	10.2	28.4	63.0	1.22
290	-.2	-27.7	-2.1	27.8	63.0	1.26
232	-.2	-27.6	-2.1	27.8	63.0	1.27
301	8.7	-16.4	5.9	27.8	63.0	1.27
245	-27.5	-.2	-2.2	27.7	63.0	1.28
294	3.9	-18.5	7.4	26.9	63.0	1.34
227	4.8	-18.2	6.9	26.8	63.0	1.35
257	-6.3	6.2	11.6	26.4	63.0	1.38
54	-.1	-15.5	10.7	26.3	63.0	1.39
263	-8.5	-25.3	-1.6	25.4	63.0	1.48
295	2.5	-13.8	9.6	25.2	63.0	1.50

Table 2.7.10.1-9 $P_m + P_b$ Stresses for Support Disk 30-Foot Side-Drop, 31.82° Orientation, Thermal Case 2

	Stresses (ksi)			Stress	Stress	Margin of
Section	Sx	Sy	Sxy	Intensity (ksi)	Allow(ksi)	Safety
274	-46.7	-73.6	12.6	78.6	90.0	.15
208	-48.2	-72.9	11.7	77.5	90.0	.16
266	-55.0	-67.7	12.5	75.3	89.8	.19
200	-56.2	-66.9	12.0	74.7	89.8	.20
275	-44.5	-68.5	12.5	73.9	90.0	.22
267	-54.5	-62.9	12.2	71.6	90.0	.26
209	-49.5	-66.3	10.7	71.5	90.0	.26
74	-45.8	-65.3	9.1	68.9	89.8	.30
238	-51.3	-62.3	10.5	68.7	90.0	.31
82	-45.3	-63.7	10.7	68.6	90.0	.31
173	-52.1	-62.7	9.8	68.6	90.0	.31
137	-47.2	-64.7	8.7	68.3	89.8	.31
145	-46.6	-62.5	10.0	67.3	90.0	.34
201	-53.2	-60.5	9.5	67.1	90.0	.34
234	-1.7	-56.5	19.0	66.6	90.0	.35
176	-53.3	-59.1	9.4	66.0	90.0	.36
276	-43.5	-58.9	12.1	65.5	90.0	.37
235	-11.8	-59.1	18.4	65.4	90.0	.38
241	-49.9	-58.2	10.5	65.3	90.0	.38
18	-60.5	-55.1	6.8	65.1	89.8	.38

Table 2.7.10.1-10 P_m Stresses for Support Disk 30-Foot Side-Drop, 49.46° Orientation, Thermal Case 1

	Stresses (ksi)			Stress	Stress	Margin of
Section	Sx	Sy	Sxy	Intensity (ksi)	Allow(ksi)	Safety
246	-19.3	8.0	10.6	34.5	63.0	.82
27	-18.1	7.0	8.4	30.2	63.0	1.09
85	-25.6	2.5	5.3	30.0	63.0	1.10
300	10.0	-13.7	8.9	29.7	63.0	1.12
234	3.6	-13.6	11.8	29.2	63.0	1.15
245	-28.3	-.2	-1.8	28.4	63.0	1.22
269	-28.3	-.9	.3	28.3	63.0	1.23
243	-17.9	8.1	5.5	28.2	63.0	1.23
235	-4.5	-9.9	13.1	26.8	63.0	1.35
29	-26.8	-.2	-.6	26.8	63.0	1.35
103	-11.2	7.8	9.2	26.4	63.0	1.39
65	-13.1	-5.4	12.1	25.4	63.0	1.48
229	-16.1	3.5	8.0	25.3	63.0	1.49
257	-10.6	4.7	9.6	24.6	63.0	1.56
242	-23.8	-.2	-1.9	24.0	63.0	1.63
28	-21.5	-5.6	-6.7	23.9	63.0	1.63
298	-.3	-23.9	-1.3	23.9	63.0	1.63
5	-17.6	-7.3	9.9	23.5	63.0	1.68
265	-9.1	11.0	5.7	23.2	63.0	1.72
26	-22.9	-.3	-2.1	23.1	63.0	1.72

Table 2.7.10.1-11 $P_m + P_b$ Stresses for Support Disk 30-Foot Side-Drop, 49.46° Orientation, Thermal Case 1

	Stresses (ksi)			Stress	Stress	Margin of
Section	Sx	Sy	Sxy	Intensity (ksi)	Allow(ksi)	Safety
74	-46.5	-60.1	11.0	66.2	90.0	.36
137	-47.3	-59.1	10.5	65.2	90.0	.38
27	-62.1	-16.6	11.7	64.9	90.0	.39
274	-42.1	-59.5	10.5	64.4	90.0	.40
208	-43.3	-59.3	10.0	64.1	90.0	.40
24	-62.0	-30.5	7.7	63.8	90.0	.41
21	-60.7	-38.6	7.0	62.7	90.0	.44
18	-60.3	-43.0	6.7	62.6	90.0	.44
75	-45.4	-55.1	10.7	62.0	90.0	.45
266	-51.7	-52.1	10.1	62.0	90.0	.45
200	-51.1	-51.9	9.3	60.9	90.0	.48
32	-58.6	-43.6	5.6	60.4	90.0	.49
138	-47.3	-52.6	9.7	60.1	90.0	.50
209	-43.6	-53.6	9.2	59.0	90.0	.52
82	-44.8	-53.4	9.0	59.0	90.0	.52
275	-40.3	-53.4	10.1	58.9	90.0	.53
173	-47.8	-51.9	8.7	58.8	90.0	.53
238	-47.3	-51.2	9.2	58.6	90.0	.54
267	-50.9	-45.8	9.5	58.2	90.0	.55
246	-54.7	-6.6	11.9	57.5	90.0	.57

Table 2.7.10.1-12 P_m Stresses for Support Disk 30-Foot Side-Drop, 49.46° Orientation, Thermal Case 2

	Stresses (ksi)			Stress	Stress	Margin of
Section	Sx	Sy	Sxy	Intensity (ksi)	Allow(ksi)	Safety
246	-21.1	11.3	11.1	39.3	63.0	.60
243	-19.6	10.5	5.7	32.1	63.0	.96
245	-31.2	-.2	-1.9	31.3	63.0	1.01
300	10.0	-13.5	9.4	30.1	63.0	1.09
85	-25.2	2.1	6.2	30.0	63.0	1.10
234	3.1	-13.4	12.2	29.4	63.0	1.14
27	-17.1	5.5	8.4	28.2	63.0	1.24
269	-27.3	-1.3	1.4	27.4	63.0	1.30
235	-4.8	-9.9	13.4	27.2	63.0	1.31
103	-11.5	8.1	9.4	27.2	63.0	1.32
242	-26.2	-.2	-2.0	26.4	63.0	1.39
257	-11.1	5.8	9.9	26.0	63.0	1.42
229	-16.4	3.6	8.2	25.9	63.0	1.44
65	-12.9	-5.5	12.4	25.8	63.0	1.44
29	-25.0	-.2	-.9	25.1	63.0	1.51
244	-24.7	-14.0	.6	24.7	63.0	1.55
240	-15.8	5.3	5.9	24.2	63.0	1.61
256	-23.6	-.2	-1.4	23.7	63.0	1.66
298	-.3	-23.5	-1.4	23.6	63.0	1.67
265	-8.9	11.3	5.8	23.3	63.0	1.71

Table 2.7.10.1-13 $P_m + P_b$ Stresses for Support Disk 30-Foot Side-Drop, 49.46° Orientation, Thermal Case 2

	Stresses (ksi)			Stress	Stress	Margin of
Section	Sx	Sy	Sxy	Intensity (ksi)	Allow(ksi)	Safety
274	-44.8	-62.5	11.5	68.1	90.0	.32
27	-64.6	-21.4	11.7	67.5	90.0	.33
208	-45.6	-61.8	10.8	67.2	90.0	.34
74	-47.7	-60.6	11.0	66.9	89.8	.34
24	-64.3	-34.1	7.6	66.1	90.0	.36
137	-47.8	-59.2	10.2	65.2	89.8	.38
21	-62.5	-41.6	7.0	64.6	90.0	.39
275	-43.4	-57.6	11.4	63.9	90.0	.41
75	-47.3	-56.9	10.7	63.8	90.0	.41
266	-52.4	-54.1	10.3	63.6	89.8	.41
18	-60.7	-44.8	6.6	63.1	89.8	.42
200	-52.1	-53.5	9.6	62.5	89.8	.44
209	-45.8	-56.4	10.0	62.4	90.0	.44
238	-50.6	-53.9	10.0	62.4	90.0	.44
173	-50.6	-54.2	9.5	62.0	90.0	.45
32	-59.4	-45.0	5.6	61.3	89.9	.47
267	-53.0	-49.4	10.1	61.4	90.0	.47
138	-48.7	-53.9	9.6	61.3	90.0	.47
246	-58.6	-5.3	11.9	61.1	90.0	.47
82	-45.2	-55.2	9.2	60.7	90.0	.48

Table 2.7.10.1-14 P_m Stresses for Support Disk 30-Foot Side-Drop, 77.92° Orientation, Thermal Case 1

	Stresses (ksi)			Stress	Stress	Margin of
Section	Sx	Sy	Sxy	Intensity (ksi)	Allow(ksi)	Safety
27	-26.3	14.3	7.4	43.1	63.0	.46
246	-25.2	12.9	9.6	42.5	63.0	.48
85	-30.5	10.5	4.1	41.8	63.0	.51
269	-31.4	9.1	-1.3	40.5	63.0	.55
29	-37.9	-.1	-.4	37.9	63.0	.66
243	-23.6	12.2	4.8	37.1	63.0	.70
245	-36.1	-.3	-1.6	36.1	63.0	.74
5	-24.4	-18.4	12.3	34.1	63.0	.85
24	-22.7	9.6	3.9	33.2	63.0	.90
26	-33.0	-.3	-1.9	33.1	63.0	.90
265	-16.6	13.5	6.8	33.1	63.0	.90
28	-30.7	-2.3	-6.0	31.9	63.0	.97
256	-31.8	-.2	-1.0	31.8	63.0	.98
240	-19.7	11.2	2.8	31.4	63.0	1.00
242	-31.0	-.2	-1.8	31.1	63.0	1.03
254	-21.2	7.9	4.7	30.6	63.0	1.06
23	-28.5	-.2	-2.3	28.7	63.0	1.19
244	-28.3	-7.8	.5	28.3	63.0	1.22
65	-16.7	-4.7	12.8	28.3	63.0	1.23
262	-15.2	12.4	1.2	27.7	63.0	1.27

Table 2.7.10.1-15 $P_m + P_b$ Stresses for Support Disk 30-Foot Side-Drop, 77.92° Orientation, Thermal Case 1

	Stresses (ksi)			Stress	Stress	Margin of
Section	Sx	Sy	Sxy	Intensity (ksi)	Allow(ksi)	Safety
27	-64.6	-5.4	11.1	66.6	90.0	.35
24	-64.8	-22.4	7.7	66.2	90.0	.36
22	-61.1	-37.9	8.4	63.8	90.0	.41
65	-54.7	-12.7	17.7	61.1	90.0	.47
246	-54.6	1.6	11.6	60.9	90.0	.48
75	-49.8	-42.0	12.0	58.5	90.0	.54
241	-53.8	-35.9	10.2	58.4	90.0	.54
54	-54.3	-14.1	13.6	58.4	90.0	.54
9	-45.1	-37.3	16.3	58.0	90.0	.55
19	-54.9	-36.3	7.3	57.4	90.0	.57
243	-56.2	-14.3	5.8	57.0	90.0	.58
21	-55.7	-25.2	4.4	56.3	90.0	.60
25	-53.8	-33.8	6.2	55.6	90.0	.62
5	-43.9	-45.8	10.6	55.5	90.0	.62
51	-52.9	-29.0	7.5	55.0	90.0	.64
74	-45.3	-40.7	10.9	54.1	90.0	.66
238	-48.2	-35.1	9.3	53.0	90.0	.70
31	-49.9	-35.1	6.4	52.3	90.0	.72
268	-50.1	-22.4	7.4	51.9	90.0	.73
244	-48.3	-31.9	8.3	51.8	90.0	.74

Table 2.7.10.1-16 P_m Stresses for Support Disk 30-Foot Side-Drop, 77.92° Orientation, Thermal Case 2

	Stresses (ksi)			Stress	Stress	Margin of
Section	Sx	Sy	Sxy	Intensity (ksi)	Allow(ksi)	Safety
246	-25.2	13.4	9.7	43.2	63.0	.46
27	-25.9	14.1	7.4	42.6	63.0	.48
85	-30.7	10.6	4.1	42.1	63.0	.50
269	-31.2	9.2	-1.1	40.4	63.0	.56
243	-23.7	12.8	4.5	37.6	63.0	.67
29	-37.4	-.1	-.4	37.4	63.0	.69
245	-36.2	-.3	-1.6	36.3	63.0	.74
5	-24.4	-18.6	12.3	34.1	63.0	.85
24	-22.4	9.7	3.7	32.9	63.0	.91
26	-32.5	-.3	-1.9	32.6	63.0	.93
265	-16.1	13.8	6.5	32.6	63.0	.93
256	-32.1	-.2	-1.0	32.1	63.0	.96
240	-19.8	11.2	2.9	31.5	63.0	1.00
28	-30.3	-2.0	-6.0	31.5	63.0	1.00
242	-31.1	-.2	-1.8	31.2	63.0	1.02
254	-21.4	8.5	4.3	31.2	63.0	1.02
65	-16.9	-4.8	12.9	28.5	63.0	1.21
244	-28.5	-7.6	.7	28.5	63.0	1.21
23	-28.1	-.2	-2.3	28.3	63.0	1.22
253	-27.9	-.2	-1.4	28.0	63.0	1.25

Table 2.7.10.1-17 $P_m + P_b$ Stresses for Support Disk 30-Foot Side-Drop, 77.92° Orientation, Thermal Case 2

	Stresses (ksi)			Stress	Stress	Margin of
Section	Sx	Sy	Sxy	Intensity (ksi)	Allow(ksi)	Safety
27	-64.7	-6.0	11.1	66.7	90.0	.35
24	-63.6	-22.0	7.4	64.9	90.0	.39
22	-59.8	-37.1	8.2	62.4	90.0	.44
65	-55.2	-12.8	17.8	61.7	90.0	.46
246	-55.1	1.8	11.6	61.5	90.0	.46
54	-54.7	-14.2	13.7	58.9	90.0	.53
9	-45.5	-37.6	16.4	58.5	90.0	.54
241	-53.0	-35.5	10.1	57.6	90.0	.56
75	-48.8	-41.1	11.7	57.3	90.0	.57
243	-55.4	-13.4	5.4	56.1	90.0	.60
19	-53.5	-35.0	7.2	56.0	89.9	.61
5	-43.9	-46.2	10.6	55.7	90.0	.62
25	-53.9	-33.1	6.2	55.6	90.0	.62
21	-54.8	-24.8	4.5	55.5	90.0	.62
51	-52.1	-28.4	7.2	54.2	90.0	.66
74	-44.1	-39.2	10.6	52.6	89.8	.71
244	-49.0	-31.7	8.5	52.5	90.0	.71
238	-47.7	-34.6	9.3	52.5	90.0	.71
103	6.4	49.1	9.9	51.3	90.0	.76
76	25.2	49.4	6.8	51.2	90.0	.76

Table 2.7.10.1-18 P_m Stresses for Support Disk 30-Foot Side-Drop, 90° Orientation, Thermal Case 1

	Stresses (ksi)			Stress	Stress	Margin of
Section	Sx	Sy	Sxy	Intensity (ksi)	Allow(ksi)	Safety
27	-31.0	25.4	.0	56.4	63.0	.12
77	-19.0	28.8	4.5	48.7	63.0	.29
269	-19.0	28.8	-4.5	48.7	63.0	.29
85	-20.9	26.6	.2	47.4	63.0	.33
277	-20.9	26.6	-.2	47.4	63.0	.33
54	-24.8	19.4	.3	44.2	63.0	.43
246	-24.8	19.4	-.3	44.2	63.0	.43
29	-43.6	-.2	.0	43.6	63.0	.44
28	-35.8	6.7	.0	42.5	63.0	.48
24	-26.8	13.6	.0	40.3	63.0	.56
26	-38.4	-.4	.0	38.4	63.0	.64
6	-19.1	-30.4	-11.3	37.4	63.0	.68
5	-19.1	-30.4	11.3	37.4	63.0	.68
273	.3	37.0	.4	37.0	63.0	.70
81	.3	37.0	-.4	37.0	63.0	.70
51	-22.8	12.1	.2	34.9	63.0	.80
243	-22.8	12.1	-.2	34.9	63.0	.80
53	-33.8	-.3	-.3	33.8	63.0	.86
245	-33.8	-.3	.3	33.8	63.0	.86
23	-33.6	-.2	.0	33.6	63.0	.88

Table 2.7.10.1-19 $P_m + P_b$ Stresses for Support Disk 30-Foot Side-Drop, 90° Orientation, Thermal Case 1

	Stresses (ksi)			Stress	Stress	Margin of
Section	Sx	Sy	Sxy	Intensity (ksi)	Allow(ksi)	Safety
77	-15.9	40.4	3.8	56.8	90.0	.59
269	-15.9	40.4	-3.8	56.8	90.0	.59
27	-31.0	25.4	-2.3	56.6	90.0	.59
246	-33.6	15.4	-2.5	49.2	90.0	.83
54	-33.6	15.4	2.5	49.2	90.0	.83
85	-20.3	28.6	-.8	48.9	90.0	.84
277	-20.3	28.6	.8	48.9	90.0	.84
28	-35.8	6.7	7.2	44.8	90.0	1.01
5	-25.6	-35.0	13.0	44.1	90.0	1.04
6	-25.6	-35.0	-13.0	44.1	90.0	1.04
29	-43.6	-.2	.2	43.6	90.0	1.06
273	.7	41.2	.4	41.2	90.0	1.19
81	.7	41.2	-.4	41.2	90.0	1.19
24	-26.8	13.6	-4.0	41.1	90.0	1.19
257	-35.3	-1.0	-10.8	40.5	90.0	1.22
65	-35.3	-1.0	10.8	40.5	90.0	1.22
26	-38.4	-.4	-.2	38.4	90.0	1.34
10	-29.6	-19.7	-10.6	36.3	90.0	1.48
9	-29.6	-19.7	10.6	36.3	90.0	1.48
63	-33.6	-11.3	6.7	35.5	90.0	1.54

Table 2.7.10.1-20 P_m Stresses for Support Disk 30-Foot Side-Drop, 90° Orientation, Thermal Case 2

	Stresses (ksi)			Stress	Stress	Margin of
Section	Sx	Sy	Sxy	Intensity (ksi)	Allow(ksi)	Safety
27	-30.6	25.4	.0	56.0	63.0	.13
77	-18.8	28.8	4.5	48.4	63.0	.30
269	-18.8	28.8	-4.5	48.4	63.0	.30
85	-20.8	26.5	.2	47.3	63.0	.33
277	-20.8	26.5	-.2	47.3	63.0	.33
54	-24.7	19.4	.3	44.1	63.0	.43
246	-24.7	19.4	-.3	44.1	63.0	.43
29	-43.1	-.2	.0	43.1	63.0	.46
28	-35.4	6.7	.0	42.1	63.0	.50
24	-26.4	13.5	.0	39.9	63.0	.58
26	-37.9	-.4	.0	37.9	63.0	.66
6	-19.0	-30.5	-11.3	37.4	63.0	.69
5	-19.0	-30.5	11.3	37.4	63.0	.69
273	.3	36.9	.4	36.9	63.0	.71
81	.3	36.9	-.4	36.9	63.0	.71
51	-22.8	12.1	.2	34.8	63.0	.81
243	-22.8	12.1	-.2	34.8	63.0	.81
53	-33.7	-.3	-.3	33.7	63.0	.87
245	-33.7	-.3	.3	33.7	63.0	.87
23	-33.1	-.2	.0	33.1	63.0	.90

Table 2.7.10.1-21 $P_m + P_b$ Stresses for Support Disk 30-Foot Side-Drop, 90° Orientation, Thermal Case 2

Section	Stress (ksi)			Stress Intensity (ksi)	Stress Allow (ksi)	Margin of Safety
	Sx	Sy	Sxy			
77	-15.7	40.2	3.9	56.4	90.0	.59
269	-15.7	40.2	-3.9	56.4	90.0	.59
27	-30.6	25.4	-2.2	56.1	90.0	.60
246	-33.5	15.4	-2.4	49.1	90.0	.83
54	-33.5	15.4	2.4	49.1	90.0	.83
85	-20.2	28.6	-0.8	48.8	90.0	.84
277	-20.2	28.6	0.8	48.8	90.0	.84
28	-35.4	6.7	7.1	44.4	90.0	1.03
5	-25.3	-34.9	13.0	44.0	90.0	1.05
6	-25.3	-34.9	-13.0	44.0	90.0	1.05
29	-43.1	-0.2	0.2	43.1	90.0	1.09
273	0.7	41.1	0.3	41.1	90.0	1.19
81	0.7	41.1	-0.3	41.1	90.0	1.19
24	-26.4	13.5	-3.9	40.7	90.0	1.21
257	-35.3	-1.0	-10.8	40.6	90.0	1.22
65	-35.3	-1.0	10.8	40.6	90.0	1.22
26	-37.9	-0.4	-0.2	38.0	90.0	1.37
10	-29.8	-19.8	-10.6	36.5	90.0	1.47
9	-29.8	-19.8	10.6	36.5	90.0	1.47
63	-33.5	-11.3	6.7	35.4	90.0	1.54

Table 2.7.10.1-22 Summary of Stress Evaluations of Support Disk - 30-Foot End-Drop

Table Number	g Load	Thermal Case	Stress Evaluation	Minimum Margin of Safety
2.7.10.1-23	55	1	$P_m + P_b$	+.02
2.7.10.1-24	55	4	$P_m + P_b$	+.01

Table 2.7.10.1-23 $P_m + P_b$ Stresses for Support Disk 30-Foot End-Drop, Thermal Case 1

Node	Principal Stresses (ksi)			Stress Intensity (ksi)	Allowable Stress (ksi)*	Margin of Safety
	S1	S2	S3			
86	69.7	0.0	-2.9	72.6	90.0	0.24
474	88.4	5,.3	0.0	88.4	90.0	0.02
1129	81.4	4.0	0.0	81.4	90.0	0.11
1444	88.4	5.8	0.0	88.4	90.0	0.02
1564	69.7	0.0	-2.9	72.6	90.0	0.24
2236	81.4	4.0	0.0	81.4	90.0	0.11
2558	88.4	5.8	0.0	88.4	90.0	0.02
2680	69.7	0.0	-2.9	72.6	90.0	0.24
3332	81.4	4.0	0.0	81.4	90.0	0.11
3647	88.4	5.8	0.0	88.4	90.0	0.02
3765	69.7	0.0	-2.9	72.6	90.0	0.24
4407	81.4	4.0	0.0	81.4	90.0	0.11

*3.0 S_m = 3.0 x 30.0 ksi at 500°F.

Table 2.7.10.1-24 $P_m + P_b$ Stresses for Support Disk 30-Foot End-Drop, Thermal Case 4

Node	Principal Stresses (ksi)			Stress Intensity (ksi)	Allowable Stress (ksi)	Margin of Safety
	S1	S2	S3			
86	70.4	0.0	-2.9	73.3	90.0	0.23
474	89.3	5.9	0.0	89.3	90.0	0.01
1129	82.3	4.0	0.0	82.3	90.0	0.09
1444	89.3	5.9	0.0	89.3	90.0	0.01
1564	70.4	0.0	-2.9	73.3	90.0	0.23
2236	82.3	4.0	0.0	82.3	90.0	0.09
2558	89.3	5.9	0.0	89.3	90.0	0.01
2680	70.4	0.0	-2.9	73.3	90.0	0.23
3332	82.3	4.0	0.0	82.3	90.0	0.09
3647	89.3	5.9	0.0	89.3	90.0	0.01
3765	70.4	0.0	-2.9	73.3	90.0	0.23
4407	82.3	4.0	0.0	82.3	90.0	0.09

*3.0 S_m = 3.0 x 30.0 ksi at 500°F.

2.7.10.2 Stress Evaluation of Tie Rods and Spacers

The tie rods and spacers in the BWR basket are evaluated for structural adequacy following a free drop of the Universal Transport Cask 30 feet onto a flat, unyielding surface. The design deceleration for the cask for the hypothetical accident 30-ft end-drop is 60 *g*.

The structural capacity of the spacers supporting the basket is evaluated by hand calculations using classical analysis. Accident loading resulting from the 30-ft drop of the fuel basket is compared with stress limit of 0.7 S_u in accordance with Section III, Subsection NG of the ASME Code [19].

The tie rods serve basket assembly purposes and are not part of the load path for the condition evaluated. The tie rods are loaded during fabrication by a 190 ft-lb preload. Under drop conditions, the preload will be reduced. The tie rod design is, therefore, acceptable by inspection, and no detailed evaluation of the rods is required.

During the end-drop, the spacers are loaded with the weight of the support disks, the aluminum heat transfer disks, one end plate, and the weight of the spacers. The load is resisted by the effective area of six spacers. The compressive stresses are calculated on the effective area of the spacer.

The material allowable stress is conservatively selected at a bounding temperature of 500°F. The temperature near the outer edge of the support disks (at the tie rods) is below 500°F.

2.7.10.2.1 Design Criteria

Stress limits	=	0.7 S_u (accident condition, more limiting than 2.4 S_m)
Loading criteria (g)	=	60 *g* (accident condition)
Evaluation temperature	=	500°F

Basket Parameters

Fuel basket weight	=	**18,199** lb
Bottom weldment weight	=	**623** lb

Fuel tube weight (56 tubes) = 4,665 lb
Rod diameter = 1.625 in.
Spacer outer diameter = 3.0 in.

Materials [21]
Tie rod = SA 479 Type 304 Stainless Steel
Spacer = SA 479 Type 304 Stainless Steel

Material Allowables
Type 304 stainless steel: S_m = 17,500 psi (500°F)
S_u = 63,500 psi (500°F).

2.7.10.2.2 30-Foot End-Drop Condition—Results

The deceleration assumed for the BWR basket in the 30-ft end-drop is 60 g. The spacers are loaded with the weight of the support disks, the aluminum heat transfer disks, one end plate, and the weight of the spacers. These loads are calculated as follows:

Total weight of basket = 18,199 lb
Less weight of bottom weldment = -623 lb
Less weight of fuel tubes = -4,665 lb
1-g-load on spacers = 12,911 lb
Applied g level = 60 *g*

Therefore, Accident condition
load on spacers = 12,911 x 60 = 774,660 lb

As a result of the end-drop, all spacers are compressed, thus distributing the load through the entire wall of the split spacer. The split spacer at each of six locations supporting the weight of the support disks is equal to the net area of the spacer and is calculated as

$$A = (3.14 \times (3.0^2 - 1.75^2))/(4) = 4.66 \text{ in}^2.$$

The average compressive stress, S_c, in the spacer is

S_c = (774,600)/(6 x 4.66) = 27,706 psi.

The allowable stress for SA479 Type 304 SS under accident conditions of transport is 0.7 S_u:

S_u = 63,500 psi
0.7 S_u = 0.7 x 63,500 = 44,450 psi.

The margin of safety, which is defined as $\frac{0.7S_u}{S_c} - 1$, is

(44,450 / 27,706) - 1 = + 0.60.

Therefore, the spacers are structurally adequate for a 60 *g* end impact under accident conditions.

2.7.10.3 Buckling Evaluation of Support Disk

During the impact following a 30-ft side-drop of the Universal Transport Cask onto an unyielding surface, the support disk is subjected to compressive loading in the plane of the disk. For cask impact orientations other than on the side, loads acting perpendicular to the plane of the support disk (out of plane) may also be applied. The compressive in-plane loadings in conjunction with the bending moments resulting from the out-of-plane loadings require that buckling of the support disk be a design consideration. The acceptance criteria are contained in NUREG/CR-6322.

2.7.10.3.1 Method of Support Disk Buckling Analysis

The support disk buckling evaluation is based on the acceptance criteria of NUREG/CR-6322, which requires that both normal conditions of transport and hypothetical accident conditions be addressed.

The BWR fuel basket support disk material is SA 533, TYPE B, Class 2 with the following characteristics:

The yield strength	S_y = 59.3 ksi at 750°F	(Conservative)
	S_y = 70.0 ksi at -40°F	(Thermal Case 1)
	S_y = 60.5 ksi at 650°F	(Conservative)
The modulus of elasticity	E = 24.60 $(10)^3$ ksi at 750°F	(Conservative)
	E = 29.90 $(10)^3$ ksi at -40°F	(Thermal Case 1)
	E = 25.56E $(10)^3$ ksi at 650°F	(Conservative)

The dynamic amplification factor g = 60 g for the 30-ft side-drop
= 55 g for the 30-ft end-drop

Thermal Case 2 or 4 is bounding for Thermal Case 3. Conservative temperatures are used in the analysis.

2.7.10.3.2 Detailed Support Disk Buckling Analysis

Four thermal conditions are defined in Section 2.7.10.1.1. For these thermal conditions, the maximum forces and moments are determined for the side-drop condition for different radial orientations of the support disk. The buckling evaluation of the support disk web is based on Interaction Equations 31 and 32 in NUREG/CR-6322. These two equations adopt the "Limit Analysis Design" approach for structural members that experience stresses beyond the yield limit of the material, i.e., for members deformed inelastically as a result of both axial load and bending moment. Other equations applicable to the calculations are listed in this section.

Buckling stresses are calculated for both the strong and the weak axes of the support disk webs. In a side-drop condition, the bending moments are in-plane and are about the strong axis. For the weak axis buckling evaluation, the compressive forces from the side-drop are combined with the moments resulting from the end-drop.

Detailed calculations for the accident condition buckling evaluation are performed in a spreadsheet format by using the equations from NUREG/CR-6322. The load amplification factors are 60 g for the side-drop and 55 g for the end-drop. The calculational methodology is the same as the one discussed in Section 2.7.8.3.2 for the PWR support disk buckling analysis.

The loading conditions and the terminology used in the buckling evaluation are also the same as those discussed in Section 2.7.8.3.2.

For the buckling evaluation parameters, different values are associated with the weak and strong axes of the support disk web. The weak axis corresponds to the 0.625-in. support disk thickness and is associated with the moments that would buckle the webs with an out-of-plane motion. Moments that would buckle the support disk web in the plane of the support disk are associated with the strong axis of the web.

Weak-Axis Buckling

For the weak-axis buckling evaluation, the parameters are as follows for (Section 17):

Parameter	Value	Parameter	Value
t	0.625 in.	λ	0.431
b	0.66 in.	P_y	A x S_y = 24,956 ksi
A	0.413 in^2	F_a	43.22
L	6.278 in.	C_c	91.32
I	b t^3 /12 = 0.0134 in^4	P_{cr}	30.31
r	0.18	F_e	250.42
K	0.800	P_e	198.33
KL/r	27.83	M_p	3.83
Z	bt^2 /4 = 0.0614	M_m	3.83
E	25,560 ksi	C_m	0.85
S_y	60.5 ksi		

Using the cross-sectional stresses calculated at each of the sections shown in Figures 2.6.15.6-2 through 2.6.15.6-5 for the 30-ft side-drop condition, the maximum corresponding compressive forces are combined with the maximum out-of-plane moment resulting from the 30-ft end-drop condition to obtain the conservative maximum interaction coefficients.

For weak axis buckling, the minimum margin of safety is +0.002 for the 90° radial basket orientation at Section 17 (thermal stresses are included).

The calculated minimum margins of safety for the drop orientations discussed in Section 2.6.13.6.1 are presented in Table 2.7.10.3-1. The location of the sections identified in the table are shown in Figures 2.6.13.14-2 through 2.6.13.14-5.

Strong-Axis Buckling

For the strong-axis buckling evaluation, the parameters are as follows for (Section 274):

Parameter	Value	Parameter	Value
t	0.65 in.	λ	0.418
b	0.625 in.	P_y	A x S_y = 24.091
A	0.406 in^2	F_a	42.687
L	6.278 in.	C_c	90.491
I	b t^3 /12 = 0.014 in^4	P_{cr}	29.481
r	0.188	F_e	260.68
K	0.800	P_e	203.334
KL/r	26.766	M_p	3.91
Z	bt^2 /4 = 0.066	M_m	3.87
E	24,600 ksi	C_m	0.85
S_y	59.3 ksi		

Using the cross-sectional stresses evaluated for each of the sections shown in Figures 2.6.15.6-2 through 2.6.15.6-5, the maximum corresponding compressive forces in conjunction with the maximum in-plane moment produces the maximum interaction coefficients. Because the location of the maximum force and the maximum moment may not coincide, the calculation of the interaction coefficient is conservative. The maximum magnitude of the moment is used, regardless of sign, to ensure the most severe condition.

For strong-axis buckling, the minimum margin of safety is +0.33 for the 31.8° radial basket orientation at Section 274 (thermal stresses are included).

The calculated minimum margins of safety for the drop orientations discussed in Section 2.6.13.6.1 are presented in Table 2.7.10.3-2. The location of the sections identified in the table are shown in Figures 2.6.15.6-2 through 2.6.15.6-5.

Table 2.7.10.3-1 Minimum Margins of Safety from Buckling Evaluation of BWR Support Disks (Weak Axis)

Section No.	G-Load*	Disk Drop Orientation	Heat Case	MS1	MS2
270	60	0	1	+0.334	+0.294
270	60	0	2	0.165	0.130
270	60	0	2 + thermal load	0.041	0.001
270	60	31.82	1	0.461	0.431
270	60	31.82	2	0.282	0.253
270	60	31.82	2 + thermal load	0.139	0.102
270	60	49.46	1	0.589	0.571
239	60	49.46	2	0.353	0.312
17	60	49.46	2 + thermal load	0.158	0.111
239	60	77.92	1	0.448	0.396
239	60	77.92	2	0.258	0.213
17	60	77.92	2 + thermal load	0.120	0.062
47	60	90	1	0.461	0.410
13	60	90	2	0.11	0.023
17	60	90	2 + thermal load	0.06	0.002

* Includes out-of-plane moment due to 30-ft end-drop impact of 55 *g*.

Table 2.7.10.3-2 Minimum Margins of Safety from Buckling Evaluation of BWR Support Disk (Strong Axis)

Section No.	G-Load	Disk Drop Orientation	Heat Case	MS1	MS2
298	60	0	1	+1.24	+0.833
298	60	0	2	1.22	0.818
298	60	0	2 + thermal load	0.847	0.511
274	60	31.82	1	0.600	0.552
274	60	31.82	2	0.587	0.539
274	60	31.82	2 + thermal load	0.391	0.339
274	60	49.46	1	0.990	0.993
246	60	49.46	2	0.877	0.753
246	60	49.46	2 + thermal load	0.605	0.490
243	60	77.92	1	0.914	0.763
246	60	77.92	2	0.927	0.760
246	60	77.92	2 + thermal load	0.722	0.569
53	60	90	1	1.63	1.160
81	60	90	2	1.268	0.889
53	60	90	2 + thermal load	1.320	0.913

2.7.10.4 Fuel Tube Analysis

The fuel tube provides a foundation and sealed cavity to mount BORAL poison plates within the fuel basket structure and does not provide a structural function relative to the support of the fuel assembly. The fuel tube design is presented in Figure 2.6.15-3. To ensure that the fuel tube remains functional when the cask is subjected to design load conditions, a structural evaluation of the tube is performed for both the end- and side-impact load conditions.

2.7.10.4.1 Fuel Tube End-Impact Analysis

During the postulated cask end impact, fuel assemblies are supported by the cask bottom for the bottom-end-drop and the lid for the top-end-drop. Fuel assembly load is not carried by the fuel tubes. Therefore, the fuel tube for the end-impact load is evaluated by considering the weight of the fuel tube subjected to the cask deceleration carried by the minimum tube cross section. The minimum tube cross section is located at the contact point of the tube with the bottom weldment. The BWR fuel tube bearing analysis is bounded by the PWR analysis based on weight (See Section 2.7.8.4.1 for details).

2.7.10.4.2 Fuel Tube Side-Impact Analysis

During the cask side-impact load configuration, the fuel tube is supported by the fuel basket 40 stainless steel support disks. The fuel basket support disks are spaced at 3.205 in. (which is slightly more than one half of the fuel tube width of 5.90 in.) and support the full length of the fuel tube. Considering the fuel tube subjected to the 60 *g* side impact deceleration and the 40 support locations provided by the basket support disks, the fuel tube shear stress is

Impact shear load = (60)(700)/40 = 1,050 lb

Shear area of tube = (0.048)(5.90)(2) = 0.566 in^2

Shear stress of tube = 1,050/0.566 = 1,855 psi.

A temperature of 750°F is conservatively used to determine the allowable stresses. The yield strength of Type 304 stainless steel at 750°F is 17,300 psi. Using 8,650 psi, an allowable shear stress equivalent to half the yield strength of the tube wall material, results in a large positive margin of safety. The conservative evaluation of the tube loading resulting from its own mass during the side-impact configuration indicates that the tube structure will maintain position and will function.

The load transfer of the fuel assembly to the weight of the fuel basket support disk in the side impact is through direct bearing and compression of the distributed load of the fuel assembly through the fuel tube to the support disk web. Two load conditions are considered in the fuel tube evaluation. The first considers the fuel assembly load as a distributed pressure on the inside surface of the fuel tube. The second postulates that the fuel assembly grid is located at the center of the span between the support disks and produces a localized distributed load over the effective area of the grid.

Two different ANSYS finite element models of the tube are developed for these two load conditions since the fuel assembly structural performance for either load is nonlinear. As shown in the following, the first model represents a fuel tube section with a length of three spans, i.e.,

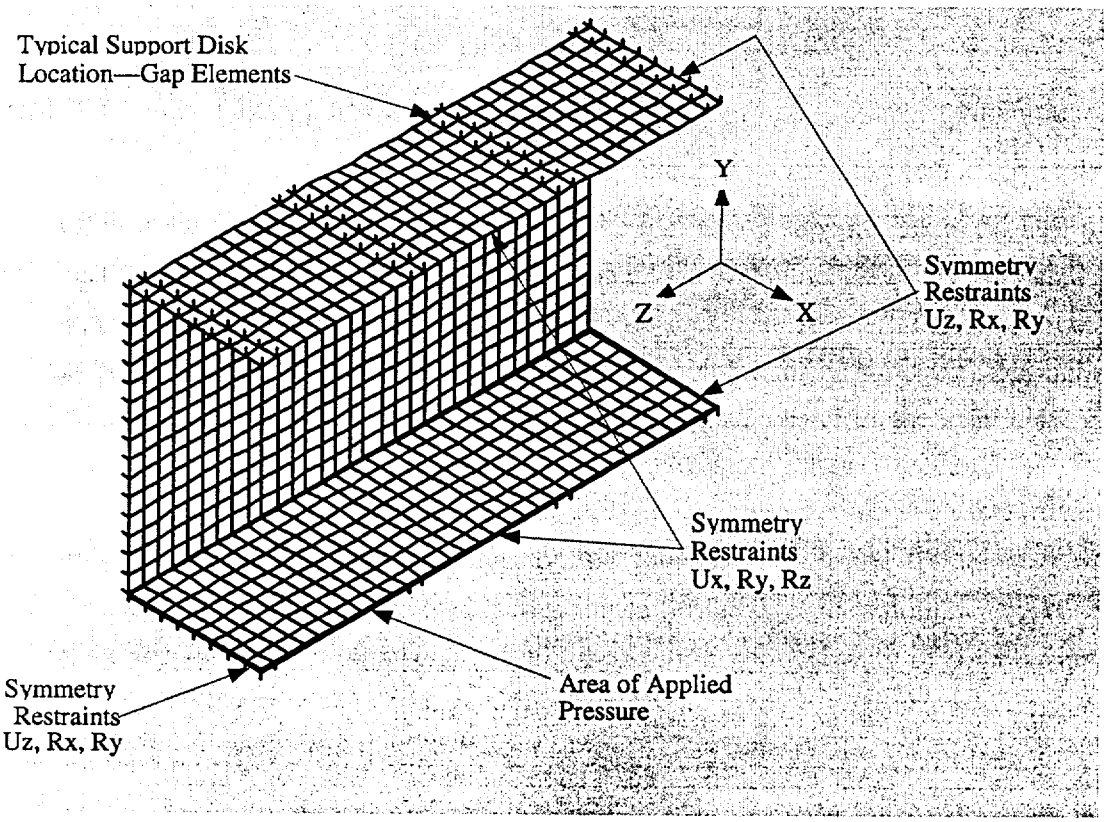

the model is supported at four locations by support disks. The model conservatively considers the fuel tube wall thickness of 0.048 inch as the only material subjected to a distributed pressure load representative of the fuel assembly deceleration of 60g. Fuel assembly stiffness is not considered in the development of the imposed pressure load on the fuel tube.

The fuel tube is modeled with the ANSYS plastic, quadrilateral shell element (SHELL43). The support disks are represented as rigid gap elements (CONTAC52). The outer nodes of the gap

elements are fully restrained in all three translational directions. Edge restraints were applied to the model to represent symmetry boundary conditions. The effective load on the fuel tube due to the 60g deceleration of the assembly is applied as a pressure to the inside area of the fuel tube.

The finite element analysis results show that the maximum stress in the tube is 19.5 ksi, which is local to the sections of the tube resting on the support disks. At 750°F the ultimate strength for Type 304 stainless steel is 63.1 ksi. The margin of safety is:

$$MS = \frac{63.1}{19.5} - 1 = +2.24$$

The analysis shows that the maximum total strain is 0.0078 inch/inch. Defining the acceptable elastic-plastic response of the stainless steel as one half of the material failure strain of 0.40 in./in. at 750°F [24], the resulting margin of safety is:

$$MS = \frac{0.40/2}{0.0078} - 1 = +\text{Large}$$

Similarly, the margin of safety for elastic-plastic stress becomes

$$MS = \frac{63.1 - 17.3}{19.5 - 17.3} - 1 = +\text{Large}$$

where the yield strength of Type 304 stainless steel is 17.3 ksi at 750°F.

The second finite element model is used to evaluate the load condition with the fuel assembly grid located at the center of the span between two support disks. The fuel tube is subjected to a localized distributed load over the effective area of the grid. As shown in the following, the model is a quarter-symmetry periodic section of the fuel tube. As in the finite element model used for the distributed pressure case, this model conservatively considers a fuel tube wall thickness of 0.048 inch. The BORAL plate (0.135 inch) and stainless steel cover plate (0.018 inch) are conservatively not included in the model. The tube wall is modeled with ANSYS SHELL43 elements. The support disks are modeled with CONTAC52 elements. A uniform pressure corresponding to the fuel assembly weight with the 60g load is applied to the elements at the grid location of the model. The displacement in the Y direction for the nodes at the grid location of the model are coupled to represent the structural rigidity of the spacer grid.

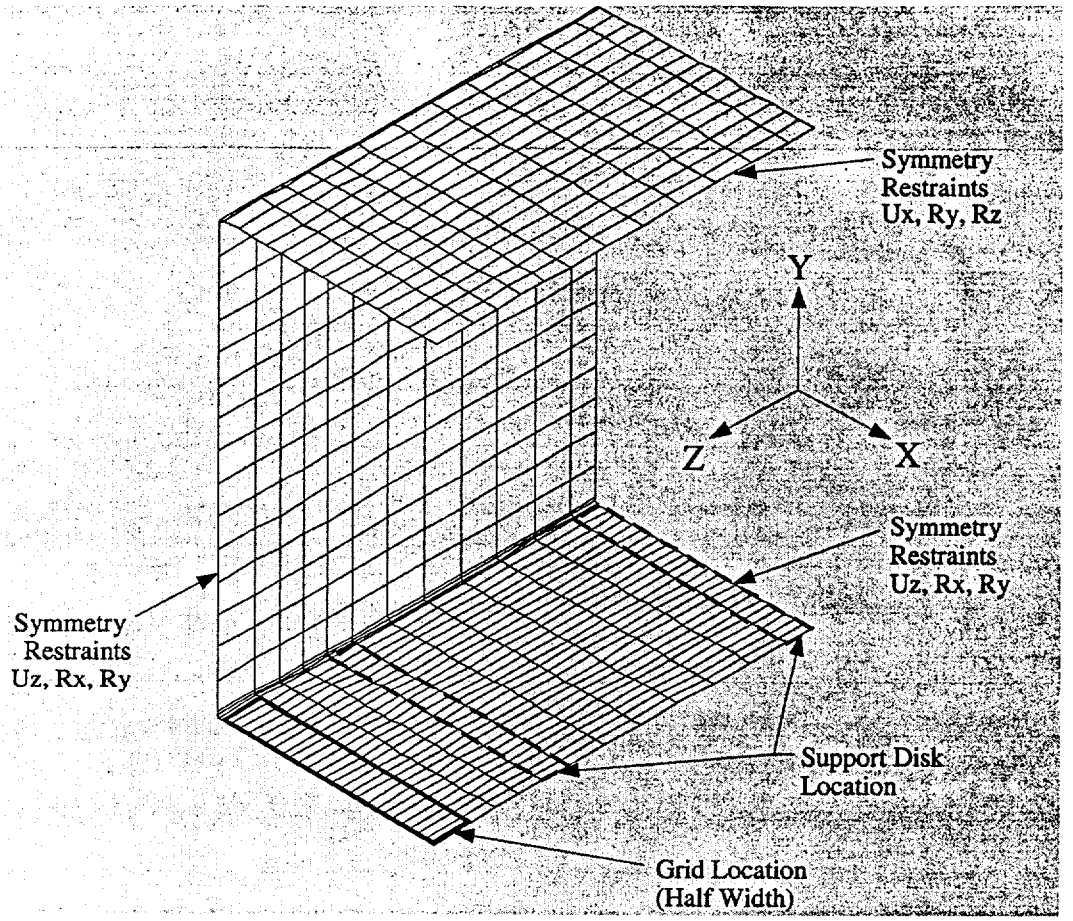

The finite element analysis results show that the maximum stress in the tube is 38.1 ksi. At 750°F the ultimate strength for Type 304 stainless steel is 63.1 ksi. The margin of safety is:

$$MS = \frac{63.1}{38.1} - 1 = +0.66$$

The analysis shows that the maximum total strain is 0.10 inch/inch. Defining the acceptable elastic-plastic response of the stainless steel as one half of the material failure strain of 0.40 in./in. at 750°F [24], the resulting margin of safety is:

$$MS = \frac{0.40/2}{0.10} - 1 = +1.0$$

Similarly, the margin of safety for elastic-plastic stress becomes:

$$MS = \frac{63.1 - 17.3}{38.1 - 17.3} - 1 = +1.2$$

where the yield strength of Type 304 stainless steel is 17.3 ksi at 750°F.

Both the maximum total strain and the elastic-plastic stress analyses indicate that the tube position within the support basket is maintained.

Assurance that the BORAL remains attached to the fuel tube is evaluated by considering that loads produced by the BORAL plate and stainless steel attachment plate, assuming a 60g load, are carried by the attachment plate weld. Total load and resultant stress on the weld are calculated as:

$F_{b/ss} = (g)(\rho)(t)(w)(l)$ Load exerted by BORAL/Stainless Steel Attachment Plate

where:

- g = acceleration (g)
- ρ = density of material (lb/in^3) (The density of aluminum (0.098 lb/in^3) is conservatively used for the BORAL.
- t = thickness of material (in.)
- w = width of material (in.)
- l = length of material section (in.)

The forces on the weld due to a 12-inch section of BORAL (F_b) and a 12-inch section of stainless steel plate (F_{ss}) are:

$F_b = (60g)(0.098\ lb/in^3)(0.135\ in)(5.45\ in)(12\ in) = 51.9\ lbs.$

$F_{ss} = (60g)(0.291\ lb/in^3)(0.018\ in)(5.79\ in)(12\ in) = 21.8\ lbs.$

The total load (F_t) on a 1-inch attachment for a 12-inch section is $F_t = 73.7$ lbs (51.9 + 21.8) lbs

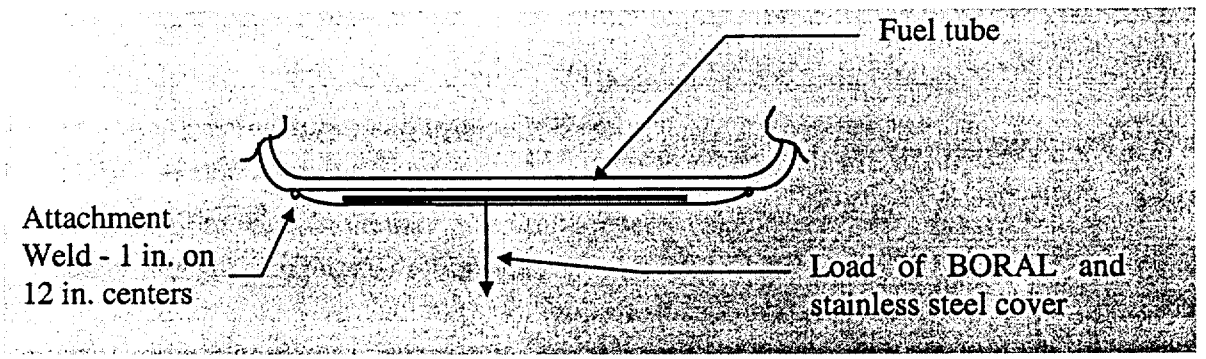

The resulting weld stress is: $\sigma = P/A = (73.7 \text{ lbs}/2) / (1 \text{ in}) (0.018 \text{ in}) = 2{,}074 \text{ psi}$

Since the weld material is Type 304 stainless steel, the margin of safety (at 750°F) is:

$$MS = \frac{17{,}300}{2{,}047} - 1 = +7.5$$

Therefore, the BORAL remains enclosed on each outer surface of the fuel tube wall.

2.7.10.5 Basket Weldment Analysis for 30-Foot End-Drop

The responses of the top and bottom weldment plates of the fuel basket assembly to a 60 *g* accident condition deceleration load are examined. Two finite element models representing the BWR basket top and bottom weldments are constructed for structural evaluation. The structural evaluations are performed at normal condition temperatures; therefore, prior to the structural evaluation portion of the analyses, the steady-state temperature distribution in the top and bottom weldment models is determined by applying fixed temperatures to the outer circular edge and to the node at the intersection of the symmetry planes. These fixed temperatures are obtained from the normal condition thermal analysis with -40°F ambient temperature and maximum heat generation. The material allowable stresses are based on the maximum temperature of the weldments determined for normal conditions with 100°F ambient temperature and maximum heat generation.

During the temperature solution portion of the analyses, the finite element models are constructed by using ANSYS three-dimensional thermal shell elements (SHELL57). During the structural evaluation portion of the analyses, the finite element models are constructed by using ANSYS three-dimensional, six-degrees-of-freedom, elastic shell elements (SHELL63) in the weldment plate and structural support region. The top nuts/pads are modeled by using BEAM 4 elements. Contact between the structural supports plates and between the structural support ring were modeled by using CONTACT 52 elements. The finite element models represent one-quarter sections of the weldments.

The top and bottom weldments are 1.0 in. thick and are fabricated from SA-240, Type 304 stainless steel. The top weldment supports its own weight and 56 fuel tubes (without the fuel assemblies) during a top-end-drop. Eight structural plates, eight tie-rod top nuts, and a

circumferential ring support the top weldment and its loads during a top-end-drop. These structural components are modeled as zero-translation restraints in the direction of the end-drop. The finite element models of the top and bottom weldments are presented in Figures 2.6.15.13-1 and 2.6.15.13-2, respectively.

2.7.10.5.1 Results of Basket Weldment Analyses (30-Foot End-Drop)

The maximum stress intensities (SI) for primary membrane plus primary bending ($P_m + P_b$) for the 30-ft end-drop analysis are 49.27 ksi for the top weldment and 56.67 ksi for the bottom weldment as tabulated below. The corresponding minimum margins of safety are +0.26 and +0.12 as shown below:

Component/Condition	$P_m + P_b$ (ksi)	Allowable S_u (ksi)	MS
Top Weldment/30-ft Drop	49.49	62.56	+0.26
Bottom Weldment/30-ft Drop	56.93	63.22	+0.11

Because a large radial temperature gradient occurs through the weldments, the maximum stress intensities presented in the preceding table do not occur at the maximum temperature of the models, and comparing these stress intensities with stress allowables on the basis of the maximum temperature is overly conservative. Therefore, the stress evaluation is performed on a nodal basis. That is, using ANSYS, the maximum stress at each node in each model is compared with the maximum allowable stress at the temperature of the node being evaluated.

For hypothetical accident conditions, the following criteria are used to evaluate the nodal stress intensities for the top and bottom weldment:

$$P_m + P_b < 3.6\ S_m \text{ or } S_u, \text{ whichever is less.}$$

(Note that for Type 304 stainless steel in these temperature ranges, S_u is smaller than 3.6 S_m.)

The margin of safety is

$$MS = \frac{\text{Allowable Stress}}{\text{Nodal Stress Intensity}} - 1.$$

2.7.10.5.2 Top Weldment Structural Rib Buckling Evaluation

The structural ribs on the top weldment are subjected to axial loads during a top-end-drop. End constraints on the ribs during a top-end-drop are fixed at the end welded to the top weldment and free at the other end. Because no closed solutions are readily available for evaluating a plate for buckling loads with end constraints matching those of the top weldment ribs, a closed-form solution for the buckling of a column is used to analyze a 1-in. section of one of the ribs.

For a column under axial loading with one end of the structural rib fixed and the other end free, the critical load (P_{cr}) is determined by

$$P_{cr} = \frac{\pi^2 EI}{(KL)^2}$$

where: I = moment of inertia
E = modulus of elasticity
L = length of the column
K = effective length factor (K = 2 for a column, one end fixed; other end free).

Evaluating a 1-in. section of one of the ribs at the maximum weldment temperature of 515°F yields

$$P_{cr} = \frac{\pi\left(25.7\times10^6 \text{ lbf/in}^2\right)\frac{1}{12}(1.0 \text{ in})(0.5 \text{ in})^3}{(2\times10.25 \text{ in})^2} = 6{,}288 \text{ lb.}$$

For the 30-ft top-end-drop, the sum of the forces on the nodes representing the ribs is a maximum of 26,945 lb. Thus, the maximum load (P) on a 1-in. section of one of the structural ribs is 1,152 lb.

Thus, the margin of safety for buckling of one of the structural ribs of the top weldment during a 30-ft top-end-drop is

$$MS = \frac{6{,}288 \text{ lb}}{1{,}152 \text{ lb}} - 1 = +4.45$$

2.7.10.5.3 Conclusions

As shown in this section, both the top and bottom weldments maintain positive margins of safety when subjected to the 30-ft end-drop conditions. As shown in the top weldment structural rib buckling calculation, the actual maximum load (P) on one of the structural ribs of the top weldment during a 30-ft drop is much less than the predicted buckling load (P_{cr}). Therefore, the top and bottom weldments are structurally adequate.

2.7.11 Summary of Damage to Cask Due to Hypothetical Accident Conditions

The analysis results reported in Sections 2.7.1 and 2.7.2 (30-ft drop, and puncture accidents) are summarized in Tables 2.7.11-1 and 2.7.11-2, respectively. The results shown in Tables 2.7.11-1 and 2.7.11-2 demonstrate that the damage incurred by the Universal Transport Cask during the hypothetical accident is minimal and does not diminish the cask's ability to maintain the containment boundary. A 30-ft drop or a 40-in. pin puncture accident may damage the neutron shield and result in a reduction in the cask's neutron shielding ability. However, the gamma shielding remains intact to provide sufficient shielding and to satisfy the accident shielding criteria. The peak dose rates resulting from a maximum slump of 3.05 in. that could occur in the gamma shielding following a 30-ft end-drop are well below the regulatory limits (The shielding consequences of the drop accidents are discussed in Section 2.7.1.5 and Chapter 5.0).

As discussed in Section 2.7.3, stresses in the cask during the fire accident are classified as secondary by the ASME Code, Section III, Subsection NB. For accident conditions, there are no set limits on secondary stresses. Review of the applicable regulations presented for crush in Section 2.7.4 shows that crush need not be considered for the Universal Transport Cask. The conformance of the cask to immersion requirements is discussed in Sections 2.7.5 and 2.7.6. An evaluation of individual cask components for a sustained external pressure of 290 psi shows that the cask meets worst case immersion requirements.

In a 30-ft hypothetical corner-drop accident, the upper impact limiter may crush to a maximum depth of 31.1 in. As shown in Section 2.7.1.6, this has no structural consequences.

Based on the analyses of Section 2.7.1 through 2.7.6, the Universal Transport Cask fulfills the structural and shielding requirements of 10 CFR 71 for all of the hypothetical accident conditions.

Table 2.7.11-1 Summary of Maximum Calculated Stresses in Cask—30-Foot Free Drop

30-Foot Drop	Conditions*					Maximum Calculated Stress		Allowable Stress	Margin of Safety
	1		2	3	4	5	Type	Value (ksi)	(ksi)	
	100°F	-40°F								
Containment**	✓		✓	✓	✓	✓	P_m	17.5	48.0	1.74
(on end)	✓		✓	✓	✓	✓	$P_m + P_b$	33.5	62.7	0.87
Noncontainment***	✓		✓	✓	✓	✓	P_m	23.4	45.9	0.96
(on end)	✓		✓	✓	✓	✓	$P_m + P_b$	22.9	70.9	2.10
Containment**	✓		✓	✓	✓	✓	P_m	31.0	48.0	0.55
(on side)	✓		✓	✓	✓	✓	$P_m + P_b$	62.4	65.0	0.04
Noncontainment***	✓		✓	✓	✓	✓	P_m	32.1	47.3	0.47
(on side)	✓		✓	✓	✓	✓	$P_m + P_b$	68.2	70.9	0.04
Containment**	✓		✓	✓	✓	✓	P_m	18.9	48.0	1.54
(on corner)	✓		✓	✓	✓	✓	$P_m + P_b$	32.0	62.7	0.96
Noncontainment***	✓		✓	✓	✓	✓	P_m	25.8	45.9	0.78
(on corner)	✓		✓	✓	✓	✓	$P_m + P_b$	36.7	70.9	0.94
Containment**	✓		✓	✓	✓	✓	P_m	28.5	48.0	0.68
(oblique)	✓		✓	✓	✓	✓	$P_m + P_b$	62.6	69.7	0.11
Noncontainment***	✓		✓	✓	✓	✓	P_m	29.8	47.3	0.59
(oblique)	✓		✓	✓	✓	✓	$P_m + P_b$	61.5	70.9	0.15

*Conditions: 1. Ambient Temperature
2. Insolance
3. Decay Heat
4. Internal Pressure
5. Weight of Contents.

** The containment structure includes cask lid, top forging, inner shell, and bottom forging.

*** The noncontainment structure includes the outer shell and the bottom plate.

Table 2.7.11-2 Summary of Maximum Calculated Stresses in Cask— Puncture

40-In. Free Drop	Conditions*						Maximum Calculated Stress		Allowable Stress (ksi)	Margin of Safety
	1		2	3	4	5	Type	Value (ksi)		
	100°F	-40°F								
Containment** (lid)	✓		✓	✓	✓	✓	$P_m + P_b$	56.81	61.5	0.08
Noncontainment*** (on mid-length)	✓		✓	✓		✓	$P_m + P_b$	56.75	66.9	0.18
Noncontainment** (on bottom center)	✓		✓	✓			$P_m + P_b$	49.96	66.9	0.34

* Conditions: 1. Ambient Temperature
2. Insolance
3. Decay Heat
4. Internal Pressure
5. Weight of Contents.

** The containment structure includes cask lid, top forging, inner shell, and bottom inner forging.

*** The noncontainment structure includes the outer shell and the bottom plate.

2.7.12 Cask Inner Shell Buckling Analysis

Code Case N-284-1 (Metal Containment Shell Buckling Design Methods) [12] of the ASME Boiler and Pressure Vessel Code is used to analyze the Universal Transport Cask inner shell for structural stability. Structural stability ensures that the inner shell does not buckle during cask fabrication, normal conditions of transport, or hypothetical accident conditions. Fabrication stresses are evaluated in Section 2.6.11 and are shown to be very low, so that that including them in the buckling evaluation would not significantly affect the margins of safety demonstrated in this section. The buckling evaluation requirements of Regulatory Guide 7.6, Paragraph C.5, are shown to be satisfied by the results of the buckling interaction equation calculations from Code Case N-284-1.

The cask inner shell buckling design criteria, are described in Section 2.1.2.5.3.

2.7.12.1 Analysis Methodology

The structural stability of the Universal Transport Cask inner shell is analyzed in accordance with the ASME Code Case N-284-1. The data considered for the buckling evaluation includes shell geometry parameters, shell fabrication tolerances, shell material properties, theoretical elastic buckling stress values for the shell, and membrane stress components in the shell. The internal stress field that controls the buckling of a cylindrical shell consists of the longitudinal (axial) membrane, circumferential (hoop) membrane, and in-plane shear stresses. These stresses may exist singly or in combination, depending upon the applied loading. Only these three stress components are considered in the buckling analysis.

For each dynamic loading case, the stress results from the ANSYS dynamic shell analyses (Sections 2.6.7.1 through 2.6.7.4 for 1-ft cask drops and Sections 2.7.1.1 through 2.7.1.4 for 30-ft cask drops) are screened for the maximum values of the longitudinal compression, circumferential compression, or in-plane shear stresses for the individual drop load cases, regardless of where in the shell they individually occur. This was performed for all cask drop orientations.

The ANSYS analyses for both the 1-ft and 30-ft drops were performed with an internal pressure of 150 psig. The internal pressure tends to stiffen the inner shell. To compensate for this, and to bound the worst case situation, the axial and hoop stresses corresponding to this internal pressure

were combined with (added to) the compressive axial and hoop stresses from the ANSYS analyses to give maximum stress values.

Also, the ANSYS stress components used in the buckling evaluations for the normal 1-ft drop load cases conservatively include thermal peak stresses and bending stresses from thermal and drop loadings. Combining the maximum stress components in this way produces a conservative, bounding-case buckling evaluation of the inner shell. The maximum ANSYS plus internal pressure stress components used in the buckling evaluations are presented in Table 2.7.12-1.

2.7.12.2 Analysis Results

As discussed above, the worst-case combination of stress components within a given drop orientation from the ANSYS analyses, regardless of location within the shell cylinder, and including temperature and pressure effects, are determined and used for input as stress components in the buckling evaluations. These conservatively determined stress components, therefore, envelope the specific load case tables presented in Sections 2.6.7.1 through 2.6.7.4 for 1-ft cask drops and Sections 2.7.1.1 through 2.7.1.4 for 30-ft cask drops.

The results of the buckling analysis of the cask inner shell are summarized in Table 2.7.12-1. All interaction equations ratios are less than 1.0. Therefore, the buckling criteria of Code Case N-284-1 are satisfied, thus demonstrating that buckling of the Universal Transport Cask inner shell does not occur.

2.7.12.3 Detailed Code Case N-284-1 Buckling Evaluation

A step-by-step analysis procedure presented below as an example of implementing the procedure recommended in Code Case N-284-1. This same procedure was followed to determine the results presented in Table 2.7.12-1.

In the buckling evaluation, the symbols ϕ, θ, or $\phi\theta$ correspond to the longitudinal (axial) direction or stress component, circumferential (hoop) direction or stress component, and in-plane shear stress component, respectively, as used in Code Case N-284-1.

In the evaluation, the formulas for cylindrical shells (unstiffened) are used. Each of the 14 load cases presented in Table 2.7.12-1 is evaluated in the manner detailed below for Load Case "N",

the hypothetical accident condition of a 30-ft bottom oblique (75°) drop; the results are listed in the table. The manner of conservatively screening for the highest stress components and the compensation for internal pressure is described above in Section 2.7.12.1.

The geometry parameters used for the cask inner shell evaluation are presented in Table 2.7.12-2.

In the example that follows, a factor of safety (FS) of 1.34 is used in accordance with the Code Case.

Step 1. Determine Stresses: For the 30-ft bottom oblique (75°) drop (load case "N" shown in Table 2.7.12-1), the maximum individual axial, hoop, and shear stresses regardless of location in the cask inner shell from the ANSYS analysis are:

Axial Stress (ANSYS) S_ϕ = 11,840 psi (Compression)
Hoop Stress (ANSYS) S_θ = 16,880 psi (Compression)
Shear Stress (ANSYS) $S_{\phi\theta}$ = 12,440 psi.

To these values are added the effects of an internal pressure, IP = 150 psig. The tensile load due to internal pressure. Acting on the area of the cask lid with an area A_L = 3,590 in^2, the internal pressure creates a force, F = 538,521 lb. Cross sectional area of the inner shell A_S = 216 in^2. Therefore, the axial stress in the inner shell due to the internal pressure is

Axial Stress (IP) = F/A_S = 2,498 psi

The hoop stress due to internal pressure

Hoop Stress (IP) = $IP(D_i)/2t$ = 2,535 psi

where D_i = internal diameter = 67.61 in.
t = shell thickness = 2.0 in.

Combining the axial and hoop stresses from ANSYS analysis and due to the effects of internal pressure, with no compensation necessary for the shear stress, gives the stress state used for the buckling evaluation example:

S_ϕ = 14,338 psi (axial compression)
S_θ = 19,415 psi (hoop compression)
$S_{\phi\theta}$ = 12,440 psi (shear).

Step 2. Determine Capacity Reduction Factors: (Code Case N-284-1, Paragraph-1500)
The reduction in capacity due to imperfections and nonlinearity in geometry and boundary conditions is provided through the use of Capacity Reduction Factors. Capacity Reduction Factors, based on the parameters in Table 2.7.11-2 are as follows:

$\alpha_{\phi L}$ = 0.231
$\alpha_{\theta L}$ = 0.8
$\alpha_{\phi\theta L}$ = 0.8.

To directly use the Capacity Reduction Factors, the tolerance requirements of Article NE-4220 of the ASME Boiler and Pressure Vessel Code, Section III, Subsection NE must be satisfied. Article NE-4221.1 and Article NE-4221.2 set forth the "maximum difference in cross-sectional diameters" and "maximum deviation from true theoretical form for external pressure."

The requirements of Articles NE-4221.1 and NE-4221.2 are satisfied, as long as the maximum tolerances and configuration constraints are met during manufacturing:

Max ID = 67.67 in.
Min ID = 67.57 in.
Max ID - Min ID = 0.10 in.
Allowable deviation (per Subsection NE) = Nominal ID/100 = 0.677 in.
0.10 in. < 0.677 in.

Allowable deviation (per Subsection NB*) shall not exceed the smaller of

(D + 50)/200 = (67.61 + 50)/200 = 0.588 in., and

Nominal ID/100 = 0.677 in.

0.10 in. < 0.588 in.

*(Evaluation of the tolerance requirements of Subsection NB is included in the evaluation because the Universal Transport Cask is being constructed to the requirements of Subsection NB.)

Therefore, direct use of the Capacity Reduction Factors is allowed.

Step 3. Determine Plasticity Reduction Factors: (Code Case N-284-1, Paragraph-1600)

When the elastic buckling stresses exceed the proportional limit for the fabricated material, Plasticity Reduction Factors are used to account for the non-linear material properties. Plasticity Reduction Factors are determined as follows:

a. Axial Compression

$\Delta = S_\phi(FS)/S_y = (14{,}338)(1.34)/(2.07\times10^4) = 0.928$

For $0.55 < \Delta \leq 1.6$,

$\eta_\phi = 0.45/\Delta + 0.18 = (0.45/0.928) + 0.18 = 0.665$

b. Hoop Compression

$\Delta = S_\theta(FS)/S_y = (19{,}415)(1.34)/(2.07\times10^4) = 1.257$

For $0.67 < \Delta \leq 4.2$,

$\eta_\theta = 2.53/(1 + 2.29\Delta) = 2.53/(1 + 2.29 \times 1.257) = 0.652$

c. Shear

$\Delta = S_{\phi\theta}(FS)/S_y = (12{,}440)(1.34)/(2.07\times10^4) = 0.805$

For $0.48 < \Delta \leq 1.7$,

$\eta_{\phi\theta} = 0.43/\Delta + 0.1 = (0.43/0.805) + 0.1 = 0.634$

Step 4. Determine Theoretical Uniaxial Buckling Values: (Code Case N-284-1, Paragraph-1712) Elastic Buckling Coefficients are first calculated followed by the calculation of the theoretical buckling values as shown below:

$$M_\phi = L_\phi/(Rt)^{.5} = 180/(34.81 \times 2.0)^{.5} = 21.57$$

$$Et/R = [26.5(10)^6 \times 2.0] / 34.81 = 1.5228(10)^6 \text{ psi}$$

a. Axial Compression

For $M_\phi \geq 1.73$, $C_\phi = 0.605$

$S_{\phi eL} = C_\phi (Et/R) = 921{,}276$ psi

b(1). External Pressure - No End Pressure

$1.65(Rt) = 28.71$

For $3.0 \leq M_\phi < 1.65(RT)$,

$C_{\phi r} = 0.92/(M_\phi - 1.17) = 0.0451$

$S_{\theta eL} = S_{reL} = C_{\phi r} (Et/R) = 68{,}659$ psi

b(2). External Pressure - End Pressure Included

For $3.5 \leq M_\phi < 1.65(Rt)$,

$C_{\phi h} = 0.92/(M_\phi - 0.636) = 0.0439$

$S_{heL} = C_{\phi h} (Et/R) = 66{,}908$ psi

c. Shear

$8.69(Rt) = 151.23$

For $26 < M_\phi < 8.69(Rt)$,

$C_{\phi\theta} = 0.746/(M_\phi)^{.5} = 0.161$

$S_{\phi\theta eL} = C_{\phi\theta} (Et/R) = 244{,}571$ psi

Step 5. Evaluate Elastic Buckling: (Code Case N-284-1, Paragraph-1713.1)
First, the elastic buckling allowable stresses for specific loading cases are calculated. This is followed by determining the individual elastic interaction ratios, Q1 through Q4.

Elastic buckling allowable stresses are

$S_{xa} = a_{\phi L} S_{\phi eL}/FS = 159{,}050$ psi — Axial Compression alone

$S_{ha} = a_{\theta L} S_{heL}/FS = 39{,}945$ psi — Hydrostatic External Pressure

$S_{ra} = a_{\theta L} S_{reL}/FS = 40{,}991$ psi — Radial External Pressure

$S_{ta} = a_{\phi\theta} S_{\phi\theta eL}/FS = 146{,}012$ psi — In-plane Shear alone.

a. Axial Compression plus Hoop Compression (for $K < 0.5$)

$K = S_\phi/S_\theta = 0.74 > 0.5$ Therefore, go to (b) below.

b. Axial Compression plus Hoop Compression (for $K \geq 0.5$)

No interaction check is required if $S_\phi / S_{ha} < 0.5$

$S_\phi / S_{ha} = 14{,}338/39{,}945 = 0.359$

Therefore, no interaction check is required and

$Q1 = 0.0$

c. Axial Compression plus Shear

$$(S_\phi/S_{xa}) + (S_{\phi\theta}/S_{\tau a})^2 \leq 1.0$$

$$(14{,}338/159{,}050) + (12{,}440/146{,}012)^2 = 0.097$$

Therefore, Q2 = 0.082 < 1.0

d. Hoop Compression plus Shear

$(S_\theta/S_{ra}) + (S_{\phi\theta}/S_{\tau a})^2 \leq 1.0$

(19,415/39,945) + (12,440/146,012)2 = 0.481

Therefore, Q3 = 0.419 < 1.0

e. Axial Compression plus Hoop Compression plus Shear

$K_s = 1 - (S_{\phi\theta}/S_{\tau a})^2 = 0.993$

Substituting K into Equation (b):

$(S_\phi - .5*K_sS_{ha})/(K_sS_{xa} - .5*K_sS_{ha}) + (S_\theta/K_sS_{ha})^2 \leq 1.0$

However, since Q1 = 0.0 from Equation (b), then

also Q4 = 0.0

Step 6. Evaluate Inelastic Buckling: (Code Case N-284-1, Paragraph-1713.2)

First, the inelastic buckling allowable stresses for specific loading cases are calculated. This is followed by determining the individual elastic interaction ratios, Q5 through Q8.

Inelastic buckling allowable stresses are

$S_{xc} = \eta_\phi S_{xa} =$ 105,739 psi Axial compression alone

$S_{rc} = \eta_\theta S_{ra} =$ 26,741 psi Radial external pressure

$S_{\tau c} = \eta_{\phi\theta} S_{\tau a} =$ 92,567 psi In-plane shear alone.

a. Axial Compression or Hoop Compression

Axial Compression: $S_\phi/S_{xc} \leq 1.0$

$14,338/105,739 = 0.136$

Therefore, $Q5 = 0.136 < 1.0$

Hoop Compression: $S_\theta/S_{rc} \leq 1.0$

$19,415/26,741 = 0.726$

Therefore, $Q6 = 0.726 < 1.0$

b. Axial Compression plus Shear

$$S_\phi/S_{xc} + (S_{\phi\theta}/S_{\tau c})^2 \leq 1.0$$

$$14,338/105,739 + (12,440/92,567)^2 = 0.154$$

Therefore, $Q7 = 0.154 < 1.0$

c. Hoop Compression plus Shear

$$S_\theta/S_{rc} + (S_{\phi\theta}/S_{\tau c})^2 \leq 1.0$$

$$19,415/26,741 + (12,440/92,567)^2 = 0.744$$

Therefore, $Q8 = 0.744 < 1.0$

Table 2.7.12-1 Buckling Evaluation Load Cases and Results for the Universal Transport Cask

Load Case	Load Condition	Longitudinal (Axial) Stress* S_ϕ (psi)	Circumferential (Hoop) Stress* S_θ (psi)	In-plane Shear Stress $S_{\phi\theta}$ (psi)	Elastic Buckling Interaction Equations				Plastic Buckling Interaction Equations			
					Q1	Q2	Q3	Q4	Q5	Q6	Q7	Q8
A	1-Ft Top End	16,808	8,135	1,410	.129	.158	.296	.129	.345	.328	.345	.328
B	1-Ft Bottom End	16,478	7,325	1,370	.108	.155	.267	.108	.334	.276	.334	.276
C	1-Ft Side	9,418	8,235	4,230	.052	.089	.300	.052	.131	.334	.131	.335
D	1-Ft Top Corner	16,708	6,915	2,470	.102	.157	.252	.103	.342	.252	.342	.252
E	1-Ft Bottom Corner	8,478	15,165	2,050	.552	.080	.552	.269	.109	.951	.109	.951
F	1-Ft Top Oblique (75°)	12,668	7,165	430	.064	.119	.261	.064	.217	.267	.217	.267
G	1-Ft Bottom Oblique (75°)	9,668	8,585	3,760	.063	.091	.313	.063	.137	.358	.137	.358
H	30-Ft Top End	8,528	12,865	1,120	.021	.054	.314	.021	.054	.361	.054	.361
I	30-Ft Bottom End	9,648	13,565	990	.041	.061	.331	.041	.067	.394	.067	.394
J	30-Ft Side	12,308	17,125	13240	.129	.086	.426	.132	.104	.584	.127	.607
K	30-Ft Top Corner	11,858	12,555	4,940	.040	.076	.307	.041	.097	.346	.098	.348
L	30-Ft Bottom Corner	14,698	18,605	4,550	.179	.093	.455	.180	.142	.674	.143	.675
M	30-Ft Top Oblique (75°)	12,008	14,115	13,140	.068	.084	.352	.070	.099	.421	.122	.443
N	30-Ft Bottom Oblique (75°)	14,338	19,415	12,440	.196	.097	.481	.200	.136	.726	.154	.744

* Compressive stresses.

Table 2.7.12-2 Geometry Parameters for the Universal Transport Cask

Parameter	Value
t = thickness (in)	2.0
ID = inside diameter (in)	67.61
R = radius (in) = (ID+t)/2	34.81
R/t	17.40
L_ϕ = Length (in)	180.00
$(Rt)^{0.5}$	8.34
$L_\theta = 2\pi R$ = circumference (in)	218.7
$M_\phi = L_\phi/(Rt)^{0.5}$	21.57
$M_\theta = L_\theta/(Rt)^{0.5}$	26.21
ν = Poisson's ratio	0.275

THIS PAGE INTENTIONALLY LEFT BLANK

Where:

$\lambda = \pi$

L = 44.6 inches

Using the cross-section of both pipes, the moment of inertia is:

$$I_{20} = \frac{\pi}{64}(D_0^4 - D_i^4) = \frac{\pi}{64}(20^4 - 17^4) = 3{,}754 \text{ in}^4, \text{ for the } 20-\text{inch pipe, and}$$

$$I_{14} = \frac{\pi}{64}(D_0^4 - D_i^4) = \frac{\pi}{64}(14^4 - 12.5^4) = 687 \text{ in}^4 \text{ for the } 14-\text{inch pipe}$$

The total moment of inertia is 4,441 in^4.

E = 28.3E+06 psi

ρ' = effective mass per unit length of beam

= 2,812/44.6/386.4 = .163 lb-sec^2 / in^2

Substituting,

fb = 694 Hz

In accordance with Blevins, the shear and bending mode frequencies are combined as:

1/fc = 1/fs + 1/ fb

or

fc = 330 Hz

The filter frequency is conservatively selected to be 450 Hz for the side drop.

2.10.3.4.3 Results/Evaluation for the 30-Foot Side Drop

The 30-foot side drop was the only test performed at SNL using the quarter-scale model for the transport cask. Prior to lifting the scale model package to the 30-foot drop height, the torque for the retaining rods and nuts were inspected to ensure that the torque specifications were met.

High-speed cameras were positioned at two locations with respect to the model. Cameras were positioned to view the model from the end and cameras were positioned to obtain a side view of the model impacting the pad. The lateral view confirmed that the axis of the cask model was

effectively horizontal at the time of impact. There appeared to be no rocking of the cask during the drop and the model rebound was less than six inches after the initial 30-foot drop impact.

2.10.3.4.4 Impact limiter Deformation and Attachment Data

After the side drop test, it was observed that the impact limiters remained attached to the cask body model (see Figure 2.10.3-5). The impact limiters were removed and it was observed that twelve attachment rods remained intact for the top impact limiter and nine attachment rods remained intact for the bottom impact limiter. These results indicate that both impact limiters remained attached to the cask body during and after the side drop test. Upon inspection of the rods, it was determined that the rods, which failed outside the crushed region, exhibited a tensile failure at the location where the attachment rod abruptly changed diameter (threaded undercut). The design of the square cut out in the attachment rod has been reversed to allow the thread run out to terminate at the location of the previous square cut out.

Measurements of the deformed model impact limiter dimensions were obtained after the side drop test to determine the crush depth that occurred. These dimensions are tabulated below, along with the crush depth calculated by LS-DYNA for the quarter-scale model (The description of the LS-DYNA analyses supporting these values is presented in Section 2.10.3.7).

	Model Drop Test Crush Depth (inch)			LS-DYNA Crush Depth Prediction (inch)		
Location	Original Thickness	Final Thickness	Measured Crush	Original Thickness	Final Thickness	Total Crush
Side Drop–under the trunnion	3.50	0.63	2.87	3.47	1.11	2.36
Side Drop–bottom impact limiter	5.13	2.38	2.75	5.13	2.42	2.71

2.10.3.4.5 Accelerometer Data from the 30-Foot Side Drop Test

The unfiltered accelerometer traces were electronically stored to permit filtering after the tests. Three acceleration traces were obtained near the bottom of the model and three acceleration traces were obtained near the top of the model. The acceleration time histories, both the filtered and the unfiltered data with maximum accelerations, are shown in Figure 2.10.3-6 for the top end and Figure 2.10.3-7 for the bottom end locations on the cask model. Figure 2.10.3-8 shows the acceleration trace containing the maximum acceleration for the top end along with the acceleration time history computed by LS-DYNA (as described in Section 2.10.3.9). A similar

set of curves is shown in Figure 2.10.3-9 for the bottom end of the cask that compares the maximum acceleration obtained from testing to the acceleration time history obtained from the LS-DYNA analysis in Section 2.10.3.9. The peak accelerations for the quarter-scale model are shown below.

UMS® Cask Model Drop Orientation	Model Acceleration Results (g)		LS-DYNA Acceleration Prediction (g)		Design Basis Acceleration (g)
	Top Accelerometer	Bottom Accelerometer	Top Accelerometer	Bottom Accelerometer	
Side	190	198	193	210	240

2.10.3.4.6 Energy Absorption Capacity of the Impact Limiter in the 30-Foot Side Drop

The capacity to absorb energy is the function of the impact limiter. For a side impact, the energy absorption of the impact limiter can be obtained from the 30-foot side drop test results. Similarly, the results of the static test for the end drop orientation can be used to determine the energy absorption for the end orientation. The side drop acceleration time history can be integrated twice to obtain the displacement, which can be plotted versus the force (the product of the acceleration time history and the model weight, i.e., the acceleration time history in units of g). This force versus displacement time history is shown in Figure 2.10.3-10. The area under this curve corresponds to 1.46E6 inch-pounds, which is within 1% of the total energy (TE) of the side drop test (1.47E6 inch-pounds). The total energy is obtained by multiplying the model weight of 4,060 pounds times the total distance traversed, which is 360 inches plus the average of the crush depths (2.87 + 2.75)/2. From the side drop test results, the upper impact limiter has a 0.5-inch depth of uncrushed wood remaining at the trunnion cutout and the lower impact limiter has a 2.25-inch depth of uncrushed wood remaining at the maximum crush location. Thus, the upper limiter is most limiting. Since the upper impact limiter can crush until the trunnion comes into contact with the impact plane, there is an additional 0.5-inch crush depth available. Using 750,000 pounds (which represents the total force from the top and bottom impact limiter) from the force-displacement time history curve, this potential additional 0.5-inch crush distance corresponds to 0.5×(750,000) or 375,000 inch-pounds of additional energy which could be absorbed. Thus, for a side impact, the UMS® impact limiters have an additional energy absorption capacity of approximately 25% (375,000/1.46E6).

2.10.3.4.7 Summary of the Side Drop Test

The comparison of the maximum test accelerations to those computed by LS-DYNA is considered to be acceptable. The LS-DYNA results shows that the predicted accelerations are approximately 10% above the test values. Additionally, the design acceleration corresponding to the quarter-scale model is 240g. This indicates that, not only is there a 10% margin between LS-DYNA and the design basis acceleration, but there is considered to be additional margin between the predicted values and the test data. With respect to maximum crush depth, LS-DYNA was shown to provide a conservative prediction. Using the dynamic force-deflection curve, the UMS® impact limiter design is shown to have an additional 25% energy absorption capacity required to decelerate the transport cask. The side drop test performed at Sandia National Laboratory confirms that the UMS® impact limiters are adequate to limit the cask component accelerations well within the design basis accelerations.

2.10.3.5 Evaluation of the 30-Foot Oblique Drop

In Section 2.6.7.5.5, a parametric study was performed to show that for the NAC-STC cask, the side drop produces the maximum lateral accelerations. This is due to the low length to radius of gyration ratio for the STC cask. The following table compares the L/r of the UMS® and the NAC-STC casks:

Cask	L/r
UMS®	1.48
NAC-STC	1.50

Based on this comparison, it is concluded that the side drop provides bounding accelerations over shallow oblique drops. Consequently, a separate oblique drop test is not required.

2.10.3.6 Scale Model Drawings

The drawings for the ORNL and SNL quarter-scale models are included in this section for reference.

2.10.3.6.1 ORNL Drop Test Model

The detailed dimensions, welding and materials are shown on the drawings of the model body and impact limiters used in the ORNL drop tests.

Drawing Number	Sheet	Revision	Title
790-300	1	3	Drop Test Assembly 1/4 Scale Model
790-301	1 through 3	6	1/4 Scale Cask Model, NAC- UMS®
790-401	1 through 3	2	Crush Fixture, End Drop, UMS® Testing
790-602	1	0	Lower Impact Limiter, 1/4 Scale Model, NAC-UMS®
790-603	1	0	Upper Impact Limiter, 1/4 Scale Model, NAC-UMS®

2.10.3.6.2 SNL Drop Test Model

The detailed dimensions, welding and materials are shown on the drawings of the model body and impact limiters used in the SNL drop test.

Drawing Number	Sheet	Revision	Title
790-308	1 and 2	0	1/4 Scale Cask Body 2001 Drop Confiramation NAC-UMS®
790-309	1	0	Drop Test Assembly, 2001 Drop Confirmation NAC-UMS®
790-302	1 and 2	3	Lower Impact Limiter, 1/4 Scale Model, NAC-UMS®
790-303	1 and 2	6	Upper Impact Limiter, 1/4 Scale Model, NAC-UMS®

2.10.3.7 LS-DYNA Analyses of the UMS® Quarter-Scale Model

The top end, top corner, and side impact analyses were performed for the finite element model shown in Figure 2.10.3-11 using LS-DYNA. The model in Figure 2.10.3-11 is a half-symmetry model and is constructed of 8-node brick and 4 node shell elements. The cask body section of the model consists of brick elements using an elastic material. The elastic modulus of the cask body was adjusted to allow the cross-sectional modulus of the finite element model to be equal to that of the quarter-scale model. The weight and the CG of the finite element model correspond to that of the quarter-scale test model. The cask contents weight, including the mass of the canister lids, is distributed in the brick elements along the length of the cask. In the full-scale design, the canister lids are positioned to be in contact with the cask body upper forging, which is a massive ring that is insensitive to the localized loading of the canister lids. For this reason, it is only required that the weight and CG of the finite element model accurately represent the quarter-scale model. The model contains a detailed representation of the trunnion and the cutout (trunnion pocket) in the top impact limiter. The impact limiters are attached to the cask ends by beam elements corresponding to the attachment bolts for the impact limiter. The redwood and

the balsa wood were modeled as an isotropic foam material. The room temperature stress-strain curves used as input into the LS-DYNA model were obtained by dynamic crush testing of redwood and balsa wood specimens as described in Tables 2.6.7.5-3 and 2.6.7.5-4.

To account for the deformation of the Type 304 stainless steel shells and gussets, these components were modeled with an elasto-plastic material. The LS-DYNA material Type 24 was used ("Piecewise_Linear_Plasticity"). The required input data for the stainless steel consists of the stress-strain data contained in Section 2.6.7.5.

2.10.3.7.1 Boundary Conditions and Initial Conditions

LS-DYNA "Surface_to_Surface" contact interfaces are employed between the cask body and the impact limiter shells. The unyielding surface is modeled as being flat using the Rigidwall_Geometric_Flat" option in LS-DYNA. Symmetry boundary conditions are imposed on the nodes in the X-Z plane for all drops. An initial velocity of 527.4 in./sec is applied to the entire model to represent the 30-foot drops. A uniform gravitational field corresponding to 386.4 in/sec^2 is also applied in the direction of the drop.

Three drop orientations are considered in this evaluation: top end, CG over top corner, and side drop. The end drop provides the maximum axial accelerations. The corner drop results in the largest crush depth of the limiter. The side drop provides the maximum acceleration in the lateral direction of the cask.

2.10.3.7.2 Results

To obtain results from LS-DYNA, nodes of interest are used to record output data. The nodes are located on the cask body at the plane of symmetry approximately 10 inches from the impact limiters. These data nodes correspond to the location of the accelerometers mounted on the quarter-scale model. For the side drop, the nodes record the lateral acceleration, and for the end drop they record the axial acceleration. For the CG over corner orientation, the output acceleration corresponds to the direction of the drop.

The LS-DYNA output is in the form of displacement and acceleration time histories. However, the acceleration time histories contain high frequency components that do not represent the response of the cask to the external impact. Therefore, the acceleration time histories are filtered

to obtain true accelerations corresponding to the impact. For this evaluation, the Butterworth low-pass filter in LS-DYNA's post-processor is used with a filter frequency of 450 Hz for the lateral direction and 550 Hz for the axial direction (refer to Sections 2.10.3.4.2 and 2.10.3.3.2, respectively). The Butterworth filter is used in NUREG/CR-6608 to filter the acceleration of the impact tests for a steel billet in the side drop and end drop orientation.

The following table shows the maximum accelerations for the three 30-foot drop cases.

UMS® Cask Model Drop Orientation	Model Acceleration Results (g)		LS-DYNA Acceleration Prediction (g)		Design Basis Acceleration (g)
	Top Accelerometer	Bottom Accelerometer	Top Accelerometer	Bottom Accelerometer	
Top Corner	121	N/A	143	N/A	240
Top End	207	N/A	226	N/A	240
Side	190	198	193	210	240

As the table shows, the maximum predicted acceleration of 226g occurs during the top end drop. Acceleration time-history plots are provided in Figures 2.10.3-8 and 2.10.3-9 for the side drop and Figures 2.10.3-12 and 2.10.3-13 for the top end and top corner drops, respectively. In all cases, the LS-DYNA prediction is greater than the quarter-scale drop test results.

A comparison of the predicted crush depth to the actual crush depth is provided in the following table:

Location	Model Drop Test Crush Depth (inch)			LS-DYNA Crush Depth Prediction (inch)		
	Original Thickness	Final Thickness	Measured Crush	Original Thickness	Final Thickness	Total Crush
Top End Drop	—	—	2.00	—	—	2.21
Top Corner Drop	—	—	2.95	—	—	3.36
Side Drop–under the trunnion	3.50	0.63	2.87	3.47	1.11	2.36
Side Drop–bottom impact limiter	5.13	2.38	2.75	5.13	2.42	2.71

The table shows that LS-DYNA accurately predicts the amount of crush experienced during the drop tests except in regions where extreme irregular deformation occur (i.e. directly below the trunnion and corner). Figure 2.10.3-14 shows a direct comparison between the side drop test and the LS-DYNA analysis. As the figure shows, LS-DYNA provides a reasonable prediction of the crush depth that occurs in the drop accident.

The force-displacement curves for the end, corner and side drops are plotted in Figures 2.10.3-15 through 2.10.3-18. The corresponding energy dissipated by the impact limiter is computed by determining the area under the force-displacement curve. The following table summarizes the peak load, maximum deflection and the energy dissipated during the drop event.

Description	Drop Configuration			
	End	**Corner**	**Side (Top Limiter)**	**Side (Bottom Limiter)**
Peak Load, lbf	850,777	687,759	376,209	406,470
Maximum Deflection, in.	2.68	4.98	3.20	3.31
Energy Dissipated, in-lb ($\times 10^6$)	1.48	1.46	0.73	0.73

The energy associated with the 30-foot drop for a scaled model design weight of 4,060 pounds is 1.46×10^6 in-lb. The table shows that the energy dissipated by the impact limiters matches the energy associated with the 30-foot drop analyses.

Figure 2.10.3-1 Typical Filtered Acceleration Time History for the Quarter-Scale Model Top End Drop, Overlayed with the Unfiltered Data

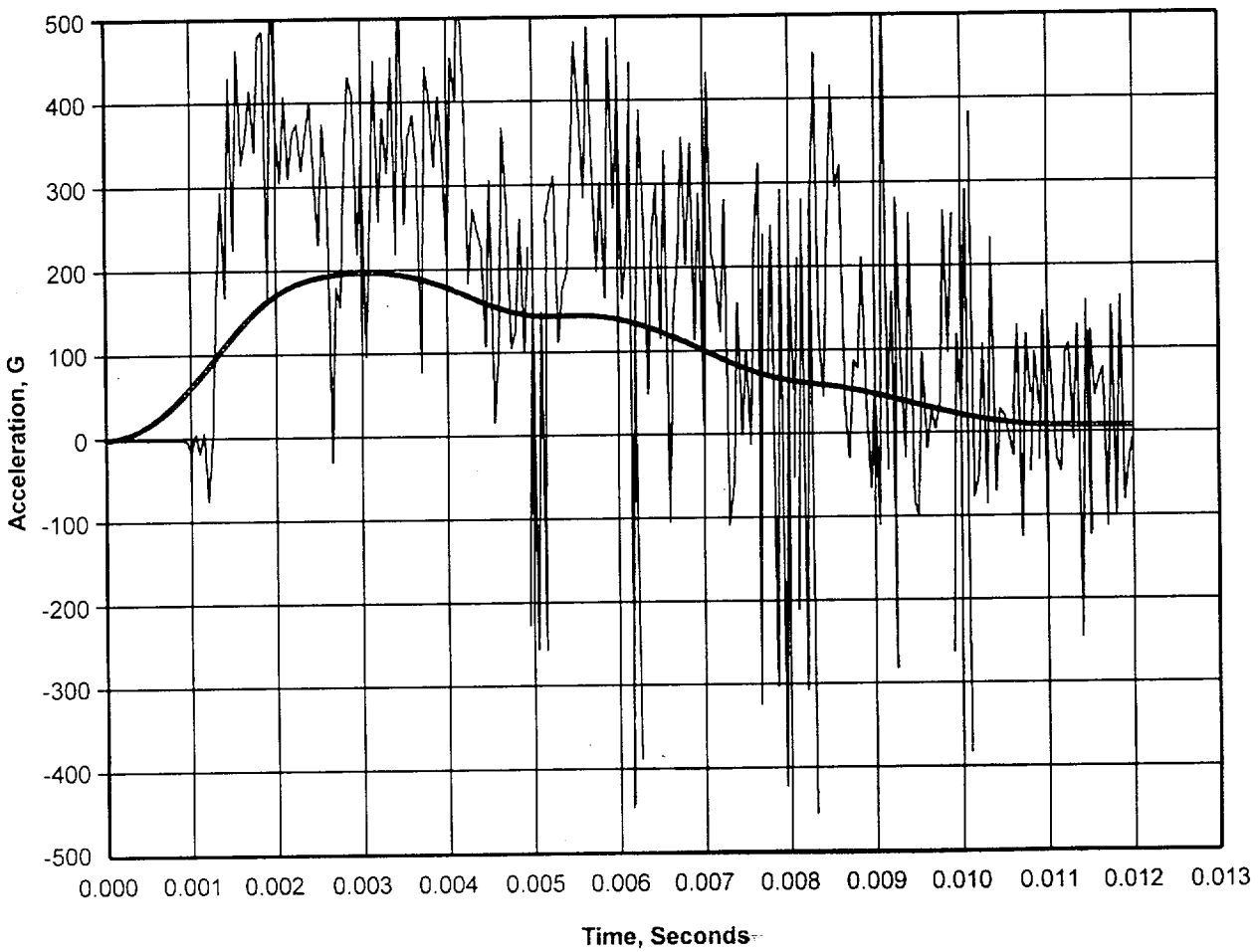

Figure 2.10.3-2 Force-Displacement Curve for Static Test 1 (End Drop Orientation) for a 45° Section of the Quarter-Scale Model Upper Impact Limiter

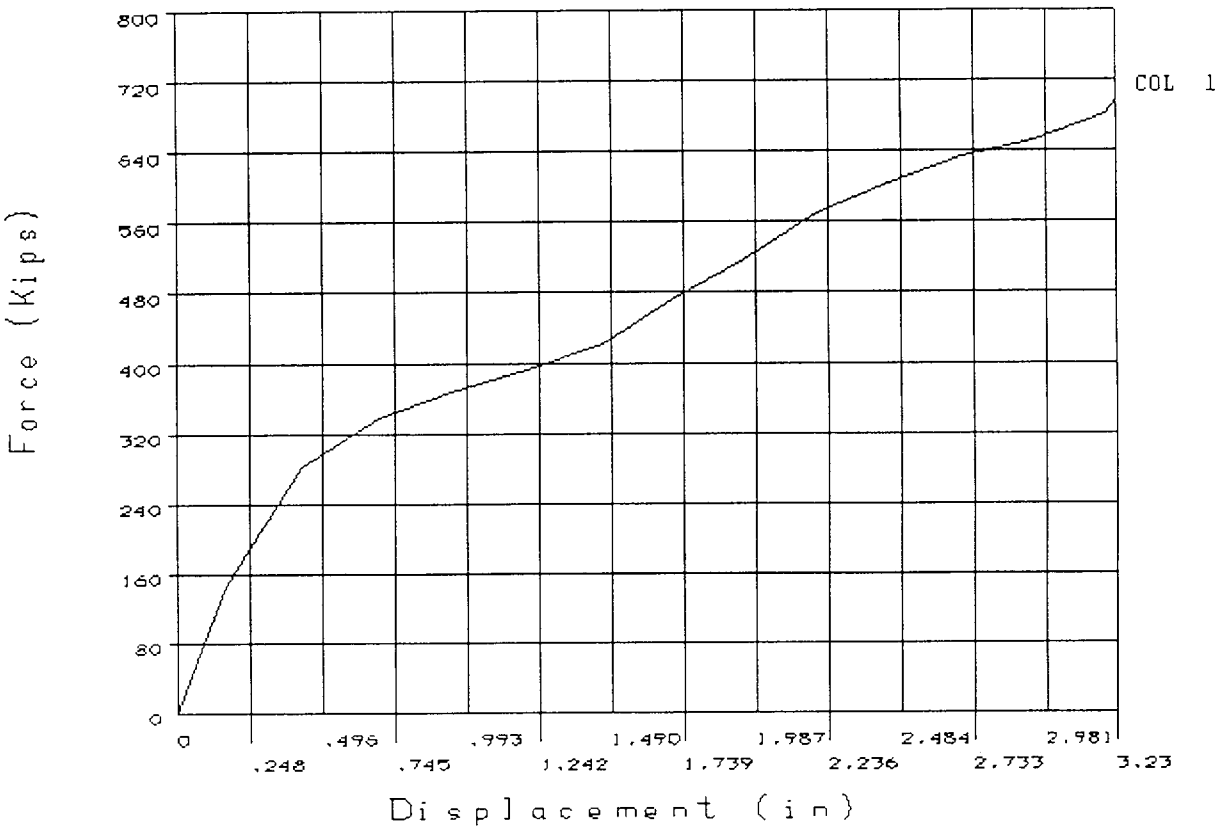

Note:

Forces correspond to a full quarter-scale model of the UMS® upper impact limiter. The forces have been factored by 1.058 to account for the dynamic crush strength of redwood.

Figure 2.10.3-3 Force-Displacement Curve for Static Test 2 (End Drop Orientation) for a 45° Section of the Quarter-Scale Model Upper Impact Limiter

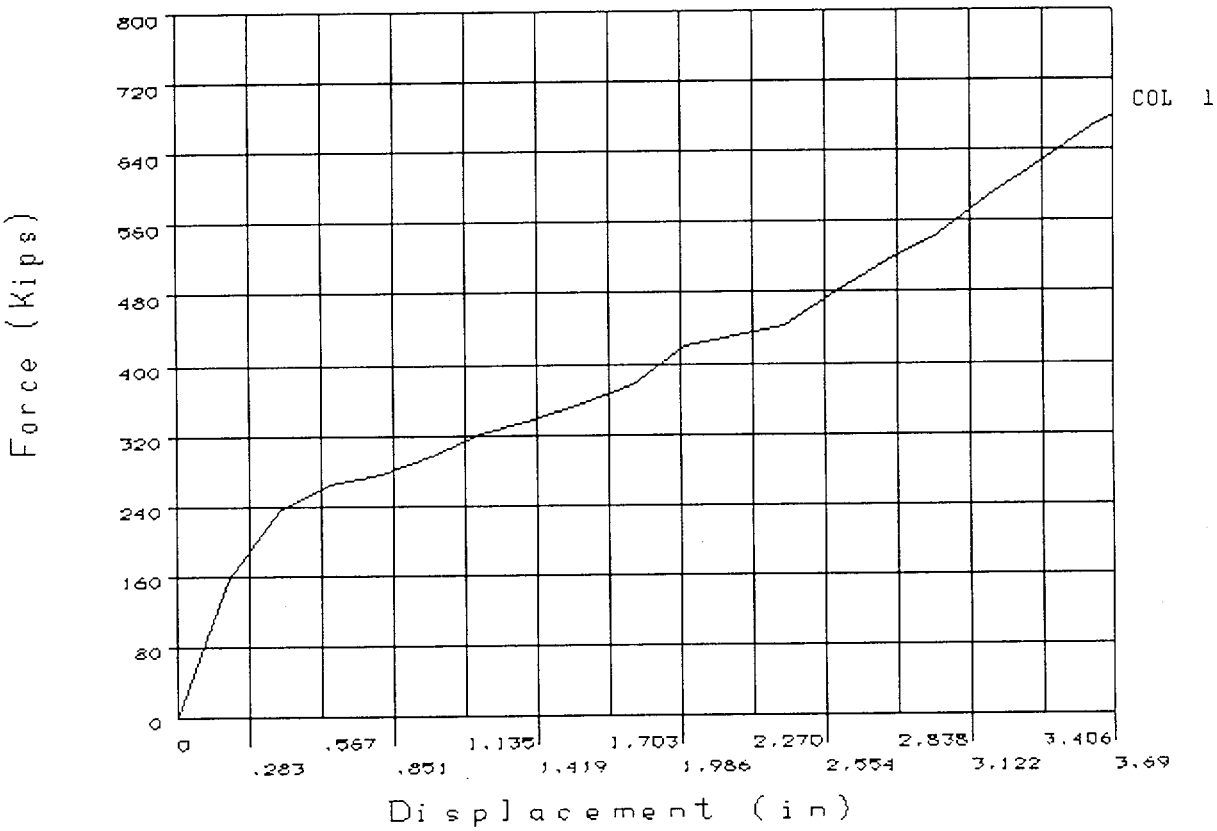

Note:

Forces correspond to a full quarter-scale model of the UMS® upper impact limiter. The forces have been factored by 1.058 to account for the dynamic crush strength of redwood.

Figure 2.10.3-4 Typical Filtered Acceleration Time History for the Quarter-Scale Model Top Corner Drop, Overlayed with the Unfiltered Data

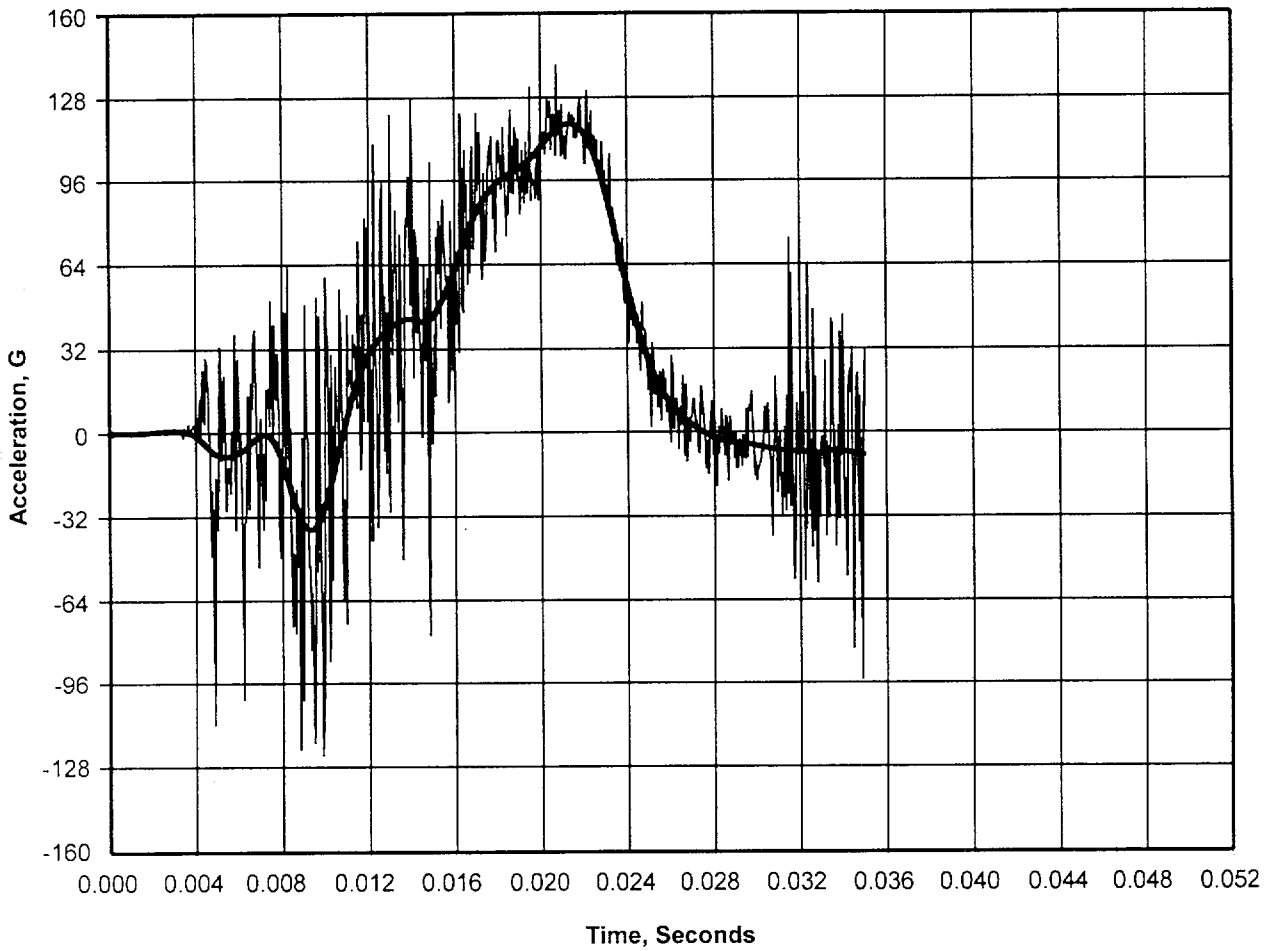

Figure 2.10.3-5 UMS® Quarter-Scale Side Drop Accelerometer Locations

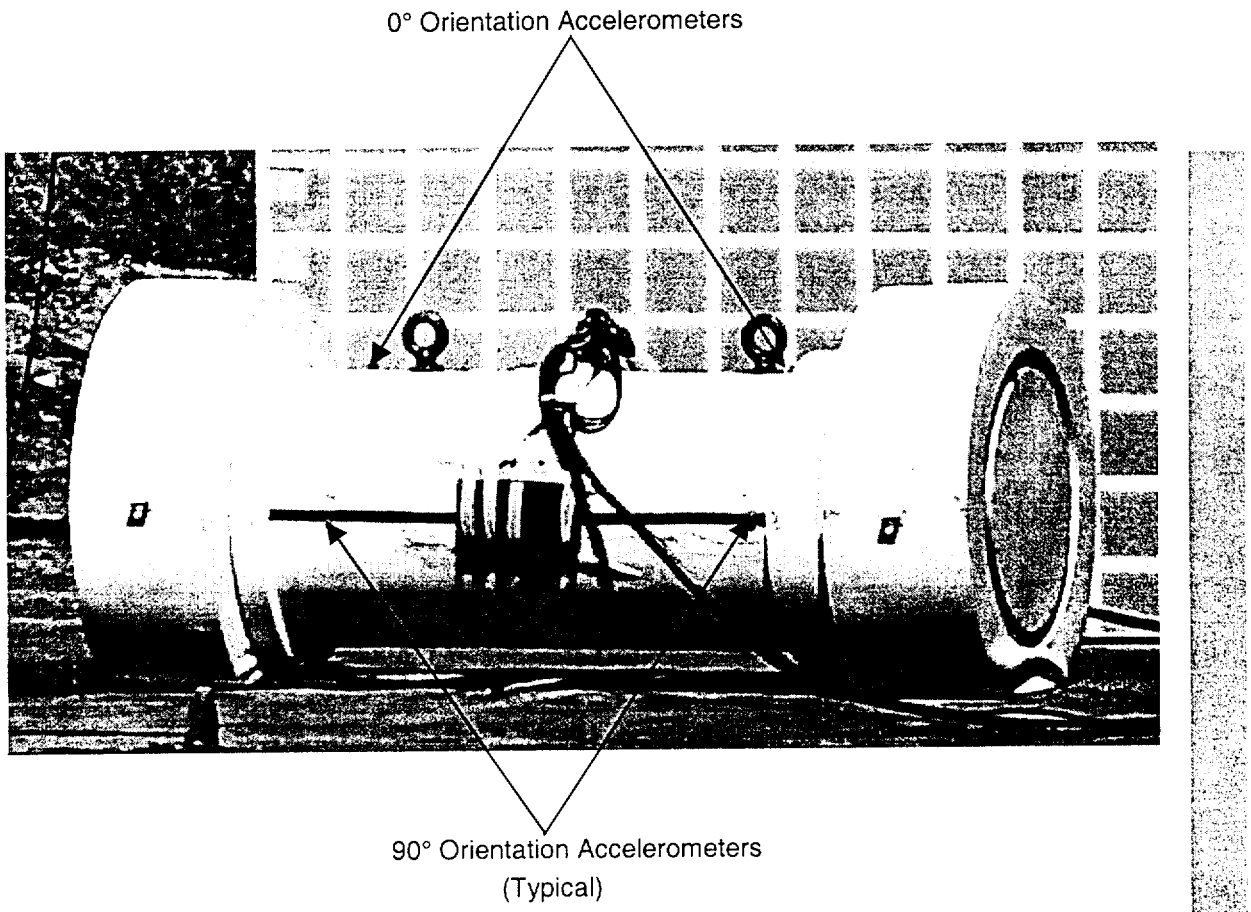

Side drop, at SNL, March 2001

Figure 2.10.3-6 Typical Filtered Acceleration (Top Accelerometer) Time History for the Quarter-Scale Model Side Drop, Overlayed with the Unfiltered Data

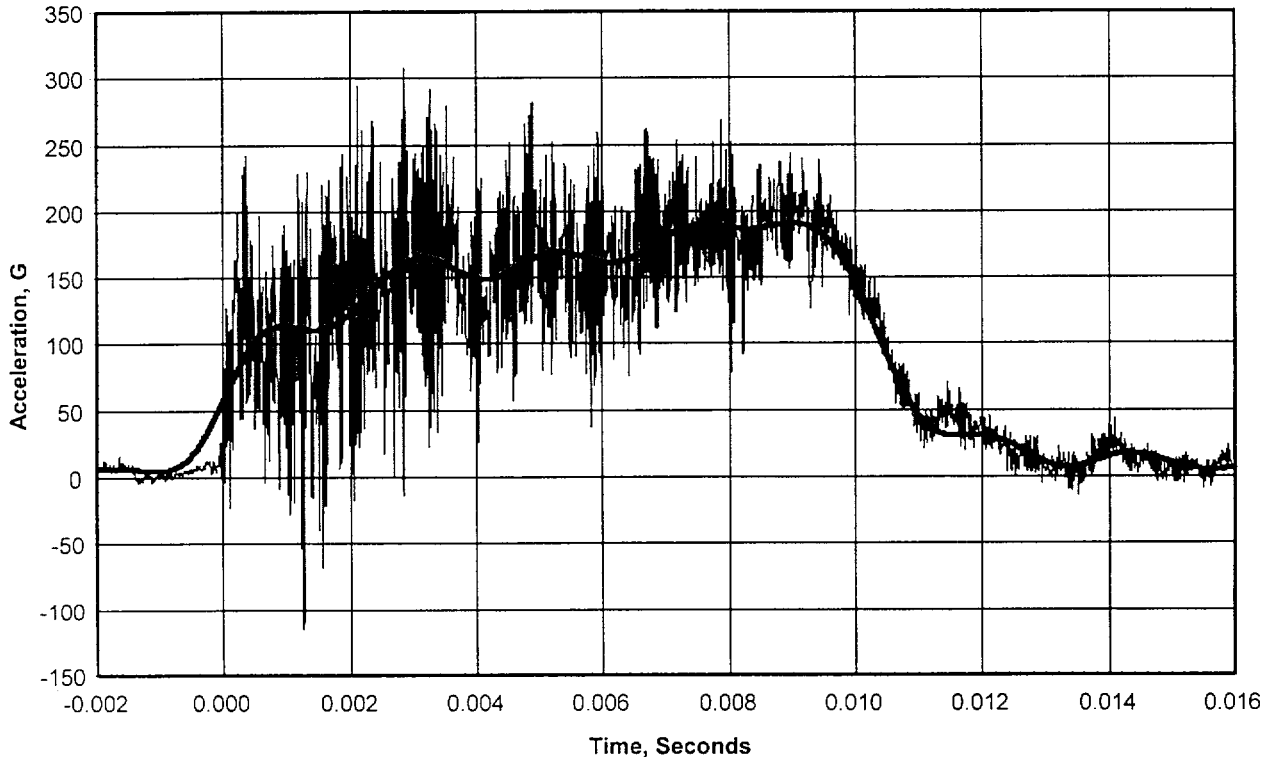

Figure 2.10.3-7 Typical Filtered Acceleration (Bottom Accelerometer) Time History for the Quarter-Scale Model Side Drop, Overlayed with the Unfiltered Data

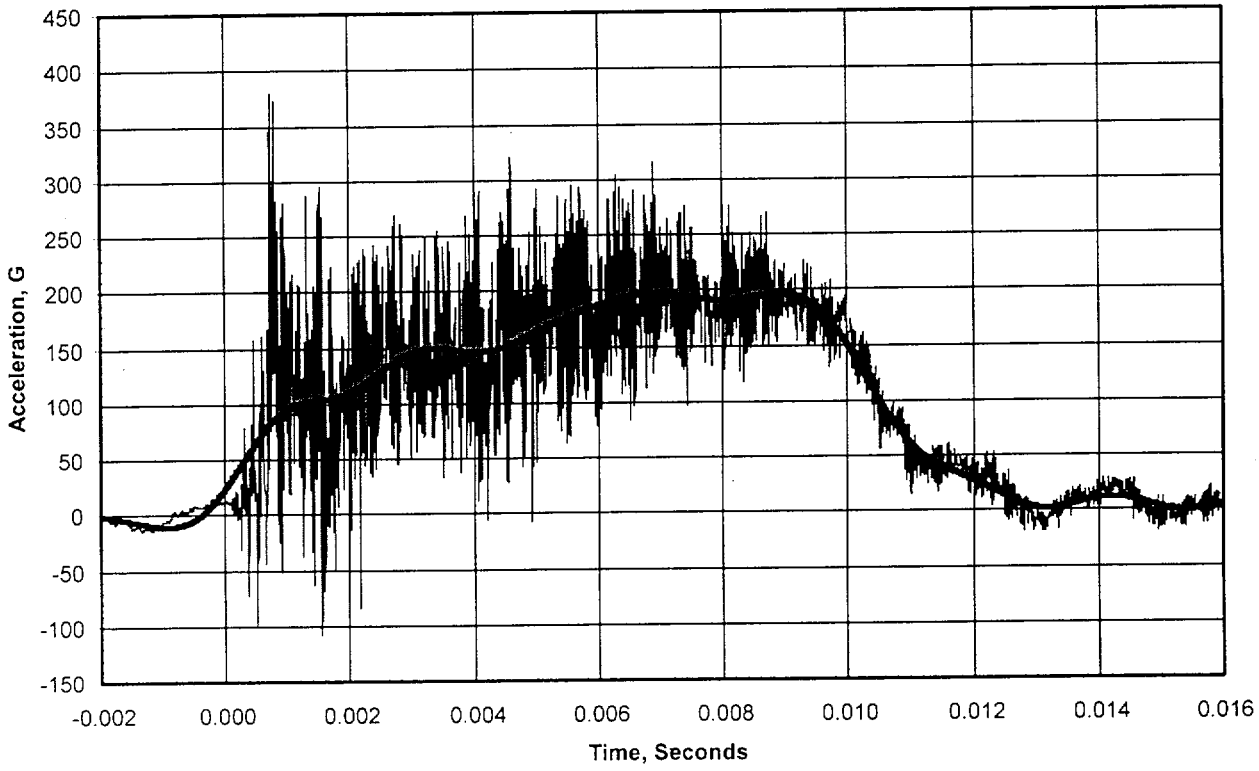

Figure 2.10.3-8 Comparison of Quarter-Scale Side Drop (LS-DYNA and Drop Test) Results (Upper Accelerometer)

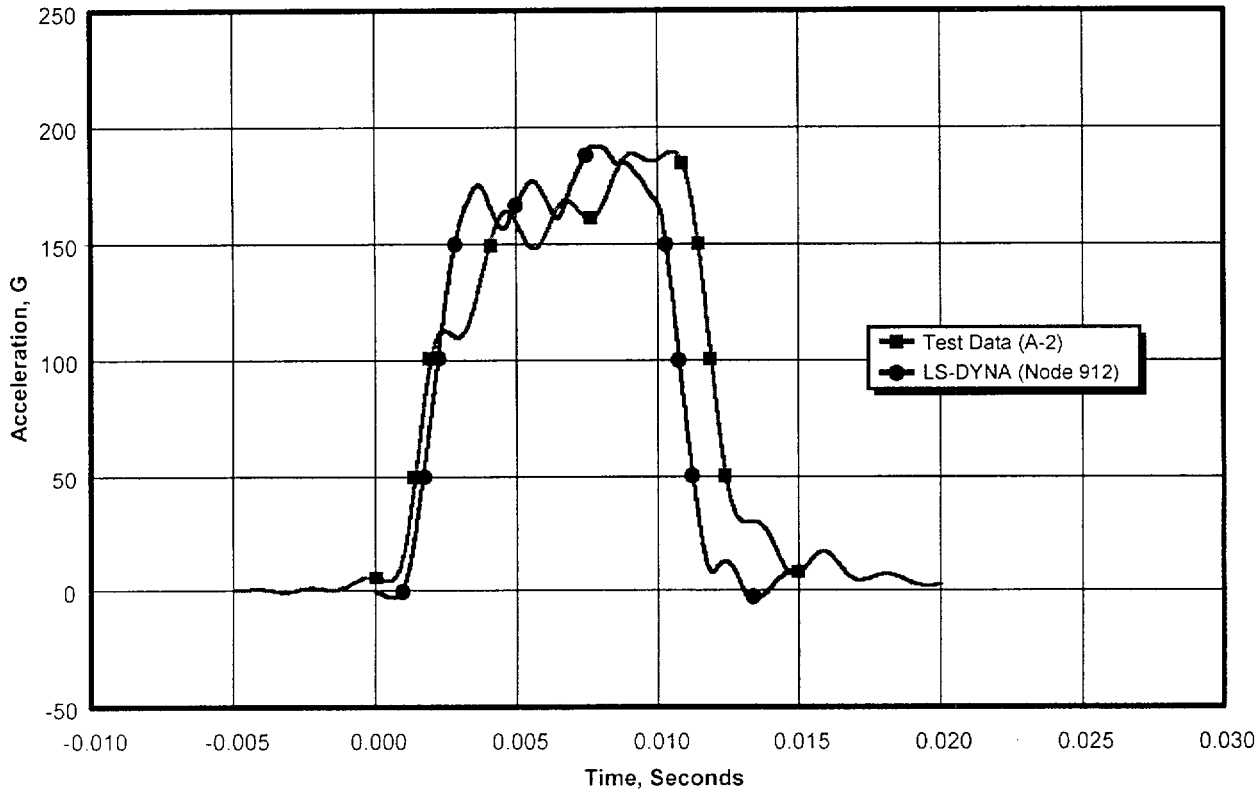

Figure 2.10.3-9 Comparison of Quarter-Scale Side Drop (LS-DYNA and Drop Test) Results (Lower Accelerometer)

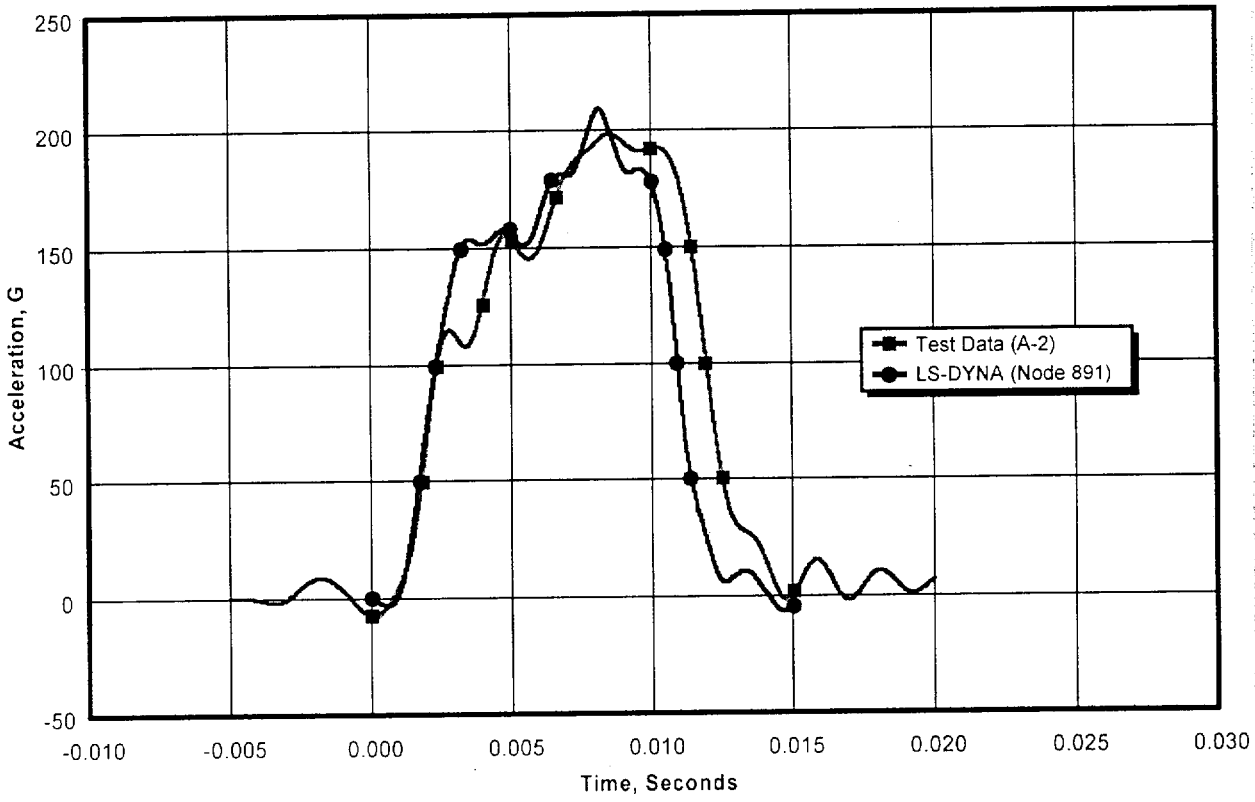

Figure 2.10.3-10 Quarter-Scale Test Model Side Drop Force-Displacement Curve

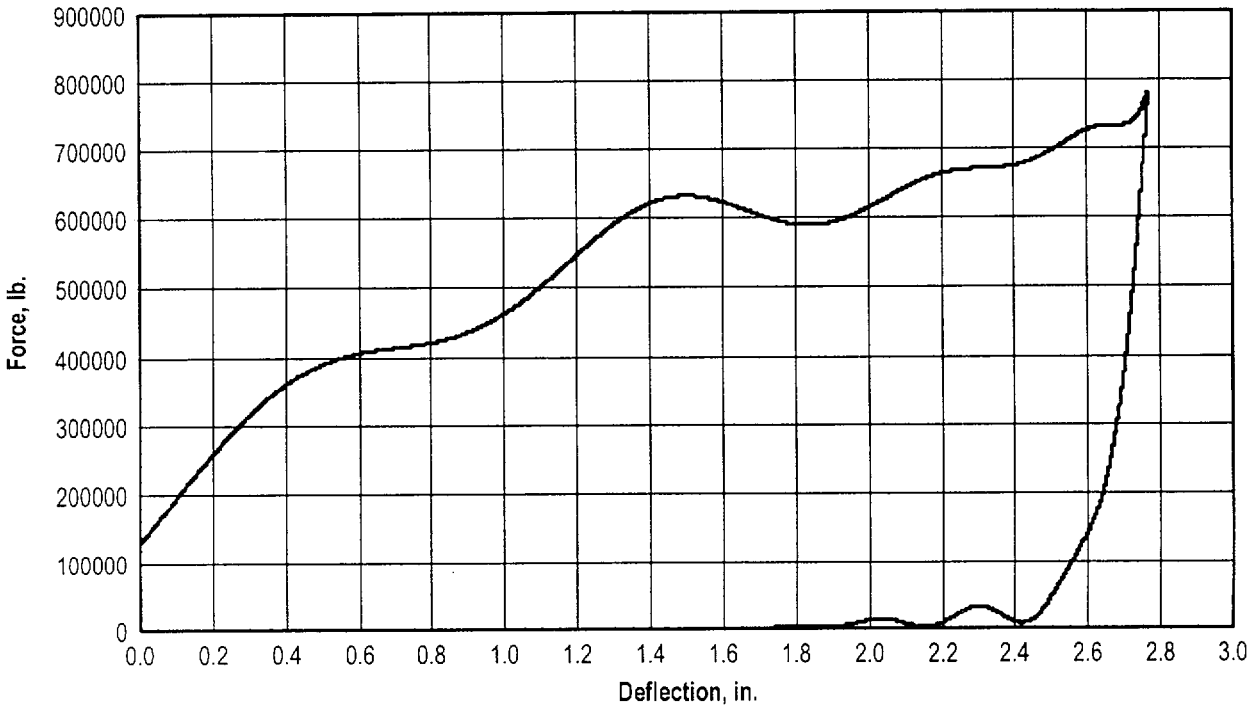

Figure 2.10.3-11 LS-DYNA Quarter-Scale Model

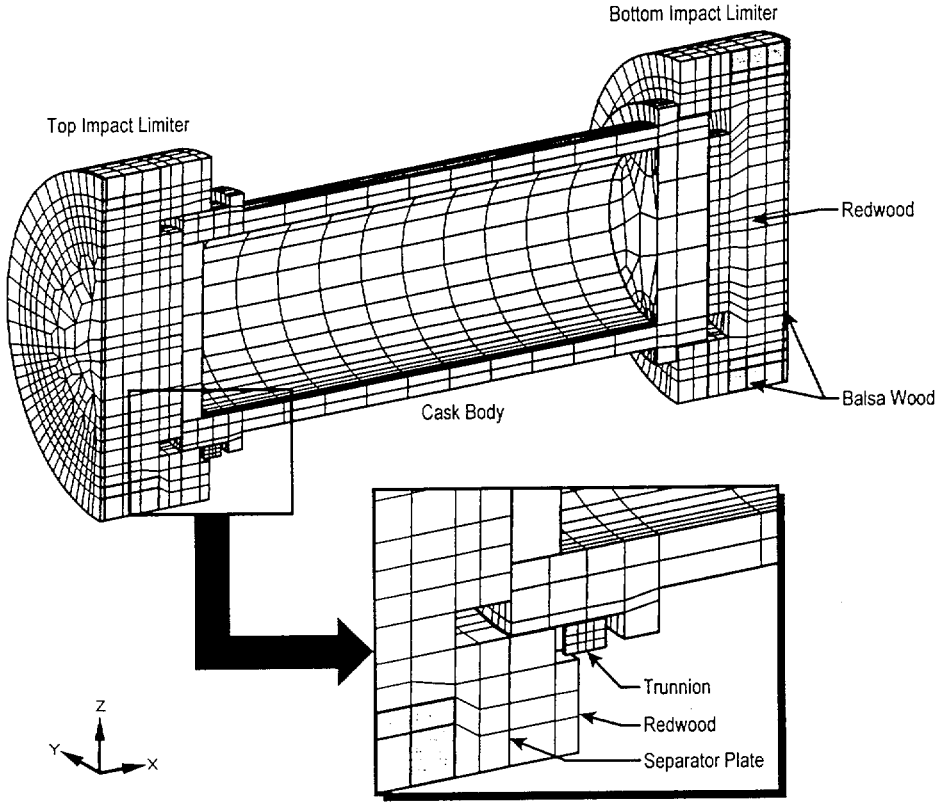

Figure 2.10.3-12 Comparison of Quarter-Scale Top End Drop (LS-DYNA and Drop Test) Results

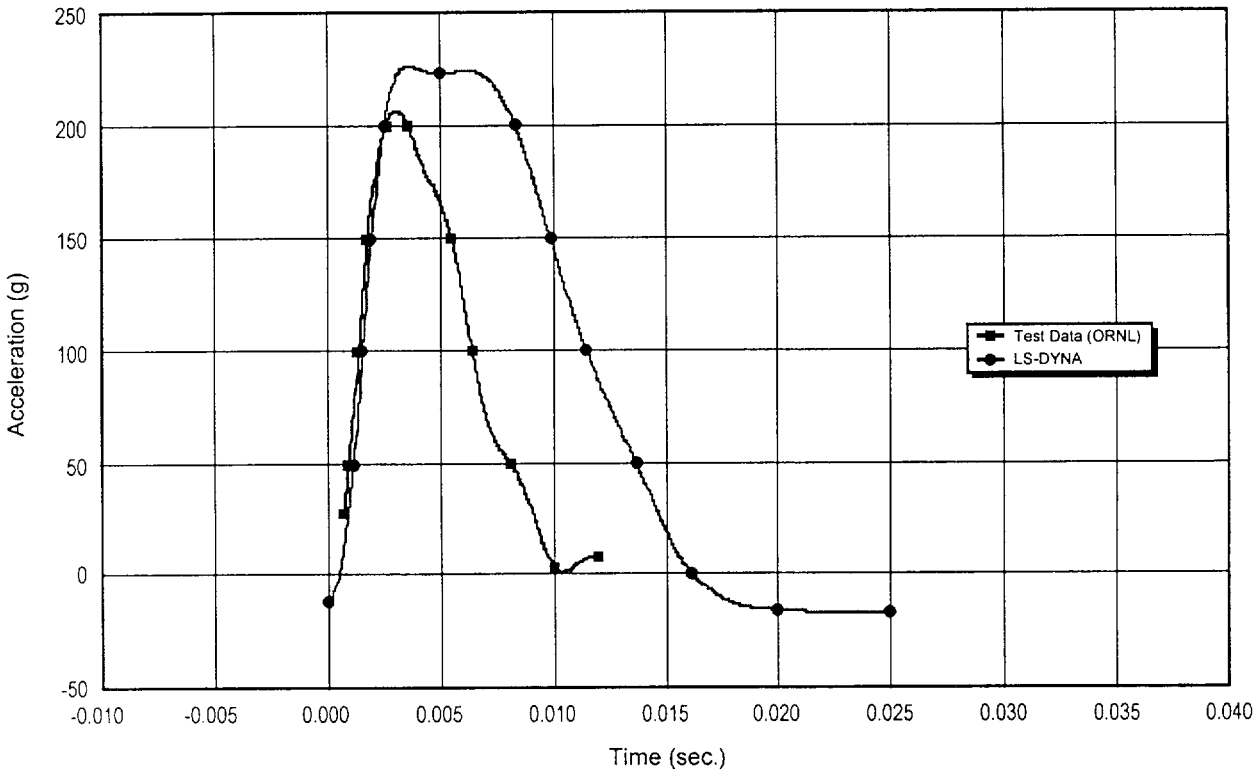

Figure 2.10.3-13 Comparison of Quarter-Scale Top Corner Drop (LS-DYNA and Drop Test) Results

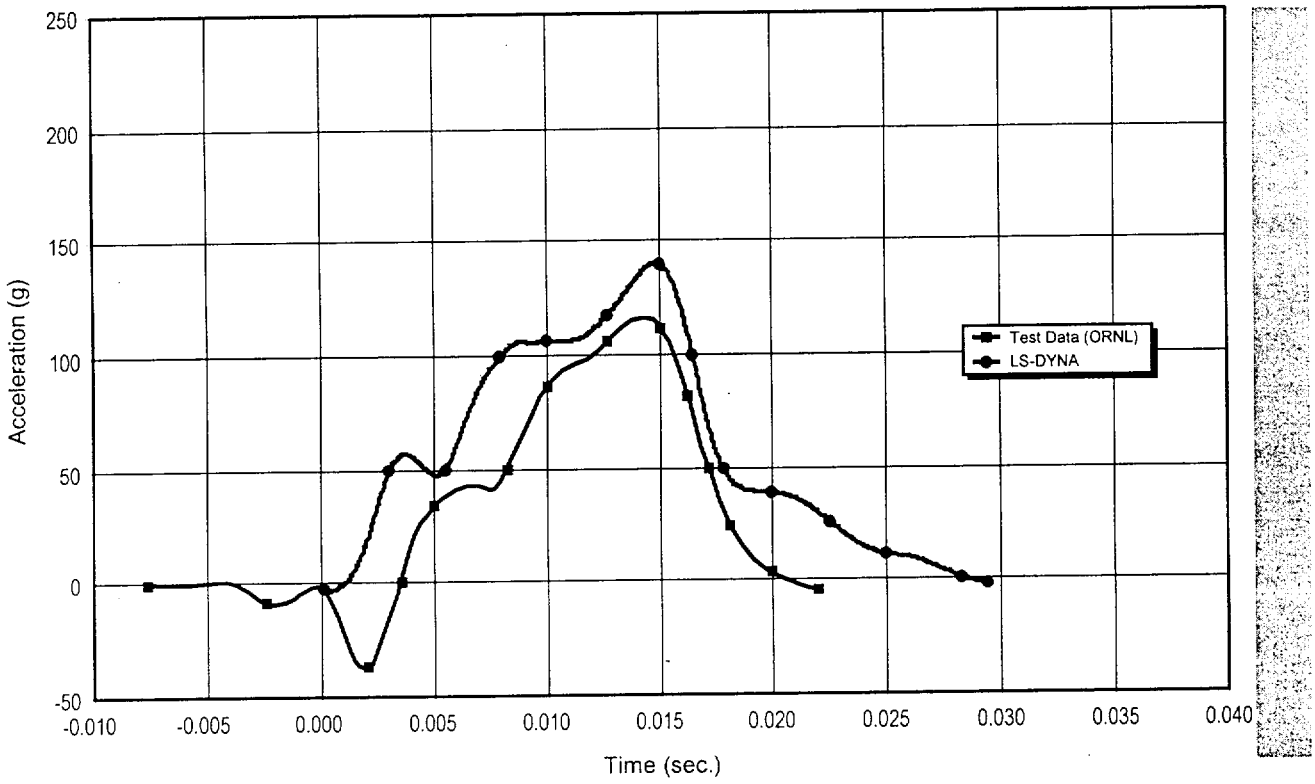

Figure 2.10.3-14 Comparison of Quarter-Scale Test Model and LS-DYNA Deformation During the Side Drop

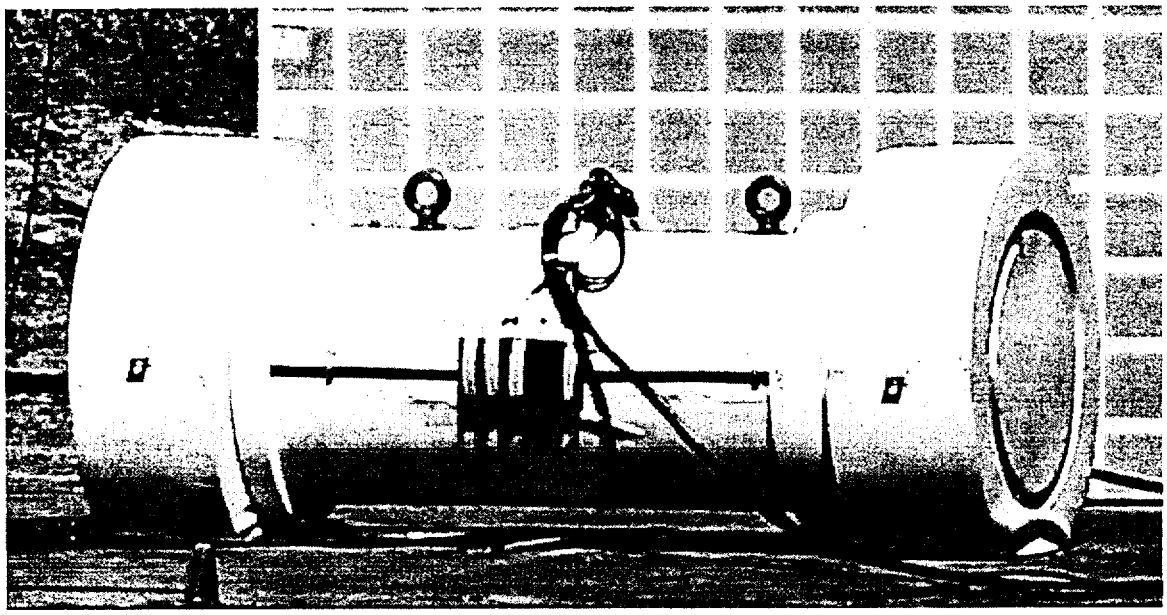

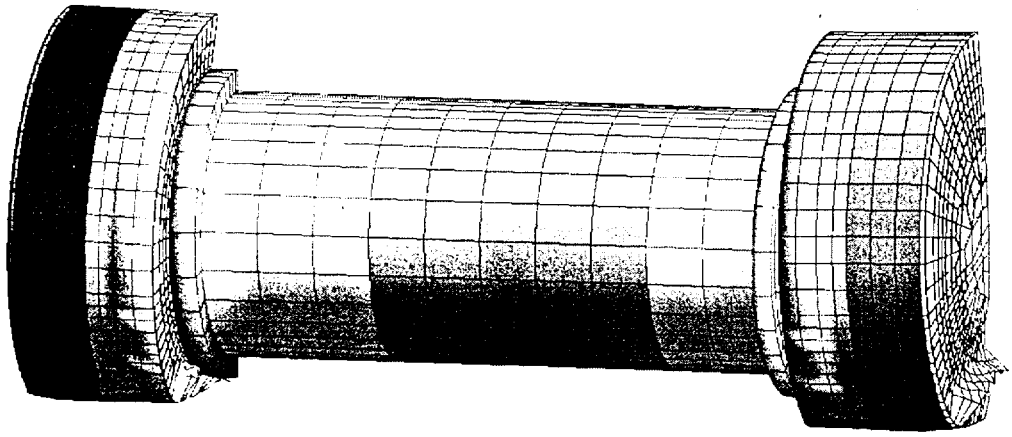

Figure 2.10.3-15 Quarter-Scale Impact Limiter Force-Displacement Curve in the End Drop

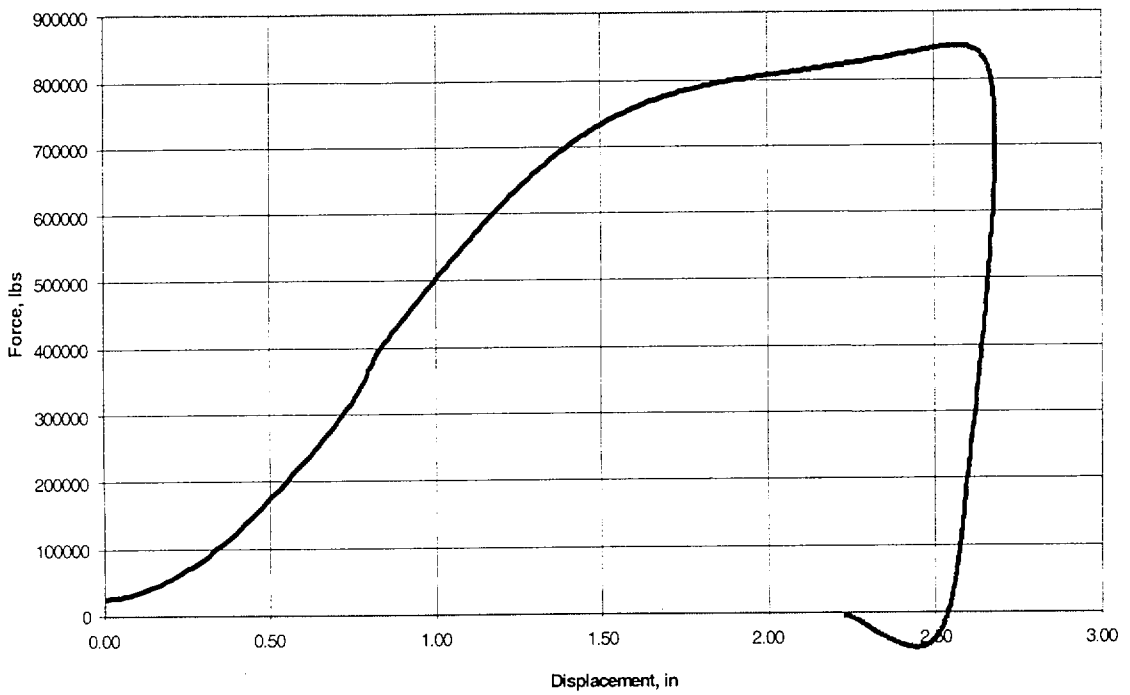

Figure 2.10.3-16 Quarter-Scale Impact Limiter Load-Deflection Curve in the Corner Drop

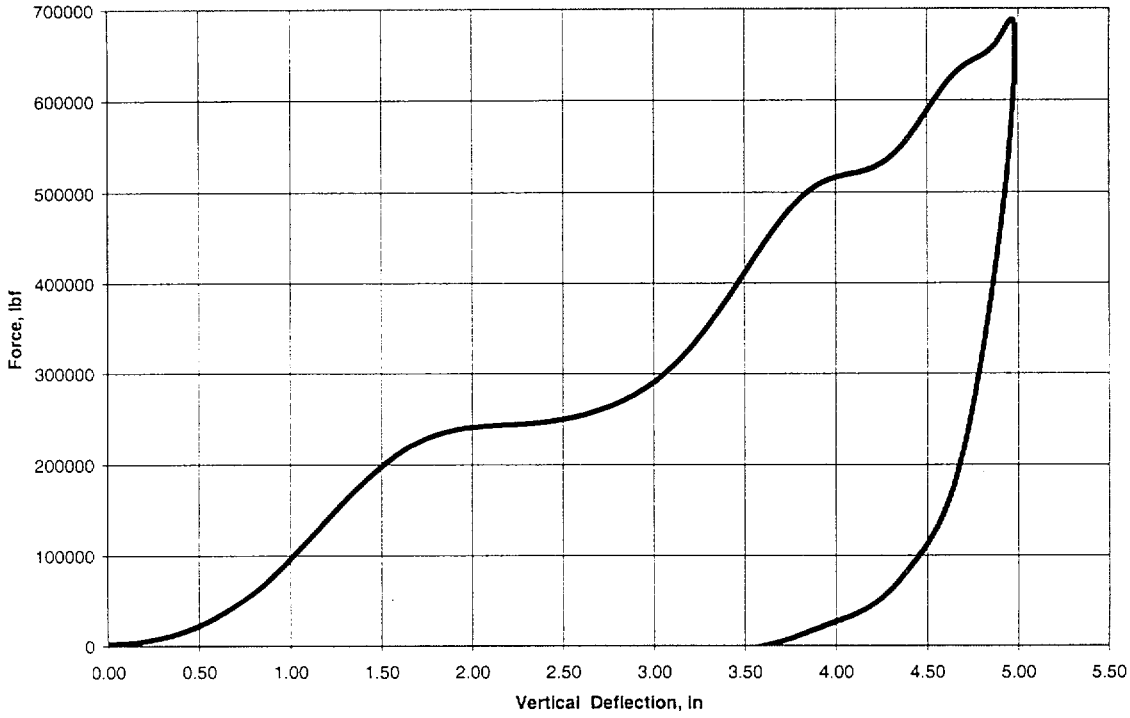

Figure 2.10.3-17 Quarter-Scale Impact Limiter Load-Displacement Curve in the Side Drop (Top Accelerometer)

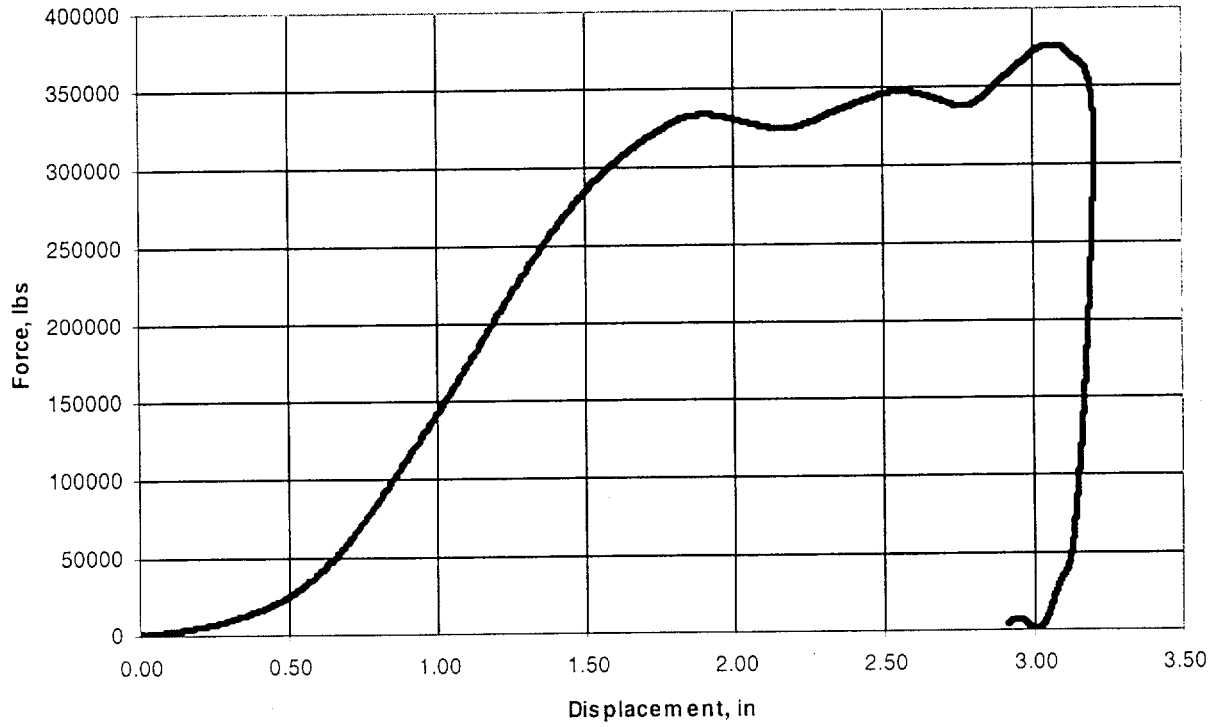

Figure 2.10.3-18 Quarter-Scale Impact Limiter Force-Displacement Curve during the Side Drop (Bottom Accelerometer)